

REPORT 1228

CALCULATED SPANWISE LIFT DISTRIBUTIONS, INFLUENCE FUNCTIONS, AND INFLUENCE COEFFICIENTS FOR UNSWEPT WINGS IN SUBSONIC FLOW¹

BY FRANKLIN W. DIEDERICH AND MARTIN ZLOTNICK

SUMMARY

Spanwise lift distributions have been calculated for nineteen unswept wings with various aspect ratios and taper ratios and with a variety of angle-of-attack or twist distributions, including flap and aileron deflections, by means of the Weissinger method with eight control points on the semispan. Also calculated were aerodynamic influence coefficients which pertain to a certain definite set of stations along the span, and several methods are presented for calculating aerodynamic influence functions and coefficients for stations other than those stipulated.

The information presented herein can be used in the analysis of untwisted wings or wings with known twist distributions, as well as in aeroelastic calculations involving initially unknown twist distributions.

INTRODUCTION

In the design and development of an airplane, a knowledge of the spanwise lift distribution on the wing is important in predicting the structural loads and the stability characteristics. For high-speed airplanes having flexible wings, the calculation of the spanwise lift distribution is an aeroelastic rather than a purely aerodynamic problem. In aeroelastic calculations means are required for calculating the spanwise lift distribution for angle-of-attack (or twist) distributions which are initially unknown. Aerodynamic influence functions or coefficients constitute the most convenient of these means.

As used in this report, the term "aerodynamic influence function" refers to a function which, when multiplied by the spanwise angle-of-attack or twist distribution and integrated over the span, yields the lift (per unit span) at some station on the wing. This function may be considered to be lift distributions on the given wing corresponding to angle-of-attack distributions given by delta (impulse) functions. In a mathematical sense this function is the Green's function for whatever equation is used to relate lift distributions to angle-of-attack distributions.

Similarly, "aerodynamic influence coefficients" are defined as numbers which, when multiplied by the values of the angle-of-attack at several discrete stations on the wing and summed, yield the lift (per unit span) at a station on the wing. The values of the influence function at the given stations

thus constitute an approximation to a set of influence coefficients; they are not true aerodynamic influence coefficients in the sense used herein, because, in general, an integral can be represented only approximately by a finite summation. However, if proper weighting factors are used, a very good approximation to the integral can usually be obtained by a summation involving relatively few terms. Therefore, aerodynamic influence coefficients may be considered to be (and calculated as) weighted values of the corresponding influence functions at the given stations.

Lift influence functions and coefficients may thus be obtained from certain lift distributions. One of the most satisfactory techniques developed in recent years for calculating the spanwise lift distribution on a wing in subsonic flow has been the Weissinger L-method (ref. 1), which can be applied to a large variety of plan forms and yields solutions of sufficient accuracy for all practical purposes without requiring an unduly long time for the calculations. This method may be considered as a simplified lifting-surface theory because the calculation of the lift on the wing is treated as a boundary-value problem, the boundary condition being that the downwash angle induced by the bound and trailing vortices is equal to the geometric angle of attack at the three-quarter-chord line.

In the present report, symmetrical and antisymmetrical lift distributions and some associated aerodynamic parameters have been calculated by means of the Weissinger method with eight control points on the semispan for several continuous and discontinuous angle-of-attack conditions on nineteen unswept wings having various aspect ratios and taper ratios.² A convenient matrix formulation of the Weissinger method was used in conjunction with the Bell Telephone Laboratories X-66744 relay computer at the Langley Laboratory to make the calculations. This formulation, which is described in appendix A, is based on a re-derivation of the Weissinger method using matrix techniques rather than the "mechanical-quadrature" formulas used by Weissinger. If the same stations on the span are used, as was done in the calculations described in this report, the resulting methods are identical; however, with the matrix method the stations can be located on the span in an arbitrary manner, whereas in the conventional Weissinger method they must be located in a certain prescribed manner.

¹ Supersedes NACA TN 3014, "Calculated Spanwise Lift Distributions and Aerodynamic Influence Coefficients for Unswept Wings in Subsonic Flow" by Franklin W. Diederich and Martin Zlotnick, 1953.

² Results of similar calculations for 61 swept wings are presented in NACA Technical Note 3476 entitled "Calculated Spanwise Lift Distributions and Aerodynamic Influence Coefficients for Swept Wings in Subsonic Flow" by Franklin W. Diederich and Martin Zlotnick, 1955.

Aerodynamic influence coefficients have been calculated for these nineteen wings for the prescribed set of stations along the span and are presented herein, and several methods for calculating aerodynamic influence functions and coefficients for any arbitrary set of stations from the numerical results of this report are also presented. The influence coefficients calculated in this manner can be used in aeroelastic analyses similar to that of reference 2.

SYMBOLS

A	aspect ratio
b	wing span
b_{att}	aileron span
b_f	flap span
C_{BM}	root bending-moment coefficient for unit angle of attack, $\frac{4 \times \text{Bending moment}}{qSb}$
C_{D_i}	induced-drag coefficient at a unit angle of attack
C_L	lift coefficient at a unit angle of attack
$C_{L\alpha}$	lift-curve slope per radian for additional-type loading
$C_{L_{1/2}}$	lift coefficient for half of antisymmetrically loaded wing at a unit tip angle of attack, $\frac{L_{1/2}}{q \frac{S}{2}}$
C_l	rolling-moment coefficient, $\frac{\text{Rolling moment}}{qSb}$
$C_{l_d} = -C_{l_p}$	
C_{l_p}	coefficient of damping in roll
C_{l_p/α_s}	rolling-moment coefficient for unit aileron deflection
c	wing chord
\bar{c}	average chord, S/b
c_l	section lift coefficient
$[I_{C_{BM}}]$	integrating matrix for C_{BM} (see appendix A)
$[I_{C_L}]$	integrating matrix for C_L (see appendix A)
$[I_{C_{L_{1/2}}}]$	integrating matrix for $C_{L_{1/2}}$ (see appendix A)
$[I_{C_l}]$	integrating matrix for C_l (see appendix A)
$L_{1/2}$	lift on one semispan
M	free-stream Mach number
$[Q]$	aerodynamic-influence-coefficient matrix
q	dynamic pressure
S	wing area
V	free-stream velocity
y, η	lateral ordinates
y_o	spanwise location of discontinuity
\bar{y}	spanwise center-of-pressure location
α	angle of attack, radians
α_s	effective angle of attack for unit flap deflection, $\frac{\partial c_l / \partial \delta}{\partial c_l / \partial \alpha}$
Γ	vortex strength
Γ^*	dimensionless vortex strength, $\frac{4\Gamma}{bV} = c^* c_l$

δ	flap or aileron deflection angle, radians
$\theta \equiv \cos^{-1} y^*$	
$\theta_o \equiv \cos^{-1} y_o^*$	
$\vartheta \equiv \cos^{-1} \eta^*$	
Λ	sweepback angle, deg
λ	taper ratio
Subscripts:	
a	antisymmetrical
ail	aileron
C	continuous
D	discontinuous
f	flap
L	left
R	right
s	symmetrical
t	tip
Superscript:	
$*$	dimensionless with respect to semispan $b/2$
Matrix notation:	
$[]$	row matrix
$\{ \}$	column matrix
$[]$	general matrix (not a row or a column matrix, but need not be square)
$[]$	diagonal matrix
$[1]$	unit (identity) matrix
In matrix notation, a prime indicates the transpose of the matrix.	

PRESENTATION OF CALCULATED RESULTS

SPANWISE LIFT DISTRIBUTIONS

Geometric characteristics of the nineteen plan forms treated in this report are indicated in table I. Lift distributions due to the following continuous symmetric and antisymmetric angle-of-attack distributions have been calculated for each of these plan forms:

Symmetric angle-of-attack distributions:

- Constant ($\alpha=1$)
- Linear ($\alpha=|y^*|$)
- Quadratic ($\alpha=y^{*2}$)
- Cubic ($\alpha=|y^{*3}|$)
- Straight-line ($\alpha=\frac{c_l}{c} |y^*|$)

Antisymmetric angle-of-attack distributions:

- Linear ($\alpha=y^*$)
- Quadratic ($\alpha=y^{*2}$ for $y^* \geq 0$; $\alpha=-y^{*2}$ for $y^* \leq 0$)
- Cubic ($\alpha=y^{*3}$)
- Quartic ($\alpha=y^{*4}$ for $y^* \geq 0$; $\alpha=-y^{*4}$ for $y^* \leq 0$)
- Quintic ($\alpha=y^{*5}$)

The straight-line angle-of-attack condition was included to represent actual structural twists where the surface of the wing is generated by straight lines so that the product $c^* \alpha$, the deflection of the leading edge, varies linearly with y^* ; that is,

$$c^* \alpha = c_l^* y^* \alpha_l$$

or, for unit twist at the tip,

$$\alpha = \frac{c_t^*}{c^*} y^*$$

For untapered wings, the straight-line lift distribution is the same as the linear lift distribution, and for wings of zero taper ratio, it is undefined.

Lift distributions for flap-type and aileron-type angle-of-attack distributions are also presented. A correction which has been made for the spanwise discontinuity in the angle of attack is derived in appendix B. The values of b_f/b and b_{at}/b (ratios of the flap span to the total span and the aileron span to the total span, respectively) for which the lift distributions have been calculated are 0.1, 0.2, 0.3, 0.4, 0.5, 0.6, 0.7, 0.8, 0.9, and 1.0. As is usual, the flaps have been taken to be inboard and the ailerons outboard. The lift distribution for any flap or aileron configuration may be obtained, however, by linear superposition; thus, the lift distribution for an outboard flap extending, for example, from $y^*=0.5$ to $y^*=1.0$ can be obtained by subtracting the lift distribution for the inboard flap ($\frac{b_f}{b}=0.5$) from the additional lift distribution ($\frac{b_f}{b}=1.0$). A similar procedure can be used for inboard ailerons.

The lift distributions pertaining to each plan form are given in one figure, parts (a) and (b) showing the lift distribution due to symmetric and antisymmetric continuous angle-of-attack distributions, respectively, and parts (c) and (d) showing the lift distribution due to flaps and ailerons, respectively. Lift distributions for plan forms with an aspect ratio approaching zero have been taken from reference 3 and are included herein in figure 1 for the sake of completeness. (As indicated in ref. 3, the lift distribution for a wing of very low aspect ratio is independent of the plan form, provided the trailing edge is not re-entrant.) The lift distributions on the nineteen wings considered in the present report are presented in figures 2 to 20. Table I serves as a table of contents for this group of figures.

AERODYNAMIC PARAMETERS

The aerodynamic parameters $C_{L\alpha}$, C_{BM} , \bar{y}^* , C_{Dv} , $C_{L\alpha}$, and $C_{L1/2}$ for the nineteen plan forms considered are compiled in table II. The values of C_L and C_{BM} for a unit effective flap deflection are presented in table III, and the values of $C_{L1/2}$ and $C_{L\alpha}$ for a unit effective aileron deflection are presented in table IV. These lift and moment coefficients pertain directly to full-chord flaps and ailerons set at an angle of attack of 1 radian. For partial-chord flaps and ailerons deflected by an angle of δ radians, these coefficients must be multiplied by the quantity $\alpha\delta$.

AERODYNAMIC INFLUENCE COEFFICIENTS FOR STIPULATED STATIONS

Aerodynamic influence coefficients for symmetric and antisymmetric lift distributions were obtained as shown in appendix A and are presented as the matrices $[Q_s]$ and $[Q_a]$ in tables V(a) and V(b), respectively. Each influence-coefficient matrix in the table applies to a given plan form.

These influence-coefficient matrices are used to calculate the spanwise lift distribution for any continuous angle-of-attack condition from the following matrix expressions:

$$\begin{aligned} \{\Gamma^*_s\} &= C_{L_s}[Q_s]\{\alpha_s\} \\ \text{and} \\ \{\Gamma^*_a\} &= C_{L_a}[Q_a]\{\alpha_a\} \end{aligned} \quad (1)$$

for the symmetrical and antisymmetrical distributions, respectively, where α is the angle of attack at stations $y^*=0.9808, 0.9239, 0.8315, 0.7071, 0.5556, 0.3827, 0.1951$, and 0 and Γ^* is the desired lift at these stations. In this report the convention is that the angle of attack for the station nearest the wing tip ($y^*=0.9808$) is the first element of the angle-of-attack matrix $\{\alpha\}$ and the lift at the same station is the first element of the lift-distribution matrix $\{\Gamma^*\}$. The matrices $[Q_s]$ and $[Q_a]$ of table V are arranged accordingly.

AERODYNAMIC INFLUENCE FUNCTIONS AND COEFFICIENTS FOR ARBITRARY STATIONS

The influence coefficients described in the preceding section are satisfactory for many purposes; for instance, the stipulated stations at which the lift is given are convenient for plotting spanwise lift distributions because the points are concentrated near the wing tip where the curvature of the lift distributions is greatest. In some cases, however, other considerations may determine the points on the span at which the lift is to be calculated. For instance, when the influence coefficients are to be used in an aeroelastic analysis, the location of the stations may be dictated by the structural characteristics of the wing; also, if lift distributions are to be calculated for the sake of comparison with experimental results, this comparison can be facilitated by calculating the lift at the same stations at which it is measured and thus avoiding the necessity of graphical or numerical interpolation.

As pointed out in the Introduction, the method described in appendix A can be used to calculate influence coefficients for arbitrary stations. However, this procedure requires re-calculation of these coefficients from scratch. In the following sections several other methods are described for obtaining aerodynamic influence functions and coefficients for arbitrary stations from the information presented in this report.

INFLUENCE COEFFICIENTS OBTAINED BY USING INTERPOLATING MATRICES

One way of constructing an influence-coefficient matrix for any stations from the matrices presented herein is to calculate interpolating matrices which give the angles of attack at $y^* = 0.9808, 0.9239, 0.8315, 0.7071, 0.5556, 0.3827, 0.1951$, and 0 in terms of the angles of attack at the given stations and the values of the lift at the given stations in terms of those at the stations $y^* = 0.9808, 0.9239, 0.8315, 0.7071, 0.5556, 0.3827, 0.1951$, and 0. The desired influence-coefficient matrix would then be obtained by postmultiplying the one given herein by the angle-of-attack interpolating matrix and premultiplying it by the lift interpolating matrix.

In order to illustrate the nature of these calculations, a pair of matrices are calculated for stations at every tenth of the semispan by linear interpolation. (The stations at which the angle of attack is given and those at which the lift is to be found need not be the same, but here, as in most cases, they are chosen to be the same as a matter of convenience.)

With linear interpolation,

$$\alpha_{0.9808} = 0.808\alpha_{1.0} + 0.192\alpha_{0.9}$$

$$\alpha_{0.9239} = 0.239\alpha_{1.0} + 0.761\alpha_{0.9}$$

$$\alpha_{0.8315} = 0.315\alpha_{0.9} + 0.685\alpha_{0.8}$$

.

$$\alpha_0 = \alpha_0$$

which can be written in matrix form as

$$\begin{bmatrix} \alpha_{0.9808} \\ \alpha_{0.9239} \\ \alpha_{0.8315} \\ \alpha_{0.7071} \\ \alpha_{0.5556} \\ \alpha_{0.3827} \\ \alpha_{0.1951} \\ \alpha_0 \end{bmatrix} = \begin{bmatrix} 0.808 & 0.192 & 0 & 0 & 0 & 0 & 0 & 0 & 0 & 0 & 0 & 0 \\ 0.239 & 0.761 & 0 & 0 & 0 & 0 & 0 & 0 & 0 & 0 & 0 & 0 \\ 0 & 0.315 & 0.685 & 0 & 0 & 0 & 0 & 0 & 0 & 0 & 0 & 0 \\ 0 & 0 & 0.071 & 0.929 & 0 & 0 & 0 & 0 & 0 & 0 & 0 & 0 \\ 0 & 0 & 0 & 0 & 0.556 & 0.444 & 0 & 0 & 0 & 0 & 0 & 0 \\ 0 & 0 & 0 & 0 & 0 & 0 & 0.827 & 0.173 & 0 & 0 & 0 & 0 \\ 0 & 0 & 0 & 0 & 0 & 0 & 0 & 0 & 0.951 & 0.049 & 0 & 0 \\ 0 & 0 & 0 & 0 & 0 & 0 & 0 & 0 & 0 & 0 & 0 & 1.000 \end{bmatrix} \begin{bmatrix} \alpha_{1.0} \\ \alpha_{0.9} \\ \alpha_{0.8} \\ \alpha_{0.7} \\ \alpha_{0.6} \\ \alpha_{0.5} \\ \alpha_{0.4} \\ \alpha_{0.3} \\ \alpha_{0.2} \\ \alpha_{0.1} \\ \alpha_0 \end{bmatrix}$$

where the rectangular matrix on the right side of the equation is the desired angle-of-attack interpolating matrix.

Similarly, for the lift distribution,

$$\Gamma^*_{1.0} = 0$$

(This information is known from physical considerations; to calculate $\Gamma^*_{1.0}$ by extrapolation from $\Gamma^*_{0.9808}$ and $\Gamma^*_{0.9239}$ would give a spurious value.)

$$\Gamma^*_{0.9} = \Gamma^*_{0.8315} + \frac{0.0685}{0.0924} (\Gamma^*_{0.9239} - \Gamma^*_{0.8315}) = 0.741\Gamma^*_{0.9239} + 0.259\Gamma^*_{0.8315}$$

$$\Gamma^*_{0.8} = \Gamma^*_{0.7071} + \frac{0.0929}{0.1244} (\Gamma^*_{0.8315} - \Gamma^*_{0.7071}) = 0.747\Gamma^*_{0.8315} + 0.253\Gamma^*_{0.7071}$$

.

$$\Gamma^*_0 = \Gamma^*_0$$

or, in matrix form,

$$\begin{Bmatrix} \Gamma^*_{1.0} \\ \Gamma^*_{0.9} \\ \Gamma^*_{0.8} \\ \Gamma^*_{0.7} \\ \Gamma^*_{0.6} \\ \Gamma^*_{0.5} \\ \Gamma^*_{0.4} \\ \Gamma^*_{0.3} \\ \Gamma^*_{0.2} \\ \Gamma^*_{0.1} \\ \Gamma^*_0 \end{Bmatrix} = \begin{bmatrix} 0 & 0 & 0 & 0 & 0 & 0 & 0 & 0 & 0 & 0 & 0 \\ 0 & 0.741 & 0.259 & 0 & 0 & 0 & 0 & 0 & 0 & 0 & 0 \\ 0 & 0 & 0.747 & 0.253 & 0 & 0 & 0 & 0 & 0 & 0 & 0 \\ 0 & 0 & 0 & 0.953 & 0.047 & 0 & 0 & 0 & 0 & 0 & 0 \\ 0 & 0 & 0 & 0.293 & 0.707 & 0 & 0 & 0 & 0 & 0 & 0 \\ 0 & 0 & 0 & 0 & 0.679 & 0.321 & 0 & 0 & 0 & 0 & 0 \\ 0 & 0 & 0 & 0 & 0.100 & 0.900 & 0 & 0 & 0 & 0 & 0 \\ 0 & 0 & 0 & 0 & 0 & 0.559 & 0.441 & 0 & 0 & 0 & 0 \\ 0 & 0 & 0 & 0 & 0 & 0.026 & 0.974 & 0 & 0 & 0 & 0 \\ 0 & 0 & 0 & 0 & 0 & 0 & 0.513 & 0.487 & 0 & 0 & 0 \\ 0 & 0 & 0 & 0 & 0 & 0 & 0 & 0 & 1.000 & 0 & 0 \end{bmatrix} \begin{Bmatrix} \Gamma^*_{0.9308} \\ \Gamma^*_{0.9239} \\ \Gamma^*_{0.8315} \\ \Gamma^*_{0.7071} \\ \Gamma^*_{0.5556} \\ \Gamma^*_{0.3827} \\ \Gamma^*_{0.1951} \\ \Gamma^*_0 \end{Bmatrix}$$

where the rectangular matrix on the right side of the equation is the desired lift interpolating matrix.

Although linear interpolation is by far the simplest type, the results obtained with it are not so accurate as a higher-order interpolation procedure. Parabolic interpolation should be satisfactory for the angle-of-attack matrix and for most of the lift-distribution matrix, except near the wing tip. The numerical factors required for parabolic interpolation can be calculated by means of Lagrange's interpolation formula for an m th degree polynomial

$$f(y^*_n) = \sum_{k=1}^{m+1} f(y^*_k) \frac{\prod_{i=1}^{m+1} (y^*_n - y^*_i)}{\prod_{i=1}^{m+1} (y^*_k - y^*_i)}$$

where $f(y^*)$ represents either the lift or the angle-of-attack distribution, y^*_n is the station at which $f(y^*)$ is to be determined by interpolation, and y^*_1, y^*_2, \dots are the stations at which $f(y^*)$ is presumed to be known. The prime mark on the product signs is the conventional designation of the fact that the term for $i=k$ is to be omitted. For parabolic interpolation ($m=2$) this formula reduces to

$$f(y^*_n) = f(y^*_1) \frac{(y^*_n - y^*_2)(y^*_n - y^*_3)}{(y^*_1 - y^*_2)(y^*_1 - y^*_3)} + f(y^*_2) \frac{(y^*_n - y^*_1)(y^*_n - y^*_3)}{(y^*_2 - y^*_1)(y^*_2 - y^*_3)} + f(y^*_3) \frac{(y^*_n - y^*_1)(y^*_n - y^*_2)}{(y^*_3 - y^*_1)(y^*_3 - y^*_2)}$$

Near the wing tip the lift distribution cannot be approximated accurately by an ordinary parabola but can be represented instead by a linear superposition of the two functions $(1-y^*)^{1/2}$ and $(1-y^*)^{3/2}$ as suggested by V. M. Falkner. With this approximation the desired interpolating factors for y^* between 0.9239 and 1 are the two elements of the row matrix obtained by postmultiplying the row matrix by the square matrix in the equation

$$\Gamma^*(y^*_n) = [(1-y^*_n)^{1/2} (1-y^*_n)^{3/2}] \begin{bmatrix} 9.652 & -1.223 \\ -126.835 & 63.708 \end{bmatrix} \begin{Bmatrix} \Gamma^*_{0.9308} \\ \Gamma^*_{0.9239} \end{Bmatrix}$$

For $y^*_n=0.96$, for instance, the factors obtained in this manner are 0.9157 and 0.2651, so that

$$\Gamma^*_{0.96} = 0.9157\Gamma^*_{0.9308} + 0.2651\Gamma^*_{0.9239}$$

Lagrange's general interpolation formula can be used for higher-order interpolation ($m>2$), but the effort entailed in calculating the interpolating factors is not generally justified by the increase in accuracy obtainable.

Interpolating factors for α and Γ^* can also be obtained by representing these functions by Fourier series in ϑ . For the lift distribution the trigonometric interpolation formula

$$\Gamma^*(\vartheta_n) = \frac{2}{n+1} \sum_{i=1}^n \Gamma^*(\vartheta_i) \sum_{j=1}^n \sin j\vartheta_i \sin j\vartheta_n$$

can be used, where n is odd and is equal to 15 for the calculations in this report, and where, as in this report, the values

of ϑ_i are at equal increments $\vartheta_i = \frac{i\pi}{n+1}$. For the angle-of-attack distribution this formula is not applicable, because the angle-of-attack distribution cannot be represented accurately by a finite sine series and because the angle-of-attack values are presumed to be given at nonequal increments in ϑ_i . (If they were given at eight equal increments no interpolation would be required.) Although in principle a matrix-inversion method could be based on an expansion of the angle-of-attack distribution in a cosine series, the matrices to be inverted are generally ill-behaved so that the results are likely to be of doubtful accuracy.

DIRECT CALCULATION OF INFLUENCE FUNCTIONS

Relation of Green's functions to the lift distributions due to flap and aileron deflection.—Although the aerodynamic-influence-coefficient matrices discussed in the preceding section have the property that when postmultiplied by the angle-of-attack matrix $\{\alpha\}$ and multiplied by the lift-curve slope they yield the lift-distribution matrix $\{\Gamma^*\}$, their individual elements have no direct physical significance. On the other hand, a structural influence coefficient has the significance that it represents the deformation at one point caused by a unit concentrated force at another point. A corresponding type of aerodynamic influence coefficient would represent the lift at one point y^* due to a "unit concentrated angle of attack" at another point y_o^* . This angle of attack is actually an angle-of-attack distribution represented by a Dirac delta (impulse) function of the distance along the span, that is, a function which, in the limiting case as Δy_o^* approaches zero, is zero everywhere except in the interval $y_o^* \leq y^* \leq y_o^* + \Delta y_o^*$ where the ordinate is equal to $\frac{1}{\Delta y_o^*}$; the area under this function would always be 1, which justifies the use of the term "unit" in connection with this distribution. The desired influence coefficients would then be the values (at various values of y^*) of the lift distributions due to these angle-of-attack distributions for various values of y_o^* .

The desired lift distributions, which constitute Green's function for Weissinger's integral equation, can be obtained as follows. Let $\Gamma^*(y^*, y_o^*)$ be the lift distribution for a unit effective deflection of a flap which is located between $y^* = y_o^*$ and $y^* = 1$. Then the lift distribution for an angle-of-attack distribution for which the angle of attack is zero everywhere except in the interval $y_o^* \leq y^* \leq y_o^* + \Delta y_o^*$, where it is $\frac{1}{\Delta y_o^*}$ is given by

$$\frac{\Gamma^*(y^*, y_o^*) - \Gamma^*(y^*, y_o^* + \Delta y_o^*)}{\Delta y_o^*}$$

The lift distribution corresponding to the unit concentrated angle-of-attack distribution, therefore, is the limit of this expression as Δy_o^* approaches zero, which is $-\frac{\partial \Gamma^*(y^*, y_o^*)}{\partial y_o^*}$ by definition. For any given angle-of-attack distribution the lift distribution can be determined by linear superposition

of lift distributions of the Green's function type as follows:

$$\Gamma^*(y^*) = - \int_{-1}^1 \alpha(y_o^*) \frac{\partial \Gamma^*(y^*, y_o^*)}{\partial y_o^*} dy_o^* \quad (2)$$

The desired Green's function can thus be obtained by calculating $\Gamma^*(y^*, y_o^*)$ and taking its partial derivative with respect to y_o^* . A more convenient approach, however, is to consider symmetric and antisymmetric loadings separately. By a repetition of the preceding argument the following results are then obtained:

$$\Gamma_{s'}^*(y^*) = \int_0^1 \alpha_s(y_o^*) \frac{\partial \Gamma_{s'}^*(y^*, y_o^*)}{\partial y_o^*} dy_o^* \quad (3)$$

$$\Gamma_{a'}^*(y^*) = - \int_0^1 \alpha_a(y_o^*) \frac{\partial \Gamma_{a'}^*(y^*, y_o^*)}{\partial y_o^*} dy_o^* \quad (4)$$

where, as elsewhere in this report, Γ^* is the lift distribution (as a function of y^*) for an inboard flap extending over the interval $-y_o^* \leq y^* \leq y_o^*$, and $\Gamma_{a'}$ is the lift distribution for outboard ailerons extending over the intervals $y_o^* \leq |y^*| \leq 1$. The argument y_o^* in $\alpha(y_o^*)$ can be regarded simply as a variable of integration corresponding to y^* .

The desired Green's function can thus be obtained from the flap and aileron distributions given herein by differentiation with respect to y_o^* . The results presented in parts (c) and (d) of figures 1 to 20 can, for instance, be cross-plotted as functions of y_o^* ($y_o^* = \frac{b_f}{b}$ for symmetrical loadings, and $y_o^* = 1 - \frac{b_{a'1}}{b}$ for antisymmetrical loadings) for given values of y^* and the differentiation then performed graphically or numerically. These procedures, however, are tedious and relatively inaccurate. Two procedures which avoid differentiation of the lift distributions are therefore presented in the following sections; one consists in calculating the desired Green's functions directly, and the other consists in using derivatives of the angle-of-attack distribution, so that the flap and aileron distributions themselves are then the required Green's functions.

Direct calculation of Green's functions.—Inasmuch as the desired Green's functions are lift distributions corresponding to angle-of-attack distributions defined by delta functions, they can be calculated directly provided the singularities in the angle-of-attack and lift distributions are taken into account. Appendix B of this report describes the method by which the singularities in the flap-type and aileron-type angle-of-attack and lift distributions were taken into account. This method is extended to the case of impulse-type angle-of-attack distributions in appendix C. The resulting lift distributions $\Gamma_{s'}$ and $\Gamma_{a'}$ are identical with the Green's functions $\frac{\partial \Gamma_{s'}^*(y^*, y_o^*)}{\partial y_o^*}$ and $\frac{\partial \Gamma_{a'}^*(y^*, y_o^*)}{\partial y_o^*}$.

CALCULATION OF INFLUENCE COEFFICIENTS FROM GREEN'S FUNCTION

The lift distributions $\Gamma_{s'}$ and $\Gamma_{a'}$ contain logarithmic singularities at $y_o^* = y^*$ which must be split off before the

integrals in equations (3) and (4) can be evaluated numerically. Thus, if properly weighted influence coefficients are to be calculated from these influence functions, a procedure similar to the following must be used. For the symmetric case and a given value of y^* ,

$$\Gamma_{s_1}^*(y^*) = \int_0^1 [\alpha_s(y_o^*) - \alpha_s(y^*)] \Gamma_{s_1}'(y^*, y_o^*) dy_o^* + \alpha_s(y^*) \int_0^1 \Gamma_{s_1}'(y^*, y_o^*) dy_o^* \quad (5)$$

The first integral does not contain any singularity; the integrand is zero at $y_o^* = y^*$. The second integral can be evaluated explicitly and is

$$\alpha_s(y^*) \Gamma_{s_1}^*(y^*)$$

where $\Gamma_{s_1}^*(y^*)$ is the lift distribution for $\alpha=1$ over the entire span, so that the right side of equation (5) can be evaluated numerically without difficulty by using any set of integrating factors appropriate to the stations of interest, such as those of Simpson's rule if the points are equally spaced and the number of intervals between $y^*=0$ and $y^*=1$ is even.

If these integrating factors are written in the form of a diagonal matrix and designated by $[I]$, equation (5) can be written as

$$\Gamma_{s_1}^*(y^*) = [\Gamma_{s_1}'(y^*, y_o^*)] [I] \{ \alpha_s(y_o^*) - \alpha_s(y^*) \} + \alpha_s(y^*) \Gamma_{s_1}^*(y^*) \quad (6)$$

Now, if the row matrix $[1_{y^*}]$ is defined as

$$[1_{y^*}] \equiv [0 \ 0 \ 0 \ 0 \ 0 \ 1 \ 0 \ 0 \ \dots \ 0]$$

with the element 1 at the position corresponding to y^* and zeros elsewhere, if the matrix $[1_{y^*}]$ is defined as a square matrix all the rows of which are equal to $[1_{y^*}]$, and if $[1]$ represents the unit matrix, then

$$\Gamma_{s_1}^*(y^*) = [\Gamma_{s_1}'(y^*, y_o^*)] [I] \{ [1] - [1_{y^*}] \} \{ \alpha_s(y_o^*) \} + \Gamma_{s_1}^*(y^*) [1_{y^*}] \{ \alpha_s(y_o^*) \} \\ = [\Gamma_{s_1}'(y^*, y_o^*)] [I] \{ [1] - [1_{y^*}] \} \{ \alpha_s(y_o^*) \} \\ \text{or} \\ \Gamma_{s_1}^*(y^*) = C_{L\alpha} [Q_s]_{y^*} \{ \alpha_s(y_o^*) \} \quad (7)$$

where the matrix $[Q_s]_{y^*}$ defined by

$$[Q_s]_{y^*} \equiv \left[\frac{\Gamma_{s_1}^*(y^*)}{C_{L\alpha}} [1_{y^*}] + \left[\frac{\Gamma_{s_1}'(y^*, y_o^*)}{C_{L\alpha}} \right] [I] \{ [1] - [1_{y^*}] \} \right] \quad (8)$$

is the row matrix corresponding to y^* of the desired influence-coefficient matrix $[Q_s]$. The values of $\frac{\Gamma_{s_1}^*(y^*)}{C_{L\alpha}}$ can be obtained directly from the curves labeled "Constant" of parts (a) or the curves for $\frac{b_{at}}{b}=1.0$ of parts (c) of figures 1 to 20, and the calculation of $\frac{\Gamma_{s_1}'(y^*, y_o^*)}{C_{L\alpha}}$ is described in appendix C.

This calculation must be repeated for all other values of y^* to obtain Q_s , so that, finally

$$[Q_s] = \left[\frac{\Gamma_{s_1}^*(y^*)}{C_{L\alpha}} \right] + \left[\frac{\Gamma_{s_1}'(y^*, y_o^*)}{C_{L\alpha}} \right] [I] - [\sum_s] \quad (9)$$

where $[\sum_s]$ is a diagonal matrix in which the elements are the sums of the elements in the rows of the matrix

$$\left[\frac{\Gamma_{s_1}'(y^*, y_o^*)}{C_{L\alpha}} \right] [I]$$

Similarly, for an antisymmetric distribution the singularity can be split off in several ways, one of them being the following. For a given value of y^* equation (4) can be written as

$$\Gamma_{a_1}^*(y^*) = \int_0^1 [\alpha_a(y_o^*) - \alpha_a(y^*)] \Gamma_{a_1}'(y^*, y_o^*) dy_o^* - \alpha_a(y^*) \Gamma_{a_1}^*(y^*)$$

where $\Gamma_{a_1}^*(y^*)$ is the lift distribution for a unit effective displacement of a full-span aileron. In matrix notation this relation may be written as

$$\Gamma_{a_1}^*(y^*) = C_{i_d} [Q_a]_{y^*} \{ \alpha_a(y_o^*) \} \quad (10)$$

where

$$[Q_a]_{y^*} = \left[-\frac{\Gamma_{a_1}^*(y^*)}{C_{i_d}} [1_{y^*}] + \left[\frac{\Gamma_{a_1}'(y^*, y_o^*)}{C_{i_d}} \right] [I] \{ [1] - [1_{y^*}] \} \right] \quad (11)$$

The values of $\frac{\Gamma_{a_1}^*(y^*)}{C_{i_d}}$ can be obtained from the curves for

$\frac{b_{at}}{b}=1.0$ of parts (d) of figures 1 to 20. This procedure must again be repeated for each value of y^* to obtain all the rows of $[Q_a]$, with the result that

$$[Q_a] = - \left[\frac{\Gamma_{a_1}^*(y^*)}{C_{i_d}} \right] + \left[\frac{\Gamma_{a_1}'(y^*, y_o^*)}{C_{i_d}} \right] [I] - [\sum_a] \quad (12)$$

where the diagonal matrix $[\sum_a]$ consists of the sums of the elements of the rows of the matrix

$$\left[\frac{\Gamma_{a_1}'(y^*, y_o^*)}{C_{i_d}} \right] [I]$$

In order to indicate the extent of the effort involved in calculating these influence-coefficient matrices, a step-by-step summary of these calculations is given for $[Q_s]$; with the obvious modifications this procedure also applied to $[Q_a]$. In the first six steps Green's functions are calculated in accordance with the procedure indicated in appendix C; in the remaining steps $[Q_s]$ is calculated in accordance with the previous discussion in this section.

(1) For the values of $\theta_o \equiv \cos^{-1} y_o^*$ of interest, the values of $\sin n\theta_o$ (for $n=1, 3, 5, \dots, 15$) are obtained from trigonometric tables and assembled in a matrix $\{ \sin n\theta_o \}$.

(2) This matrix is premultiplied by the matrix $[\cos n\theta]^{-1}$. (See table VI.)

(3) The resulting matrix is premultiplied by the matrix $[F_a]$ containing the elements $F(\eta^*, y^*)$ defined in appendix A. The evaluation of this $[F_a]$ matrix is probably the most time-consuming part of the calculation because it does not lend itself very readily to high-speed automatic computation. For any one of the nineteen plan forms considered in this report, the matrices $2[F_a]$ and $2[F_s]$ are available upon request from the National Advisory Committee for Aeronautics.

(4) The resulting matrix is premultiplied by the matrix $[Q_a]$ given in the present report for the plan form of concern, and the matrix obtained in this manner is multiplied by the constant $1/\pi$.

(5) The values of $\Gamma_{s,D}^*$ are calculated from equation (C3) for the given values of θ_0 and for $\vartheta \equiv \frac{n\pi}{16}$, $n=1, 2, \dots, 8$; they are then divided by $C_{L\alpha}$ and assembled in a matrix $\left[\frac{\Gamma_{s,D}^*}{C_{L\alpha}} \right]$ the columns of which pertain to given values of θ_0 .

(6) The matrices obtained in steps (4) and (5) are added to obtain the matrix $\left[\frac{\Gamma_{s'}^*}{C_{L\alpha}} \right]$.

(7) Values of $\frac{\Gamma_{s_1}^*(y^*)}{C_{L\alpha}}$ are obtained by reading the values of $\frac{cc_i}{cC_{L\alpha}}$ at y^* defined by $y^* \equiv \cos \frac{n\pi}{16}$, $n=1, 2, \dots, 8$, from figures 2 to 20 for a constant value of α and multiplying them by $\frac{2}{A}$; these values are assembled in a diagonal matrix $\left[\frac{\Gamma_{s_1}^*(y^*)}{C_{L\alpha}} \right]$.

(8) The matrix obtained in step (6) is postmultiplied by the diagonal matrix of integrating factors $[I]$.

(9) The diagonal matrix $[\Sigma_s]$ is assembled from elements calculated by adding the elements in a given row of the matrix obtained in step (8).

(10) The matrices obtained in steps (7) and (8) are added to each other and that obtained in step (9) is subtracted from the sum. The resulting matrix is the desired matrix $[Q_s]$, as defined in equation (9).

The entire calculation thus involves the calculation of $8P$ values of $\frac{\sin n\theta_0}{\pi}$ and of $\Gamma_{s,D}^*$ (P being the number of stations y_0^*), four matrix multiplications, and three matrix additions, as well as the calculation of the 64 elements of the matrix $[F_a]$, if this matrix is not available.

INFLUENCE FUNCTIONS AND COEFFICIENTS FOR THE SPANWISE
DERIVATIVE OF THE ANGLE-OF-ATTACK DISTRIBUTION

Equation (3) can be integrated by parts to yield

$$\Gamma_{s'}^*(y^*) = \alpha_s(1) \Gamma_{s'}^*(y^*, 1) - \int_0^1 \frac{\partial \alpha_s(y_0^*)}{\partial y_0^*} \Gamma_{s'}^*(y^*, y_0^*) dy_0^* \quad (13)$$

where $\Gamma_{s'}^*(y^*, 1)$ is the lift distribution for a unit effective deflection of a full-span flap. Similarly, integrating equation (4) by parts yields

$$\Gamma_a^*(y^*) = \int_0^1 \frac{\partial \alpha_a(y_0^*)}{\partial y_0^*} \Gamma_{att}^*(y^*, y_0^*) dy_0^* \quad (14)$$

Here again the argument y_0^* in $\alpha(y_0^*)$ is merely a variable of integration, corresponding to y^* . In these equations the lift distributions $\Gamma_{s'}$ and Γ_{att}^* themselves serve as the influence, or Green's, functions. Neither these influence functions nor, in most cases of interest, the functions $\frac{\partial \alpha(y_0^*)}{\partial y_0^*}$ have singularities in the range of integration, so that the numerical evaluation of the integrals of equations (13) and (14), and hence, the calculation of weighted influence coefficients, can be effected very readily as follows.

With a set of integrating factors $[I]$ for the stations of interest and the identity $\alpha_s(1) = \alpha_s(0) + \int_0^1 \frac{\partial \alpha_s(y_0^*)}{\partial y_0^*} dy_0^*$, equation (13) can be written as

$$\{\Gamma_{s'}^*(y^*)\} = \alpha_s(0) \{\Gamma_{s'}^*(y^*, 1)\} + \{[\Gamma_{s'}^*(y^*, 1)] - [\Gamma_{s'}^*(y^*, y_0^*)]\} [I] \left\{ \frac{\partial \alpha_s(y_0^*)}{\partial y_0^*} \right\} \quad (15)$$

where $[\Gamma_{s'}^*(y^*, 1)]$ is a matrix all the columns of which are equal to the column matrix $\{\Gamma_{s'}^*(y^*, 1)\}$, and $[I]$ is the diagonal matrix consisting of the integrating factors. Equation (15) can be rewritten in terms of a new influence-coefficient matrix $[Q'_s]$ defined by

$$[Q'_s] \equiv \left[\left[\frac{\Gamma_{s'}^*(y^*, 1)}{C_{L\alpha}} \right] - \left[\frac{\Gamma_{s'}^*(y^*, y_0^*)}{C_{L\alpha}} \right] \right] [I] \quad (16)$$

as

$$\{\Gamma_{s'}^*(y^*)\} = \alpha_s(0) \{\Gamma_{s'}^*(y^*, 1)\} + C_{L\alpha} [Q'_s] \left\{ \frac{\partial \alpha_s(y_0^*)}{\partial y_0^*} \right\} \quad (17)$$

Similarly, with a new influence-coefficient matrix $[Q'_a]$ defined by

$$[Q'_a] \equiv \left[\frac{\Gamma_{att}^*(y^*, y_0^*)}{C_{i_d}} \right] [I] \quad (18)$$

equation (14) can be written as

$$\{\Gamma_a^*(y^*)\} = C_{i_d} [Q'_a] \left\{ \frac{\partial \alpha_a(y_0^*)}{\partial y_0^*} \right\} \quad (19)$$

The matrices $[Q'_s]$ and $[Q'_a]$ are based on the assumption that $\frac{\partial \alpha(y_0^*)}{\partial y_0^*}$ is nonsingular and continuous. However, this assumption is violated when α_s is discontinuous. Discontinuities in α result from control-surface deflection or from deflection of parts of the wing relative to the rest of the wing and can be treated in the manner indicated in appendix B or, more simply, by superposition of the lift distributions given in figures 1 to 20. In the angle-of-attack distributions for which influence coefficients are particularly useful, namely those due to structural deformations, discontinuities cannot occur.

Discontinuities in $\frac{\partial \alpha(y_0^*)}{\partial y_0^*}$ can arise if simple beam theory is used for wings with discontinuous stiffness distributions. Actually this theory is inapplicable for such wings, and the spanwise slope of the twist is never discontinuous. If, however, simple-beam theory is to be used anyway for the sake of convenience and because the errors involved are

considered to be acceptable, then the matrices $[Q'_s]$ and $[Q'_a]$ can still be used provided one of the stations is located at the point of the discontinuity in the stiffness distribution and provided suitable integrating factors are used.

The objection may be raised against the influence-coefficient matrices $[Q'_s]$ and $[Q'_a]$ that they do not actually express the lift distribution in terms of the angle-of-attack distribution but rather require its derivative. Inasmuch as the angle-of-attack distribution can always be reduced to a continuous one by splitting off the discontinuous part and treating it as described elsewhere in this report, the derivative of the angle-of-attack distribution can be obtained numerically by using numerical differentiating factors obtained from any text or numerical analysis. These differentiating factors can be assembled into a differentiating matrix which when postmultiplied by the matrix of the angle-of-attack values yields a matrix of values of the spanwise derivative of the angle-of-attack distribution. The matrices $[Q'_s]$ and $[Q'_a]$ can then be postmultiplied by this differentiating matrix in order to obtain new influence-coefficient matrices which express the lift distribution directly in terms of the angle-of-attack distribution. However, the main advantage of the method outlined in this section is that in aeroelastic calculations, for which aerodynamic influence coefficients are primarily intended, the angle-of-attack distribution usually is obtained by integrating its derivative; the use of the derivative then actually saves a calculation.

In such aeroelastic calculations the lift distributions can be considered to consist of a known "rigid wing" part (due to airplane attitude or motion, built-in twist, or control deflection), which can be calculated initially with due regard to all discontinuities, and an initially unknown part due to structural deformation; the matrices $[Q'_s]$ and $[Q'_a]$ can be used to advantage in calculating the latter part. The calculation of $\alpha(y^*)$ can then be obviated altogether, because if the structural deformations are referred to the plane of symmetry the structural part of $\alpha(y^*)$ is zero for $y^*=0$, so that the first term on the right sides of equations (15) and (17) represents a known rigid-wing lift distribution and can be included with the others. Thus, in general,

$$\{\Gamma^*\} = \{\Gamma^*\}_{\text{rigid wing}} + C_{L\alpha} [Q'] \left\{ \frac{\partial \alpha_{\text{structural}}(y_o^*)}{\partial y_o^*} \right\}$$

The separate treatment of these two parts in an aeroelastic analysis presents no difficulties and can be effected in a manner similar to that employed in reference 4 for the lift distribution due to aileron deflection; the use of $[Q']$ rather than $[Q]$ requires only the omission of one of the integrating matrices in the methods of references 2 and 4.

DISCUSSION

GENERAL LIMITATIONS OF THE RESULTS OF THIS REPORT

The Weissinger L-method, its range, and validity have been discussed in several previous papers (for example, refs. 3 and 5) so that in this section only a few comments are made about special applications.

Number of control points.—In references 1 and 5, four control points on the semispan were found to give satisfactory accuracy for the lift distributions due to constant angle of attack. In the present report, interest is centered primarily

on the lift distributions due to twist and control deflection, and for these cases the additional effort entailed in using eight rather than four control points was believed to be warranted by the resulting increase in accuracy.

Fuselage, nacelle, and tip-tank interference.—The Weissinger method and all results presented apply only to wings without fuselages, nacelles, or tip tanks. At low angles of attack the lift distribution on the wing is not affected to a large extent by the presence of the fuselage except when it covers a large part of the wing; the effect is largely localized near the wing root and is most pronounced for the constant angle-of-attack and flap-deflected cases. For the lift distributions due to twist and aileron deflection the presence of the fuselage can probably be ignored in most cases.

Nacelles also tend to affect the lift distribution primarily in their own vicinity, but these effects may be significant even for the lift distributions due to twist and aileron deflection. Tip tanks tend to increase the lift over much of the outer part of the wing to a large extent, particularly in the case of lift distributions due to twist and aileron deflection. Except for wings with very high or very low aspect ratio, these effects can hardly be underestimated and must be taken into account in designing the wing.

High angles of attack.—Potential flow breaks down at high angles of attack and the higher the Mach number the lower the angle of attack at which linearized potential-flow theories, such as the one employed in this report, fail to predict the lift distributions accurately. However, the critical design loads often occur at high angles of attack. The only suggestion that can be made is that once the rigid-wing lift distributions at high angles of attack are estimated on the basis of tests or experience, the changes in these distributions due to aeroelastic effects can be estimated by means of the results calculated in this report. This procedure cannot be justified theoretically because, although the nature of the mutual induction effects between various parts of the wing after the flow has separated is still substantially the same as before; the lifts caused by these induction effects are not those predicted by potential-flow theory. However, the changes due to aeroelastic action are small unless the speed is near the flutter or divergence speed, so that certain inaccuracies can usually be tolerated in estimating them.

Longitudinal location of the center of pressure.—The Weissinger theory yields no information regarding the location of the chordwise center of pressure; however, the assumption that at each spanwise station the section center of pressure of the angle-of-attack loading on the two-dimensional airfoil section is unchanged in three-dimensional flow has been found by lifting-surface calculations (ref. 6, for example) to be largely justified for swept and unswept wings of moderate and high aspect ratio (except near the root and tip). If this assumption is used, the longitudinal location of the wing center of pressure may be estimated. For low-aspect-ratio wings, the chordwise location of the center of pressure cannot be determined simply, and lifting-surface methods must be used. For flap and aileron deflections, accurate theoretical methods for calculating the longitudinal location of the center of pressure are not available, but the approximate methods suggested in reference 7 may be applied to obtain qualitative information.

Effective angle of attack for flap deflection.—In order to determine the loading due to flap deflection for wings of high and medium aspect ratio (for example, $A > 4$), the effective angle of attack α_s for the flap (or aileron) deflection may be approximated satisfactorily by the values obtained from two-dimensional thin-airfoil theory. Figure 21 gives a plot of the effective angle of attack α_s against flap-chord ratio c_f/c . For very low aspect ratios (approaching 0 and certainly less than 1/2) values of α_s close to 1 are indicated by linearized potential-flow theory, even for relatively small values of c_f/c . For aspect ratios from about 1/2 to 4, lifting-surface methods must be used to obtain potential-flow solutions for the lift distributions due to partial-chord control deflections.

Calculation of the roll due to sideslip $C_{l\beta}$.—The loading for the case of full-span ailerons $\frac{b_{att}}{b} = 1$ is the same as the loading on a wing with dihedral in yaw or sideslip, because in this case the loading on the wing is that due to an angle of attack equal to the product of the sideslip angle and dihedral angle on one wing, and the negative of that angle of attack on the other wing. The values of $C_{l\beta}$ given in table IV for the case of full-span aileron deflection are therefore equivalent to the parameter $C_{l\beta}$.

Some other stability derivatives can be deduced similarly from the results presented in this report.

RELATIVE MERITS OF THE VARIOUS TYPES OF AERODYNAMIC INFLUENCE COEFFICIENTS

In this report four types of aerodynamic influence coefficients have been discussed:

(1) The influence-coefficient matrices presented in table V which are obtained by solving Weissinger's integral equation by numerical methods

(2) Influence-coefficient matrices obtained from those of table V by multiplying them by interpolating matrices

(3) Influence coefficients based on Green's function

(4) Influence coefficients based on flap-type and aileron-type lift distributions, which express the lift distribution in terms of the spanwise derivative of the angle-of-attack distribution rather than the distribution itself.

The influence coefficients given in table V apply to the stations $y^* = 0.9808, 0.9239, 0.8315, 0.7071, 0.5556, 0.3827, 0.1951, \text{ and } 0$. If these stations can be used in the calculations in which the influence coefficients are to be used, the coefficients given in table V are by far the simplest to use because they require no further calculations. If these stations cannot conveniently be used, either the coefficients have to be re-calculated from scratch for the desired stations by the method described in appendix A, or, if the results presented herein are to be used, one of the other three types of influence coefficients has to be calculated. Of these two alternatives the first-mentioned is generally the one requiring the greater effort.

The second type of influence coefficients is based on the first and requires a premultiplication of their matrix by a lift interpolating matrix and the postmultiplication of that matrix by an angle-of-attack interpolating matrix. These interpolating matrices serve to relate the lift and angle of attack at the stations of interest to those at the stations specified in the preceding paragraph. The interpolating matrices can be constructed in several ways; parabolic (or possibly cubic) interpolation is probably the most satisfactory choice for the angles of attack, and for the lift distributions either this type of interpolation (with a modification at the wing tip) or trigonometric interpolation should be satisfactory. The calculation of the interpolating factors does not lend itself readily to automatic computation, but the amount of effort involved is relatively small. The two matrix multiplications can then be performed readily on automatic computation machines.

The influence coefficients based on Green's functions are similar in concept to the commonly used structural influence coefficients. The values of the influence functions $\Gamma^{*'}(y^*, y_o^*)$ and $\Gamma^{*'}(y_o^*, y^*)$ are the only aerodynamic influence coefficients discussed herein which individually have physical significance; the first two types of influence coefficients have only a collective physical significance in that they yield the values of the lift when matrix-multiplied by the angle-of-attack values. However, this individual significance of the coefficients based on Green's functions is lost once these coefficients are manipulated in the manner indicated in equations (9) and (12) to obtain aerodynamic influence coefficients useful in further computations, and the resulting influence coefficients have neither more nor less significance than the others. The computation of these coefficients requires a relatively large expenditure of effort—four matrix multiplications and three matrix additions, as well as the computation of many values of $\Gamma^{*'}_D$ or $\Gamma^{*'}_{D^*}$ (by substitution of given values of ϑ and θ_o in eq. (C3)) and a few other minor steps. Despite their conceptual attractiveness, these coefficients are therefore practically at a disadvantage compared with the other much more simply computed influence coefficients.

The influence coefficients based on flap-type and aileron-type lift distributions and on the spanwise derivatives of the angle-of-attack distributions are probably the simplest to compute (with the exception of those presented in table V); they require only the reading of the values of the lift distributions from the figures of this report at the stations of interest and for the flap and aileron spans corresponding to the stations of interest, as well as the multiplication of the matrix of these coefficients by a diagonal matrix. (For a symmetric distribution, a matrix subtraction is also called for.) As previously mentioned, the fact that these coefficients express the lift distribution in terms of the derivative of

the angle-of-attack distribution need not be a disadvantage and may actually be an advantage. The decision as to whether to use the second or the fourth type of influence coefficients (once the decision has been made that the stations implied in the first type are unsuitable) then becomes largely a matter of individual preference, guided by decisions in any given case as to the relative convenience of calculating interpolating factors or reading values from the figures in this report, and of using angle-of-attack distributions or their derivatives.

CONCLUDING REMARKS

Spanwise lift distributions have been calculated for nineteen unswept wings with various aspect ratios and taper ratios and with a variety of angle-of-attack or twist distributions, including aileron and flap deflections, by means of

Weissinger's method with eight control points on the semi-span. Also calculated by this method were aerodynamic influence coefficients which pertain to a certain definite set of stations on the span. Three methods for calculating aerodynamic influence functions and coefficients for arbitrary stations have been outlined and their relative merits discussed.

The information presented herein can be used in the analysis of untwisted wings or wings with known twist distributions, as well as in aeroelastic calculations involving initially unknown twist distributions.

LANGLEY AERONAUTICAL LABORATORY,
 NATIONAL ADVISORY COMMITTEE FOR AERONAUTICS,
 LANGLEY FIELD, VA., May 5, 1958.

APPENDIX A

MATRIX FORMULATION OF THE WEISSINGER METHOD

CALCULATION OF THE LIFT DISTRIBUTION AND INFLUENCE COEFFICIENTS

From two-dimensional thin-airfoil theory it can be shown that, if all the vorticity of a plane or parabolically cambered airfoil section is concentrated at the quarter-chord line, the downwash angle induced at the three-quarter-chord line is equal to the geometric angle of attack at the three-quarter-chord line. This circumstance leads to the Weissinger L-method in which the lifting vortex is concentrated at the quarter-chord line and the boundary conditions are satisfied at the three-quarter-chord line. The Weissinger equation (ref. 1) can be written as

$$\alpha(y^*) = \frac{1}{4\pi} \int_{-1}^1 \frac{d\Gamma^*(\eta^*)}{d\eta^*} \frac{d\eta^*}{y^* - \eta^*} + \frac{1}{8\pi} \int_{-1}^1 F(\eta^*, y^*) \frac{d\Gamma^*(\eta^*)}{d\eta^*} d\eta^* \quad (A1)$$

where

$$F(\eta^*, y^*) = \frac{1}{y^* - \eta^*} \left\{ \sqrt{\left[1 + \tan \Lambda \left(\frac{y^* - \eta^*}{c^*/2}\right)\right]^2 + \left(\frac{y^* - \eta^*}{c^*/2}\right)^2} - 1 \right\} \quad (\eta^* \geq 0)$$

$$= \frac{1}{y^* - \eta^*} \left\{ \frac{\sqrt{\left[1 + \tan \Lambda \left(\frac{y^* + \eta^*}{c^*/2}\right)\right]^2 + \left(\frac{y^* - \eta^*}{c^*/2}\right)^2}}{1 + 2 \tan \Lambda \frac{y^*}{c^*/2}} - 1 \right\} +$$

$$\frac{2 \tan \Lambda}{c^*/2} \frac{\sqrt{\left[1 + \frac{y^*}{c^*/2} \tan \Lambda\right]^2 + \left(\frac{y^*}{c^*/2}\right)^2}}{1 + 2 \tan \Lambda \frac{y^*}{c^*/2}} \quad (\eta^* \leq 0)$$

and α is the angle of attack or, more specifically, the streamwise slope of the mean-camber surface at the three-quarter-chord line.

Introduction of the trigonometric variables $\theta \equiv \cos^{-1} y^*$ and $\vartheta \equiv \cos^{-1} \eta^*$ into equation (A1) yields

$$\alpha(\theta) = \frac{1}{4\pi} \int_0^\pi \frac{d\Gamma^*(\vartheta)}{d\vartheta} \frac{d\vartheta}{\cos \vartheta - \cos \theta} - \frac{1}{8\pi} \int_0^\pi F(\vartheta, \theta) \frac{d\Gamma^*(\vartheta)}{d\vartheta} d\vartheta \quad (A2)$$

The solution of equation (A2) is effected in reference 1 by the use of trigonometric interpolation and integration formulas. An alternate solution based on matrix techniques is presented herein which leads to the identical results somewhat more simply and suggests a fairly simple setup for routine calculations.

The function Γ^* is approximated by a finite sine series, as in reference 1, so that for any value ϑ_m

$$\Gamma^*_m = \sum_n a_n \sin n\vartheta_m \quad (A3)$$

or

$$\{\Gamma^*_m\} = [\sin n\vartheta_m] \{a_n\} \quad (A4)$$

In the calculations of this report, the values of n in equation (A4) have been chosen as $n=1, 3, 5, \dots, 15$ for the symmetrical loadings and $n=2, 4, 6, \dots, 14$ for the antisymmetrical loadings; values of ϑ_m were chosen at

$$\vartheta_m = \frac{m\pi}{16}$$

with $m=1, 2, 3, \dots, 8$ for the symmetrical loadings and $m=1, 2, 3, \dots, 7$ for the antisymmetrical loadings. The use of equal increments in ϑ is essential in the method of reference 1, but any values of ϑ between 0 and $\pi/2$ could have been chosen in the matrix analysis used in the present report. This possibility of using arbitrary stations in this matrix version of Weissinger's method is an important

advantage in that it allows the direct calculation of influence coefficients for arbitrary stations. Such a calculation is complicated, however, by the fact that some of the matrices which must be inverted may be ill-behaved when nonequal increments are chosen for ϑ .

The value of $\frac{d\Gamma^*(\vartheta)}{d\vartheta}$ required in equation (A2) can be obtained from equation (A3) as

$$\frac{d\Gamma_m^*}{d\vartheta} = \sum_n n a_n \cos n\vartheta_m \quad (A5)$$

so that the first term of equation (A2) becomes

$$\frac{1}{4\pi} \int_0^\pi \frac{\sum_n n a_n \cos n\vartheta_m d\vartheta}{\cos \vartheta - \cos \theta_m} = \frac{1}{4} \sum_n n a_n \frac{\sin n\theta_m}{\sin \theta_m}$$

or, in matrix notation,

$$\left\{ \frac{1}{4\pi} \int_0^\pi \frac{d\Gamma_m^*}{d\vartheta} \frac{d\vartheta}{\cos \vartheta - \cos \theta_m} \right\} = \frac{1}{4} \begin{bmatrix} \sin n\theta_m \\ \sin \theta_m \end{bmatrix} [n] \{a_n\}$$

The values of a_n can be expressed in terms of Γ_m^* (see eq. (A4)) as

$$\{a_n\} = [\sin n\vartheta_m]^{-1} \{\Gamma_m^*\} \quad (A6)$$

so that

$$\left\{ \frac{1}{4\pi} \int_0^\pi \frac{d\Gamma_m^*}{d\vartheta} \frac{d\vartheta}{\cos \vartheta - \cos \theta_m} \right\} = [B_m] \{\Gamma_m^*\}$$

where

$$[B_m] = \frac{1}{4} \begin{bmatrix} \sin n\theta_m \\ \sin \theta_m \end{bmatrix} [n] [\sin n\vartheta_m]^{-1} \quad (A7)$$

The matrices $\begin{bmatrix} \sin n\theta_m \\ \sin \theta_m \end{bmatrix} [n]$, $[\sin n\theta_m]$, $[\sin n\theta_m]^{-1}$, and $[B_m]$ are given in table VII(a) for the symmetrical distributions and table VII(b) for the antisymmetrical distributions. As a result of the orthogonality of the sine function, the inverse of the $[\sin n\theta_m]$ matrix is the same as one-fourth its transpose except for the first and last rows. (See, for instance, ref. 8.)

The second term of equation (A2) can be integrated numerically by approximating either F or $F \frac{d\Gamma^*}{d\vartheta}$ by a cosine series. Both approximations will yield identical results, and the latter alternative is followed here. Thus let

$$F(\vartheta, \theta) \frac{d\Gamma^*(\vartheta)}{d\vartheta} = \sum_n b_n(\theta) \cos n\vartheta$$

so that

$$\frac{1}{8\pi} \int_0^\pi F(\vartheta, \theta) \frac{d\Gamma^*(\vartheta)}{d\vartheta} d\vartheta = \frac{b_0(\theta)}{8} \quad (A8)$$

Now, in matrix notation,

$$\left\{ F \frac{d\Gamma^*}{d\vartheta} \right\} = [\cos n\vartheta] \{b_n(\vartheta)\}$$

so that

$$b_0(\theta) = [[\cos n\vartheta]^{-1}]_0 \left\{ F \frac{d\Gamma^*}{d\vartheta} \right\} \\ = [F(\vartheta, \theta)] [I_1] \left\{ \frac{d\Gamma^*}{d\vartheta} \right\}$$

where $[[\cos n\vartheta]^{-1}]_0$ is the first row of the inverse of the matrix $[\cos n\vartheta]$, that is, the row corresponding to $n=0$, and $[I_1]$ consists of the same elements written in the form of a diagonal matrix.

Inasmuch as the integral of the antisymmetrical component of $F \frac{d\Gamma^*}{d\vartheta}$ is zero, $F \frac{d\Gamma^*}{d\vartheta}$ can be written for symmetrical distributions as

$$F_a \frac{d\Gamma_a^*}{d\vartheta} = \frac{F_R - F_L}{2} \frac{d\Gamma_s^*}{d\vartheta}$$

and, for antisymmetrical distributions, as

$$F_s \frac{d\Gamma_s^*}{d\vartheta} = \frac{F_R + F_L}{2} \frac{d\Gamma_a^*}{d\vartheta}$$

where

$$F_R(|\eta^*|, y^*) = F(\eta^*, y^*) \quad (\eta^* \geq 0) \quad (A9)$$

$$F_L(|\eta^*|, y^*) = F(\eta^*, y^*) \quad (\eta^* \leq 0) \quad (A10)$$

From equations (A5) and (A6) $\frac{d\Gamma^*}{d\vartheta}$ can be expressed in matrix notation as

$$\left\{ \frac{d\Gamma^*}{d\vartheta} \right\} = [\cos n\vartheta] [n] [\sin n\vartheta]^{-1} \{\Gamma^*\}$$

so that equation (A8) can be written for symmetrical distributions as

$$\left\{ \frac{1}{8\pi} \int_0^\pi F_a(\vartheta, \theta_m) \frac{d\Gamma_a^*}{d\vartheta} d\vartheta \right\} = \\ \frac{1}{8} \left[\frac{F_R - F_L}{2} \right] [I_1] [\cos n\vartheta_m] [n] [\sin n\vartheta_m]^{-1} \{\Gamma_s^*\} = 2[F_a] [D_s] \{\Gamma_s^*\} \quad (A11)$$

where

$$[D_s] = \frac{1}{16} [I_1] [\cos n\vartheta_m] [n] [\sin n\vartheta_m]^{-1}$$

Similarly, for antisymmetrical distributions

$$\left\{ \frac{1}{8\pi} \int_0^\pi F_s(\vartheta, \theta_m) \frac{d\Gamma_s^*}{d\vartheta} d\vartheta \right\} = 2[F_s] [D_a] \{\Gamma_a^*\} \quad (A12)$$

where

$$[D_a] = \frac{1}{16} [I_1] [\cos n\vartheta_m] [n] [\sin n\vartheta_m]^{-1}$$

The matrices $[D]$, $[I_1]$, and $[\cos n\theta_m][n]$ are given in table VII (a) for symmetrical distributions and table VII (b) for antisymmetrical distributions.

Equation (A1) (or its equivalent, eq. (A2)) can now be expressed completely in matrix form. For symmetrical distributions, the equation is

$$[[B_s]-2[F_d][D_s]]\{\Gamma^*_s\}=\{\alpha_s\}$$

or

$$[G_s]\{\Gamma^*_s\}=\{\alpha_s\} \quad (A13)$$

and for antisymmetrical distributions,

$$[[B_a]-2[F_s][D_a]]\{\Gamma^*_a\}=\{\alpha_a\}$$

or

$$[G_a]\{\Gamma^*_a\}=\{\alpha_a\} \quad (A14)$$

It should be noted that the $[B]$ and $[D]$ matrices are invariant with plan form and that only the $[F]$ matrices need be computed separately for each plan form; all the matrices are independent of the angle-of-attack conditions. A computing form for the elements of the F matrices is given in table VIII; this computing form includes provision for calculating the load on swept wings. Sample $2[F_d]$ and $2[F_s]$ matrices are shown in table IX.

Equations (A13) and (A14) can be expressed as

$$\{\Gamma^*\}=[G]^{-1}\{\alpha\} \quad (A15)$$

so that the elements of the matrices $[G]^{-1}$ constitute, in effect, sets of aerodynamic influence coefficients. The influence coefficients presented in table V for the plan forms treated in this report are defined as

$$[Q_s] \equiv \frac{1}{C_{L\alpha}} [G_s]^{-1}$$

and

$$[Q_a] \equiv \frac{1}{C_{L\alpha}} [G_a]^{-1}$$

so that

$$\left. \begin{aligned} \{\Gamma^*_s\} &= C_{L\alpha} [Q_s] \{\alpha_s\} \\ \{\Gamma^*_a\} &= C_{L\alpha} [Q_a] \{\alpha_a\} \end{aligned} \right\} \quad (A16)$$

The division by $C_{L\alpha}$ and by $C_{L\alpha}$ has been performed both to facilitate interpolation of the coefficients for unswept wings with plan forms other than those considered in this report and for convenience in aeroelastic calculations. Inasmuch as the lift distribution is much less sensitive to Mach number than is the overall magnitude of the lift, an influence-coefficient matrix $[Q_s]$ or $[Q_a]$ chosen for the average of the subsonic Mach number range of interest (that is, for the effective aspect ratio $A\sqrt{1-M^2}$ corresponding to that average Mach number) will serve for the entire range, provided only that for each Mach number the appropriate values of $C_{L\alpha}$ and $C_{L\alpha}$ are used in equations (A16). (See ref. 9, for instance, for simple methods of estimating Mach number effects on $C_{L\alpha}$ and $C_{L\alpha}$.)

CALCULATION OF THE AERODYNAMIC PARAMETERS ASSOCIATED WITH THE LIFT DISTRIBUTIONS

The values of the lift, induced-drag, bending-moment, and rolling-moment coefficients can be obtained conveniently by the use of the integrating matrices derived in this section.

An integrating matrix for the lift coefficient associated with symmetrical loadings can be obtained as follows:

The lift coefficient can be written as

$$C_L = \frac{A}{2} \int_0^1 \Gamma^*_s dy^*$$

If, as before, $y^* = \cos \theta$ and $\Gamma^*_s = \sum_n a_n \sin n\theta$, with $n=1, 3, 5, \dots, 15$, then

$$\begin{aligned} C_L &= \frac{A}{2} \int_0^{\pi/2} \sum_n a_n \sin n\theta \sin \theta d\theta \\ &= \frac{\pi}{8} A a_1 \end{aligned}$$

or

$$C_L = A [I_{C_L}] \{\Gamma^*_s\}$$

where

$$[I_{C_L}] = \frac{\pi}{8} [[\sin n\theta]^{-1}]_1$$

and $[[\sin n\theta]^{-1}]_1$ is the first row of the matrix $[\sin n\theta_m]^{-1}$ given in table VII(a); the matrix $[I_{C_L}]$ is given in table X.

Similarly, the integration to obtain the bending-moment coefficient for symmetrical loadings C_{BM} can be performed as follows:

The bending-moment coefficient can be written as

$$\begin{aligned} C_{BM} &= \frac{A}{4} \int_0^1 \Gamma^*_s y^* dy^* \\ &= \frac{A}{4} \int_0^{\pi/2} \sum_n a_n \sin n\theta \sin \theta \cos \theta d\theta \\ &= \frac{A}{8} \left(\frac{2}{3} a_1 + \frac{2}{5} a_3 - \frac{2}{21} a_5 + \frac{2}{45} a_7 - \frac{2}{77} a_9 + \right. \\ &\quad \left. \frac{2}{117} a_{11} - \frac{2}{165} a_{13} + \frac{2}{221} a_{15} \right) \end{aligned}$$

or

$$C_{BM} = A [I_{C_{BM}}] \{\Gamma^*_s\}$$

where the matrix

$$[I_{C_{BM}}] \equiv \frac{1}{8} \left[\begin{array}{cccc} \frac{2}{3} & \frac{2}{5} & -\frac{2}{21} & \frac{2}{45} \\ -\frac{2}{21} & \frac{2}{45} & -\frac{2}{77} & \frac{2}{117} \\ \frac{2}{45} & -\frac{2}{77} & \frac{2}{117} & -\frac{2}{165} \\ -\frac{2}{77} & \frac{2}{117} & -\frac{2}{165} & \frac{2}{221} \end{array} \right] [\sin n\theta]^{-1}$$

is given in table X.

For antisymmetrical loadings, the half-wing lift coefficient $C_{L_{1/2}}$ is obtained in the following manner:

The equation for the half-wing lift coefficient is

$$C_{L_{1/2}} = \frac{A}{2} \int_0^1 \Gamma^*_a dy^*$$

and, if $\Gamma^*_a = \sum_n a_n \sin n\theta$, with $n=2, 4, 6, \dots, 14$ as before, then

$$C_{L_{1/2}} = \frac{A}{2} \int_0^{\pi/2} \sum_n a_n \sin n\theta \sin \theta d\theta$$

$$= A \left(\frac{1}{3} a_2 - \frac{2}{15} a_4 + \frac{3}{35} a_6 - \frac{4}{63} a_8 + \frac{5}{99} a_{10} - \frac{6}{143} a_{12} + \frac{7}{195} a_{14} \right)$$

or

$$C_{L_{1/2}} = A [I_{C_{L_{1/2}}}] \{\Gamma^*_a\}$$

where the matrix

$$[I_{C_{L_{1/2}}}] \equiv \left[\frac{1}{3} \quad -\frac{2}{15} \quad \frac{3}{35} \quad -\frac{4}{63} \quad \frac{5}{99} \quad -\frac{6}{143} \quad \frac{7}{195} \right] [\sin n\theta]^{-1}$$

is given in table X.

Similarly, the rolling-moment coefficient can be obtained as follows:

The equation for the rolling-moment coefficient is

$$C_i = \frac{A}{4} \int_0^{\pi/2} \Gamma^*_a y^* dy^*$$

$$= \frac{A}{4} \int_0^{\pi/2} \sum_n a_n \sin n\theta \cos \theta \sin \theta d\theta$$

$$= \frac{\pi}{32} A a_2$$

or

$$C_i = A [I_{C_i}] \{\Gamma^*_a\}$$

where the matrix

$$[I_{C_i}] \equiv \frac{\pi}{32} [(\sin n\theta)^{-1}]_i$$

is given in table X.

The induced-drag coefficient C_{D_i} can be written as

$$C_{D_i} = \frac{A}{2} \int_0^1 \alpha_i \Gamma^*_s dy^*$$

where

$$\alpha_i(y^*) = \frac{1}{8\pi} \int_{-1}^1 \frac{d\Gamma^*_s(\eta^*)}{d\eta^*} \frac{d\eta^*}{y^* - \eta^*}$$

or

$$\{\alpha_i\} = \frac{1}{2} [B_m] \{\Gamma^*_s\}$$

For symmetrical loadings the $[I_{C_i}]$ matrix can be used to integrate the values of $\alpha_i \Gamma^*_s$, so that

$$C_{D_i} = A [I_{C_i}] \{\alpha_i \Gamma^*_s\}$$

An integrating matrix to evaluate C_{D_i} for antisymmetrical distributions can be set up similarly. However, in this report, values of C_{D_i} were calculated only for additional lift distributions.

APPENDIX B

CALCULATION OF LIFT DISTRIBUTIONS FOR DISCONTINUOUS ANGLE-OF-ATTACK CONDITIONS

The method of solving equation (A1) outlined in appendix A relies heavily on numerical integration, as does the method of reference 1. Discontinuous angle-of-attack distributions therefore cannot be analyzed as accurately as continuous ones can, because discontinuous angle-of-attack distributions are known (on the basis of knowledge of the lift distributions of wings with very low and very high aspect ratios presented in ref. 3) to give rise to logarithmic singularities in the function $\frac{d\Gamma^*}{d\eta^*}$ which occurs in the integrands of both integrals in equation (A1). Nor can a discontinuous angle-of-attack distribution be described adequately by a small number of points on the semispan; for instance, with stations located as they are for the calculations described in this report any inboard flap terminating at a value of y^* greater than 0.3827 but less than 0.5556 would, for a unit effective angle-of-attack distribution, be characterized by the angle-of-attack distribution 1, 1, 1, 0, 0, 0, 0, regardless of the exact location of the end of the flap.

These difficulties can be overcome by using the results obtained by solving equation (A1) for the case of wings of vanishingly small aspect ratio (see ref. 3), in which case the second integral vanishes. This technique is similar to the one used by Mulhopp (ref. 10) in connection with the Prandtl lifting-line equation to handle discontinuous angle-of-attack distributions. The lift distribution Γ^* is considered to consist of a "discontinuous" part Γ^*_D which is the solution to equation (A1) if the second term is neglected and of a correcting "continuous" part Γ^*_C , so that

$$\Gamma^* = \Gamma^*_C + \Gamma^*_D \tag{B1}$$

where Γ^*_D is defined implicitly by

$$\alpha = \frac{1}{4\pi} \int_0^{\pi} \frac{d\Gamma^*_D}{d\vartheta} \frac{d\vartheta}{\cos \vartheta - \cos \theta} \tag{B2}$$

and Γ^*_C is the correction that must be added to Γ^*_D to obtain a function Γ^* which satisfied equation (A1) for the given

discontinuous angle-of-attack distribution. The solution of equation (B2) for $\Gamma^*_{D_f}$ corresponding to the more common discontinuous angle-of-attack distributions is given in reference 3; specifically, for inboard flaps terminating at $y^* = y_o^* \equiv \cos^{-1} \theta_o$

$$\Gamma^*_{D_f}(\vartheta, \theta_o) = \frac{4}{\pi} \left[(\pi - 2\theta_o) \sin \vartheta - (\cos \vartheta - \cos \theta_o) \log_e \frac{\sin \frac{\vartheta + \theta_o}{2}}{\sin \frac{|\vartheta - \theta_o|}{2}} - (\cos \vartheta + \cos \theta_o) \log_e \frac{\cos \frac{\vartheta + \theta_o}{2}}{\cos \frac{\vartheta - \theta_o}{2}} \right] \quad (B3)$$

and for outboard ailerons with inner ends at $y^* = y_o^* \equiv \cos^{-1} \theta_o$

$$\Gamma^*_{D_{ait}}(\vartheta, \theta_o) = \frac{4}{\pi} \left[(\cos \vartheta - \cos \theta_o) \log_e \frac{\sin \frac{\vartheta + \theta_o}{2}}{\sin \frac{|\vartheta - \theta_o|}{2}} - (\cos \vartheta + \cos \theta_o) \log_e \frac{\cos \frac{\vartheta + \theta_o}{2}}{\cos \frac{\vartheta - \theta_o}{2}} \right] \quad (B4)$$

If equations (B1) and (B2) are substituted into equation (A2), the result is

$$\frac{1}{4\pi} \int_0^\pi \frac{\partial \Gamma^*_{D_f}(\vartheta, \theta_o)}{\partial \vartheta} \frac{d\vartheta}{\cos \vartheta - \cos \theta} - \frac{1}{8\pi} \int_0^\pi F(\vartheta, \theta) \frac{\partial \Gamma^*_{D_f}(\vartheta, \theta_o)}{\partial \vartheta} d\vartheta = R(\theta, \theta_o) \quad (B5)$$

where the function $R(\theta, \theta_o)$ is defined by

$$R(\theta, \theta_o) \equiv \frac{1}{8\pi} \int_0^\pi F(\vartheta, \theta) \frac{\partial \Gamma^*_{D_f}(\vartheta, \theta_o)}{\partial \vartheta} d\vartheta$$

or, specifically, for flaps

$$R_f(\theta, \theta_o) \equiv \frac{1}{8\pi} \int_0^\pi F_a(\vartheta, \theta) \frac{\partial \Gamma^*_{D_f}(\vartheta, \theta_o)}{\partial \vartheta} d\vartheta \quad (B6a)$$

and for ailerons

$$R_a(\theta, \theta_o) \equiv \frac{1}{8\pi} \int_0^\pi F_s(\vartheta, \theta) \frac{\partial \Gamma^*_{D_{ait}}(\vartheta, \theta_o)}{\partial \vartheta} d\vartheta \quad (B6b)$$

Comparison of equation (B5) with equation (A2) indicates that equation (B5) may be considered to be the Weissinger equation (eq. (A1) or (A2)) for the lift distribution Γ^*_c on the given wing (the plan form of which determines the function $F(\vartheta, \theta)$) corresponding to an angle-of-attack distribution $R(\theta, \theta_o)$. Inasmuch as $R(\theta, \theta_o)$ is a continuous function, as is

demonstrated presently, equation (B5) can be solved in the manner used for equation (A2). If $R(\theta, \theta_o)$ is being evaluated at the stations considered in this report ($\theta = \frac{\pi}{16}, 2 \frac{\pi}{16}, 3 \frac{\pi}{16}, \dots, \frac{\pi}{2}$), and if the eight values of R are listed in a column in the order of increasing θ , then premultiplication of this column by the matrix $[Q]$ given in this report and by the appropriate value of C_{L_α} yields the desired function Γ^*_c for the given discontinuous angle-of-attack distribution.

As indicated in equations (B6), the function $R(\theta, \theta_o)$ depends on the plan form, which determines $F(\vartheta, \theta)$, and on the position of the discontinuity in the angle-of-attack distribution, which determines $\Gamma^*_{D_f}$ and, hence, $\frac{\partial \Gamma^*_{D_f}(\vartheta, \theta)}{\partial \vartheta}$.

For flaps and ailerons,

$$\frac{\partial \Gamma^*_{D_f}}{\partial \vartheta} = \frac{4}{\pi} \left[(\pi - 2\theta_o) \cos \vartheta + \sin \vartheta \left(\log_e \frac{\sin \frac{\vartheta + \theta_o}{2}}{\sin \frac{|\vartheta - \theta_o|}{2}} + \log_e \frac{\cos \frac{\vartheta + \theta_o}{2}}{\cos \frac{\vartheta - \theta_o}{2}} \right) \right] \quad (B7a)$$

and

$$\frac{\partial \Gamma^*_{D_{ait}}}{\partial \vartheta} = \frac{4}{\pi} \left[2 \sin \theta_o + \sin \vartheta \left(\log_e \frac{\cos \frac{\vartheta + \theta_o}{2}}{\cos \frac{\vartheta - \theta_o}{2}} - \log_e \frac{\sin \frac{\vartheta + \theta_o}{2}}{\sin \frac{|\vartheta - \theta_o|}{2}} \right) \right] \quad (B7b)$$

so that the functions $\frac{\partial \Gamma^*_{D_f}}{\partial \vartheta}$ may be seen to have logarithmic singularities. The evaluation of $R(\theta, \theta_o)$ from equations (B6) by numerical methods is therefore not a trivial problem. A logarithmic singularity is integrable, however, and $F(\vartheta, \theta)$ is always continuous in ϑ and θ so that $R(\theta, \theta_o)$ must always be continuous. The integration can thus be effected readily by expanding $F(\vartheta, \theta)$ in a finite Fourier series as follows:

Let

$$\left. \begin{aligned} F_a(\vartheta, \theta) &= \sum_n P_{a_n}(\theta) \cos n\vartheta \quad (n=1, 3, 5, \dots, 15) \\ F_s(\vartheta, \theta) &= \sum_n P_{s_n}(\theta) \cos n\vartheta \quad (n=0, 2, 4, \dots, 16) \end{aligned} \right\} \quad (B8)$$

Substitution of these expressions for F and those of equations (B7) for $\frac{\partial \Gamma^*_{D_f}}{\partial \vartheta}$ into equations (B6) yields

$$\left. \begin{aligned} R_f(\theta, \theta_o) &= \frac{1}{2\pi^2} \sum_n P_{a_n}(\theta) [(\pi - 2\theta_o) I_n + J_n + K_n] \\ R_a(\theta, \theta_o) &= \frac{-1}{2\pi^2} \sum_n P_{s_n}(\theta) (J_n - K_n) \end{aligned} \right\} \quad (B9)$$

where

$$\left. \begin{aligned} I_n &\equiv \int_0^\pi \cos \vartheta \cos n\vartheta \, d\vartheta \\ J_n &\equiv \int_0^\pi \sin \vartheta \cos n\vartheta \log_e \frac{\sin \frac{\vartheta + \theta_0}{2}}{\sin \frac{\vartheta - \theta_0}{2}} \, d\vartheta \\ K_n &\equiv \int_0^\pi \sin \vartheta \cos n\vartheta \log_e \frac{\cos \frac{\vartheta + \theta_0}{2}}{\cos \frac{\vartheta - \theta_0}{2}} \, d\vartheta \end{aligned} \right\} \quad (B10)$$

These integrals can all be evaluated explicitly and are

$$\left. \begin{aligned} I_0 &= 0 \\ I_1 &= \frac{\pi}{2} \\ I_n &= 0 \quad (n=2, 3, \dots) \end{aligned} \right\} \quad (B11)$$

$$\left. \begin{aligned} J_0 &= \pi \sin \theta_0 \\ J_1 &= \frac{\pi}{4} \sin 2\theta_0 \\ J_n &= \frac{\pi}{2} \left[\frac{\sin (n+1)\theta_0}{n+1} - \frac{\sin (n-1)\theta_0}{n-1} \right] \quad (n=2, 3, \dots) \end{aligned} \right\} \quad (B12)$$

and

$$\left. \begin{aligned} K_0 &= -\pi \sin \theta_0 \\ K_1 &= \frac{\pi}{4} \sin 2\theta_0 \\ K_n &= (-1)^{n+1} \frac{\pi}{2} \left[\frac{\sin (n+1)\theta_0}{n+1} - \frac{\sin (n-1)\theta_0}{n-1} \right] \quad (n=2, 3, \dots) \end{aligned} \right\} \quad (B13)$$

With these values for I_n , J_n , and K_n , equations (B9) can be simplified to

$$\left. \begin{aligned} R_s(\theta, \theta_0) &= \frac{1}{2\pi} \sum_n P_{s_n}(\theta, \theta_0) H_n(\theta_0) \quad (n=1, 3, 5, \dots 15) \\ R_a(\theta, \theta_0) &= \frac{-1}{2\pi} \sum_n P_{s_n}(\theta, \theta_0) H_n(\theta_0) \quad (n=0, 2, 4, \dots 16) \end{aligned} \right\} \quad (B14)$$

where

$$\left. \begin{aligned} H_0 &= 0 \\ H_1 &= \frac{\pi - 2\theta_0 + \sin 2\theta_0}{2} \\ H_n &= \frac{\sin (n+1)\theta_0}{n+1} - \frac{\sin (n-1)\theta_0}{n-1} \quad (n=2, 3, \dots) \end{aligned} \right\} \quad (B15)$$

The function $R(\theta, \theta_0)$ can also be expressed in matrix form by writing equations (B8) in matrix form as

$$[F(\vartheta, \theta)] = [P_n(\theta, \theta_0)] [\cos n\vartheta]'$$

so that

$$[P_n(\theta, \theta_0)] = [F(\vartheta, \theta)] [[\cos n\vartheta]']^{-1} \quad (B16)$$

where $[\cos n\vartheta]'$ is the transpose of the matrix $[\cos n\vartheta]$. The following expressions are then obtained by combining equation (B16) with the matrix equivalent of equations (B14):

$$\left. \begin{aligned} R_s(\theta, \theta_0) &= \frac{1}{2\pi} [F_s(\vartheta, \theta)] [[\cos n\vartheta]']^{-1} \{H_n(\theta_0)\} \\ R_a(\theta, \theta_0) &= \frac{-1}{2\pi} [F_s(\vartheta, \theta)] [[\cos n\vartheta]']^{-1} \{H_n(\theta_0)\} \end{aligned} \right\} \quad (B17)$$

By using the procedure outlined in this appendix for calculating lift distributions for discontinuous angle-of-attack distributions the necessity of integrating numerically an initially unknown singular function, as required in equation (A1) or (A2), can thus be avoided; instead, the integration of the singular part of the function is performed analytically (by solving eq. (B2), as in ref. 3) and only the continuous part of the function is treated numerically (by solving eq. (B5)). As part of this procedure, a singular function has to be integrated numerically in order to evaluate $R(\theta, \theta_0)$; however, this function is known initially because it is the product of a known singular but integrable function and a known continuous function $\left(\frac{\partial \Gamma_{s,D}^*}{\partial \vartheta} \text{ and } F(\vartheta, \theta), \text{ respectively}\right)$ so that, by expanding the continuous function in a

Fourier series, the numerical integration can be effected without difficulty.

The values of $[[\cos n\vartheta]']^{-1} \{H_n(\theta_0)\}$ for flap-span ratios of 0.1, 0.2, 0.3, 0.4, 0.5, 0.6, 0.7, 0.8, and 0.9 and for aileron-span ratios of 0.1, 0.2, 0.3, 0.4, 0.5, 0.6, 0.7, 0.8, 0.9, and 1.0 are given in table XI.

APPENDIX C

CALCULATION OF THE REQUIRED GREEN'S FUNCTIONS

As pointed out in the body of this report (see eqs. (3) and (4)) the desired Green's functions are

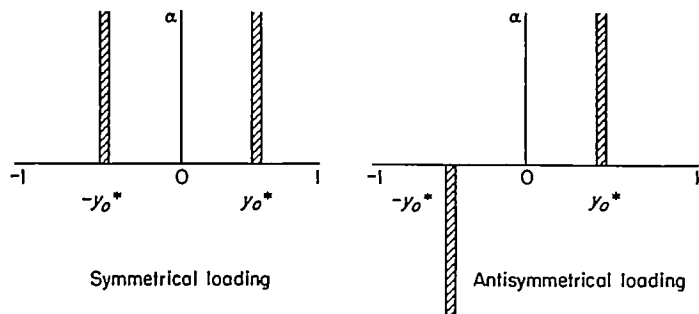
$$\frac{\partial \Gamma_{f'}^*(y^*, y_o^*)}{\partial y_o^*} \quad - \quad \frac{\partial \Gamma_{att}^*(y^*, y_o^*)}{\partial y_o^*}$$

The functions $\Gamma_{f'}$ and Γ_{att}^* can be obtained in the manner indicated in appendix B. However, in order to calculate the desired derivatives of these functions, a numerical differentiation would have to be performed with respect to y_o^* . Such a numerical differentiation is inherently inaccurate inasmuch as $\Gamma_{f'}$ and Γ_{att}^* have singularities. The desired Green's functions are therefore best calculated without using the calculated values of $\Gamma_{f'}$ and Γ_{att}^* and by using, instead, a modification of the method of appendix B.

Let

$$\left. \begin{aligned} \Gamma_{s'}^*(y^*, y_o^*) &\equiv \frac{\partial \Gamma_{f'}^*(y^*, y_o^*)}{\partial y_o^*} \\ \Gamma_{a'}^*(y^*, y_o^*) &\equiv -\frac{\partial \Gamma_{att}^*(y^*, y_o^*)}{\partial y_o^*} \end{aligned} \right\} \quad (C1)$$

Then $\Gamma_{s'}$ and $\Gamma_{a'}$ are lift distributions corresponding to impulse-type angle-of-attack distributions of the following forms:



Hence, they must satisfy equation (A1) or its equivalent, equation (A2), for these angle-of-attack distributions.

Again, as in appendix B, the lift distributions can be considered to consist of a discontinuous part, which satisfies equation (A1) for the given angle-of-attack distribution if the second integral on the right side is disregarded, and of a correction part; that is,

$$\left. \begin{aligned} \Gamma_{s'}^* &= \Gamma_{s'D}^* + \Gamma_{s'C}^* \\ \Gamma_{a'}^* &= \Gamma_{a'D}^* + \Gamma_{a'C}^* \end{aligned} \right\} \quad (C2)$$

The functions $\Gamma_{s'D}^*$ and $\Gamma_{a'D}^*$ must thus satisfy equation (B2) for the given angle-of-attack distributions. By virtue of the linearity of equation (B2) and by virtue of the definitions of the functions in terms of $\Gamma_{f'}$ and Γ_{att}^* , respectively, $\Gamma_{s'D}^*$ and $\Gamma_{a'D}^*$ can be obtained by differentiating with respect to y_o^* the solutions of equation (B2) given in

equations (B3) and (B4) for the flap and aileron angle-of-attack conditions. Thus

$$\left. \begin{aligned} \Gamma_{s'D}^* &= \frac{4}{\pi} \log_e \frac{\sin \vartheta + \sin \theta_o}{|\sin \vartheta - \sin \theta_o|} \\ \Gamma_{a'D}^* &= \frac{4}{\pi} \log_e \frac{\sin (\vartheta + \theta_o)}{\sin |\vartheta - \theta_o|} \end{aligned} \right\} \quad (C3)$$

Similarly, the functions $\Gamma_{s'C}^*$ and $\Gamma_{a'C}^*$ must satisfy equation (B5), where now $R(\theta, \theta_o)$ is defined for the symmetrical and antisymmetrical loadings, respectively, by

$$\left. \begin{aligned} R_s(\theta, \theta_o) &= \frac{1}{8\pi} \int_0^\pi F_s(\vartheta, \theta) \frac{\partial \Gamma_{s'D}^*(\vartheta, \theta_o)}{\partial \vartheta} d\vartheta \\ R_a(\theta, \theta_o) &= \frac{1}{8\pi} \int_0^\pi F_a(\vartheta, \theta) \frac{\partial \Gamma_{a'D}^*(\vartheta, \theta_o)}{\partial \vartheta} d\vartheta \end{aligned} \right\} \quad (C4)$$

The evaluation of these integrals can be effected in the manner employed for equations (B6) so that

$$\left. \begin{aligned} R_s(\theta, \theta_o) &= \frac{1}{2\pi} \sum_n P_{a_n}(\theta) H'_n(\theta_o) \quad (n=1, 3, 5, \dots, 15) \\ R_a(\theta, \theta_o) &= \frac{1}{2\pi} \sum_n P_{s_n}(\theta) H'_n(\theta_o) \quad (n=0, 2, 4, \dots, 16) \end{aligned} \right\} \quad (C5)$$

where

$$H'_n(\theta_o) \equiv 2 \sin n\theta_o \quad (C6)$$

for all values of n , and where P_{a_n} and P_{s_n} are the same values as those used in appendix B. Thus, in matrix form, for given values of θ and θ_o ,

$$\left. \begin{aligned} R_s(\theta, \theta_o) &= \frac{1}{\pi} [F_s(\vartheta, \theta)] [[\cos n\vartheta]']^{-1} \{\sin n\theta_o\} \\ R_a(\theta, \theta_o) &= \frac{1}{\pi} [F_a(\vartheta, \theta)] [[\cos n\vartheta]']^{-1} \{\sin n\theta_o\} \end{aligned} \right\} \quad (C7)$$

The values of $[[\cos n\vartheta]']^{-1} \{\sin n\theta_o\}$ are given in table VI for values of y_o^* ranging from 0 to 0.9 for symmetrical distributions and 0.1 to 0.9 for antisymmetrical distributions.

The desired Green's functions can thus be calculated in the following way. For a given value of θ_o , the values of $R_s(\theta, \theta_o)$ and $R_a(\theta, \theta_o)$ are calculated for eight equal increments of θ between 0 and $\pi/2$ from equation (C7). These values are then written as columns and premultiplied by the matrix of influence coefficients tabulated in this report for the given plan form in order to obtain

$$\frac{\Gamma_{s'C}^*(\theta, \theta_o)}{C_{L\alpha}} \quad \text{and} \quad \frac{\Gamma_{a'C}^*(\theta, \theta_o)}{C_{L\beta}}$$

for the given value of θ_o . To these values are added the

values of

$$\frac{\Gamma_{s,D}^{*'}(\theta, \theta_0)}{C_{L\alpha}} \text{ and } \frac{\Gamma_{a,D}^{*'}(\theta, \theta_0)}{C_{i_d}}$$

obtained by dividing the values of $\Gamma_{s,D}^{*'}$ and $\Gamma_{a,D}^{*'}$ calculated from equation (C3) by $C_{L\alpha}$ and C_{i_d} , respectively, for this value of θ , and the given values of θ_0 . This procedure yields

$$\frac{\Gamma_{s'}^{*'}(\theta, \theta_0)}{C_{L\alpha}} \text{ and } \frac{\Gamma_{a'}^{*'}(\theta, \theta_0)}{C_{i_d}}$$

(The division by $C_{L\alpha}$ and by C_{i_d} is performed to facilitate the further calculations required to obtain the desired influence coefficients, as explained in the body of this report.) This calculation is repeated for all the values of θ_0 for which the Green's functions are desired.

REFERENCES

1. Weissinger, J.: The Lift Distribution of Swept-Back Wings. NACA TM 1120, 1947.
2. Diederich, Franklin W.: Calculation of the Aerodynamic Loading of Swept and Unswept Flexible Wings of Arbitrary Stiffness. NACA Rep. 1000, 1950.
3. Diederich, Franklin W., and Zlotnick, Martin: Theoretical Spanwise Lift Distributions of Low-Aspect-Ratio Wings at Speeds Below and Above the Speed of Sound. NACA TN 1973, 1949.
4. Diederich, Franklin W.: Calculation of the Lateral Control of Swept and Unswept Flexible Wings of Arbitrary Stiffness. NACA Rep. 1024, 1951.
5. DeYoung, John, and Harper, Charles W.: Theoretical Symmetric Span Loading at Subsonic Speeds for Wings Having Arbitrary Plan Form. NACA Rep. 921, 1948.
6. Falkner, V. M.: The Calculation of Aerodynamic Loading on Surfaces of Any Shape. R. & M. No. 1910, British A.R.C., 1943.
7. Diederich, Franklin W.: A Simple Approximate Method for Calculating Spanwise Lift Distributions and Aerodynamic Influence Coefficients at Subsonic Speeds. NACA TN 2751, 1952.
8. Bencotter, Stanley U.: Matrix Development of Multhopp's Equations for Spanwise Air-Load Distribution. Jour. Aero. Sci., vol. 15, no. 2, Feb. 1948, pp. 113-120.
9. Diederich, Franklin W.: A Plan-Form Parameter for Correlating Certain Aerodynamic Characteristics of Swept Wings. NACA TN 2335, 1951.
10. Multhopp, H.: The Calculation of the Lift Distribution of Aerofoils. R.T.P. Translation No. 2392, British M.A.P.

TABLE I.—INDEX TO SPANWISE-LIFT-DISTRIBUTION FIGURES

[All wings are unswept]

Plan form	A	λ	Figure
----	Very low	----	1
311	1.5	0	2
312	1.5	.25	3
313	1.5	.50	4
314	1.5	1.00	5
315	1.5	1.50	6
321	3.0	0	7
322	3.0	.25	8
323	3.0	.50	9
324	3.0	1.00	10
325	3.0	1.50	11
331	6.0	0	12
332	6.0	.25	13
333	6.0	.50	14
334	6.0	1.00	15
335	6.0	1.50	16
341	12.0	0	17
342	12.0	.25	18
343	12.0	.50	19
344	12.0	1.00	20

TABLE II.—FORCE AND MOMENT COEFFICIENTS FOR ANGLE-OF-ATTACK LOADINGS

Plan form	Additional loading				Damping-in-roll loading	
	$C_{L\alpha}$	C_{BM}	\bar{y}^*	C_{D_i}	C_{i_d}	$C_{L_{iR}}$
311	1.8976	0.7701	0.4068	0.7799	0.1280	0.4448
312	1.9940	.8351	.4188	.8448	.1403	.4781
313	2.0006	.8449	.4223	.8493	.1423	.4835
314	1.9782	.8433	.4263	.8303	.1434	.4865
315	1.9459	.8363	.4293	.8041	.1438	.4871
321	2.9938	1.1765	.3930	1.0004	.2120	.7544
322	3.1747	1.3177	.4161	1.0733	.2501	.8548
323	3.1735	1.3410	.4226	1.0686	.2584	.8772
324	3.0970	1.3364	.4315	1.0198	.2642	.8912
325	3.0086	1.3174	.4379	.9679	.2661	.8948
331	4.1171	1.5537	.3774	.9950	.3083	1.1248
332	4.3381	1.7830	.4110	1.0071	.3893	1.3333
333	4.3205	1.8363	.4250	.9918	.4141	1.3904
334	4.1316	1.8479	.4419	.9409	.4334	1.4417
335	4.0252	1.8260	.4536	.8921	.4405	1.4540
341	5.0125	1.8145	.3620	.7360	.3918	1.4714
342	5.1989	2.1145	.4067	.7310	.5190	1.7797
343	5.1647	2.2164	.4291	.7126	.5700	1.9008
344	5.0026	2.2819	.4561	.6982	.6150	2.0024

TABLE III.—LIFT AND BENDING-MOMENT COEFFICIENTS FOR UNIT EFFECTIVE FLAP DEFLECTION

Plan form	$\frac{b_f}{b}=0.1$		$\frac{b_f}{b}=0.2$		$\frac{b_f}{b}=0.3$		$\frac{b_f}{b}=0.4$		$\frac{b_f}{b}=0.5$		$\frac{b_f}{b}=0.6$		$\frac{b_f}{b}=0.7$		$\frac{b_f}{b}=0.8$		$\frac{b_f}{b}=0.9$	
	C_L	C_{BM}	C_L	C_{BM}	C_L	C_{BM}	C_L	C_{BM}	C_L	C_{BM}	C_L	C_{BM}	C_L	C_{BM}	C_L	C_{BM}	C_L	C_{BM}
311	0.24786	0.07142	0.49355	0.14681	0.73368	0.22716	0.96414	0.31187	1.18127	0.39990	1.38248	0.48986	1.56275	0.57842	1.71660	0.66114	1.83434	0.73034
312	.25418	.07604	.60633	.15609	.75344	.24137	.99165	.33146	1.21746	.42537	1.42860	.52190	1.62029	.61788	1.78740	.70911	1.91973	.78762
313	.26380	.07667	.60573	.15741	.75282	.24345	.99126	.33443	1.21760	.42636	1.42964	.52704	1.62254	.62430	1.79111	.71632	1.92432	.79650
314	.24974	.07696	.49783	.15608	.74147	.24162	.97632	.33222	1.20044	.42693	1.41039	.52458	1.60173	.63196	1.78931	.71474	1.90239	.79469
315	.24461	.07456	.48785	.15338	.72704	.23774	.95828	.32729	1.17816	.42105	1.38497	.51795	1.57371	.61476	1.73984	.70710	1.87100	.78678
321	.40716	.10593	.81108	.21999	1.20459	.34386	1.57797	.47562	1.92384	.61296	2.24004	.75402	2.51688	.89211	2.74710	1.01964	2.91414	1.12266
322	.40941	.11157	.81663	.23169	1.21545	.36252	1.59631	.50262	1.95396	.64998	2.28637	.80385	2.58717	.95350	2.84940	1.10766	3.05819	1.23738
323	.40218	.11106	.80307	.23100	1.19691	.36216	1.57482	.50325	1.93047	.65244	2.26458	.80928	2.56863	.96310	2.83869	1.12242	3.05025	1.25707
324	.38379	.10695	.78788	.23329	1.14735	.35166	1.51335	.49080	1.85973	.63909	2.18823	.79841	2.48970	.95822	2.75820	1.11363	2.97270	1.25106
325	.36567	.10215	.78329	.21417	1.09860	.33891	1.45263	.47517	1.78911	.62130	2.10247	.77736	2.40690	.93723	2.67243	1.09413	2.83507	1.23183
331	.50772	.13242	1.19136	.28086	1.76562	.44742	2.29812	.62706	2.77458	.81433	3.19980	1.00764	3.55740	1.19424	3.84296	1.36332	4.03494	1.49250
332	.57630	.13332	1.15194	.28374	1.71390	.45438	2.24094	.64080	2.72100	.83880	3.16494	1.05000	3.55962	1.26480	3.90582	1.47612	4.17634	1.66278
333	.54013	.13392	1.08594	.28596	1.62270	.46002	2.13108	.65202	2.60046	.85873	3.04534	1.08330	3.45156	1.31034	3.81972	1.55034	4.11588	1.72604
334	.40986	.11700	1.09800	.25330	1.61572	.41676	2.00256	.59844	2.45790	.79758	2.89848	1.01880	3.30822	1.25268	3.69634	1.49148	3.99342	1.70754
335	.45744	.10764	.92820	.23604	1.40592	.38924	1.86948	.56658	2.30778	.76254	2.78911	.95364	3.14574	1.21980	3.62560	1.46230	3.83532	1.68312
341	.70104	.13980	1.67320	.30912	2.32488	.50964	2.96520	.72852	3.56004	.95496	4.05084	1.18956	4.44300	1.41168	4.75044	1.60944	4.93476	1.75164
342	.72096	.13104	1.44804	.29352	2.15460	.48996	2.79444	.70872	3.34692	.94152	3.85392	1.19508	4.29456	1.45536	4.69780	1.71660	4.99032	1.95600
343	.66384	.12120	1.34112	.27516	2.00940	.46560	2.62296	.68112	3.16248	.91636	3.67584	1.17900	4.14024	1.45896	4.57560	1.75200	4.92816	2.25000
344	.57324	.10416	1.17312	.24348	1.78732	.42252	2.35572	.63108	2.87280	.86436	3.38724	1.13736	3.87180	1.43736	4.34544	1.76038	4.73964	2.06820

TABLE IV.—LIFT AND ROLLING-MOMENT COEFFICIENTS FOR UNIT EFFECTIVE AILERON DEFLECTION

Plan form	$\frac{b_{afl}}{b}=1.0$		$\frac{b_{afl}}{b}=0.9$		$\frac{b_{afl}}{b}=0.8$		$\frac{b_{afl}}{b}=0.7$		$\frac{b_{afl}}{b}=0.6$		$\frac{b_{afl}}{b}=0.5$		$\frac{b_{afl}}{b}=0.4$		$\frac{b_{afl}}{b}=0.3$		$\frac{b_{afl}}{b}=0.2$		$\frac{b_{afl}}{b}=0.1$	
	$C_{L1/2}$	$C_{l\beta}$	$C_{L1/2}$	$C_{l\beta}$	$C_{L1/2}$	$C_{l\beta}$	$C_{L1/2}$	$C_{l\beta}$	$C_{L1/2}$	$C_{l\beta}$	$C_{L1/2}$	$C_{l\beta}$	$C_{L1/2}$	$C_{l\beta}$	$C_{L1/2}$	$C_{l\beta}$	$C_{L1/2}$	$C_{l\beta}$	$C_{L1/2}$	$C_{l\beta}$
311	0.86804	0.22007	0.83565	0.21686	0.76517	0.20654	0.67196	0.19005	0.56484	0.16731	0.45041	0.14069	0.32467	0.10988	0.22358	0.07712	0.12389	0.04480	0.04340	0.01653
312	.91721	.23814	.88443	.23459	.81272	.22401	.71742	.20678	.60725	.18344	.48870	.15480	.36768	.12210	.24990	.08691	.14186	.05160	.05213	.01982
313	.92597	.24134	.89309	.23774	.82106	.22706	.72522	.20961	.61430	.18599	.49476	.15701	.37256	.12386	.25341	.08817	.14394	.05235	.05291	.02010
314	.93083	.24326	.89789	.23964	.82569	.23340	.72957	.21131	.61823	.18752	.49812	.15830	.37594	.12488	.25532	.08891	.14507	.05277	.05334	.02027
315	.93179	.24383	.89885	.24020	.82665	.22943	.73052	.21182	.61913	.18797	.49893	.15870	.37690	.12519	.25581	.08913	.14537	.05291	.05345	.02031
321	1.51881	.37215	1.45671	.36906	1.32375	.34806	1.15662	.31834	.95478	.27966	.74913	.23220	.54531	.17889	.35448	.12306	.18358	.06330	.06174	.02409
322	1.65873	.42441	1.59594	.41805	1.46070	.39915	1.28349	.36834	1.08120	.32670	.86610	.27570	.64899	.21765	.43972	.16507	.24933	.09231	.09174	.03584
323	1.69173	.43704	1.62882	.43062	1.49310	.41142	1.31487	.38013	1.11081	.33771	.89286	.28557	.67158	.22584	.45631	.16131	.25983	.09618	.09579	.03714
324	1.71111	.44505	1.64829	.43917	1.51278	.41985	1.33455	.38826	1.12986	.34533	.91032	.29238	.68631	.23148	.46779	.16545	.26646	.09867	.09828	.03807
325	1.71447	.44838	1.65192	.44193	1.51704	.42284	1.33953	.39105	1.13532	.34803	.91572	.29484	.69108	.23352	.47142	.16695	.26865	.09957	.09912	.03940
331	2.39826	.55524	2.27172	.54540	2.03448	.51618	1.73508	.46914	1.40694	.40680	1.07382	.33240	.75588	.25050	.47094	.16716	.23652	.08994	.07050	.02886
332	2.65548	.66174	2.54118	.65160	2.30388	.62160	2.00280	.57288	1.66920	.50748	1.32390	.42792	.98400	.33774	.66336	.24132	.37620	.14466	.13974	.05670
333	2.73516	.69544	2.62164	.68538	2.38632	.65526	2.08704	.60624	1.75332	.53988	1.40424	.45828	1.05634	.36450	.71988	.26256	.41250	.15846	.15408	.06222
334	2.78340	.72096	2.67186	.71106	2.44146	.68142	2.14776	.63264	1.81734	.56592	1.46700	.48276	1.11120	.38580	.76314	.27894	.43926	.16360	.16416	.06606
335	2.78514	.72894	2.67558	.71928	2.45040	.69024	2.16300	.64224	1.83774	.57600	1.48962	.49260	1.12328	.39450	.77976	.28654	.44946	.17262	.16794	.06766
341	3.33884	.72884	3.18348	.71424	2.74812	.67200	2.28120	.60468	1.79496	.51696	1.32510	.41472	.89892	.30528	.53640	.19740	.25548	.10176	.07032	.03048
342	3.69132	.88500	3.49608	.87096	3.11808	.82956	2.66508	.76284	2.18876	.67416	1.71144	.56760	1.28012	.44820	.84624	.32160	.48276	.19524	.18384	.07884
343	3.81612	.94776	3.62556	.93420	3.25932	.89388	2.82012	.82336	2.36116	.74904	1.87694	.63168	1.41166	.60888	.97056	.37020	.66692	.22836	.21804	.09288
344	3.89628	1.00176	3.71364	.98904	3.36732	.95100	2.95116	.88800	2.49888	.80100	2.03716	.69120	1.56088	.66088	1.08204	.41364	.63720	.25666	.24564	.10392

TABLE V.—AERODYNAMIC-INFLUENCE-COEFFICIENT MATRICES

(a) Symmetric loadings [Q]

Plan form 311 matrix with 9 columns and 9 rows of numerical values.

Plan form 312 matrix with 9 columns and 9 rows of numerical values.

Plan form 313 matrix with 9 columns and 9 rows of numerical values.

Plan form 314 matrix with 9 columns and 9 rows of numerical values.

Plan form 315 matrix with 9 columns and 9 rows of numerical values.

Plan form 321 matrix with 9 columns and 9 rows of numerical values.

Plan form 322 matrix with 9 columns and 9 rows of numerical values.

Plan form 323 matrix with 9 columns and 9 rows of numerical values.

Plan form 324 matrix with 9 columns and 9 rows of numerical values.

Plan form 325 matrix with 9 columns and 9 rows of numerical values.

Plan form 331 matrix with 9 columns and 9 rows of numerical values.

Plan form 332 matrix with 9 columns and 9 rows of numerical values.

Plan form 333 matrix with 9 columns and 9 rows of numerical values.

Plan form 334 matrix with 9 columns and 9 rows of numerical values.

Plan form 335 matrix with 9 columns and 9 rows of numerical values.

Plan form 341 matrix with 9 columns and 9 rows of numerical values.

Plan form 342 matrix with 9 columns and 9 rows of numerical values.

Plan form 343 matrix with 9 columns and 9 rows of numerical values.

Plan form 344 matrix with 9 columns and 9 rows of numerical values.

TABLE VI.—VALUES OF $[[\cos n\delta]']^{-1} \{\sin n\theta_0\}$ FOR INFLUENCE-COEFFICIENT CALCULATIONS

(a) Symmetrical distributions

[[cos nδ]'] ⁻¹ {sin nθ ₀ } for—									
$y_0^*=0$	$y_0^*=0.1$	$y_0^*=0.2$	$y_0^*=0.3$	$y_0^*=0.4$	$y_0^*=0.5$	$y_0^*=0.6$	$y_0^*=0.7$	$y_0^*=0.8$	$y_0^*=0.9$
0	0.06482	0.12738	0.05490	0.00307	0.10825	0.12843	0.00112	0.17124	0.05804
0.25490	0.12405	0.00042	0.15587	0.27393	0.07457	0.05802	0.36868	0.08137	0.56104
0	0.14056	0.27772	0.12089	0.00637	0.24856	0.30772	0.00289	0.53340	0.46784
0.30068	0.14692	0.00050	0.19161	0.35049	0.10198	0.08935	0.73259	0.43254	-0.60905
0	0.18521	0.37593	0.17232	0.01072	0.46929	0.83031	0.08064	-0.62272	-0.05031
0.44998	0.22397	0.00082	0.35209	0.83706	0.51296	-0.38534	-0.64349	-0.04478	-0.09633
0	0.35996	0.87921	0.67744	-0.14552	-0.60008	-0.29469	-0.00127	-0.09559	-0.01272
1.28146	0.83714	-0.03954	-0.52044	-0.35834	-0.04983	-0.02158	-0.07658	-0.00696	-0.02107

(b) Antisymmetrical distributions

[[cos nδ]'] ⁻¹ {sin nθ ₀ } for—									
$y_0^*=0.1$	$y_0^*=0.2$	$y_0^*=0.3$	$y_0^*=0.4$	$y_0^*=0.5$	$y_0^*=0.6$	$y_0^*=0.7$	$y_0^*=0.8$	$y_0^*=0.9$	
0.00645	0.02547	0.01647	0.00123	0.05413	0.07706	0.00078	0.13699	0.06224	
0.01266	0.00008	0.04767	0.11171	0.03801	0.03550	0.26312	0.06036	0.51484	
0.01522	0.06011	0.03925	0.00297	0.13453	0.19984	0.00219	0.46188	0.45576	
0.01766	0.00013	0.06913	0.16861	0.06132	0.06448	0.61676	0.41617	-0.65926	
0.02619	0.10633	0.07311	0.00606	0.32476	0.70453	0.07983	-0.70452	-0.06403	
0.04032	0.00029	0.19013	0.60268	0.46138	-0.41616	-0.68476	-0.06448	-0.16004	
0.21900	0.45950	0.53108	-0.15211	-0.78405	-0.46188	-0.00232	-0.19985	-0.02992	
0.30418	-0.04053	-0.80033	-0.73472	-0.12770	-0.06636	-0.27477	-0.03550	-0.10133	
-0.64170	-0.61138	-0.16632	-0.00644	-0.16233	-0.13700	-0.00082	-0.07706	-0.01225	

TABLE VII.—MATRICES USED IN LIFT-DISTRIBUTION CALCULATIONS

(a) Symmetrical distributions

$$[\sin n\theta_m]=$$

0.19509	0.55557	0.83147	0.98079	0.98079	0.83147	0.55557	0.19509
0.38268	0.92388	0.92388	0.38268	-0.38268	-0.92388	-0.92388	-0.38268
0.55557	0.98079	0.19509	-0.83147	-0.83147	0.19509	0.55557	0.38268
0.70711	0.70711	-0.70711	-0.70711	0.70711	-0.70711	-0.70711	0.70711
0.83147	0.19509	-0.83147	0.55557	0.55557	-0.83147	0.19509	0.83147
0.92388	-0.38268	-0.38268	0.92388	-0.92388	0.38268	-0.92388	0.38268
0.98079	-0.83147	0.55557	-0.19509	0.19509	-0.83147	0.55557	-0.19509
1.00000	-1.00000	1.00000	-1.00000	1.00000	-1.00000	1.00000	-1.00000

$$[\sin n\theta_m]^{-1}=$$

0.04877	0.09567	0.13889	0.17678	0.20787	0.23097	0.24520	0.12500
0.13889	0.23097	0.24520	0.17678	0.04877	-0.09567	-0.20787	-0.12500
0.20787	0.23097	0.04877	-0.17678	-0.24520	-0.09567	0.13889	0.12500
0.24520	0.09567	-0.20787	-0.17678	-0.13889	0.23097	-0.04877	-0.12500
0.24520	-0.09567	-0.20787	0.17678	0.13889	-0.23097	-0.04877	0.12500
0.20787	-0.23097	0.04877	0.17678	-0.24520	0.09567	0.13889	-0.12500
0.13889	-0.23097	0.24520	-0.17678	0.04877	0.09567	-0.20787	0.12500
0.04877	-0.09567	0.13889	-0.17678	0.20787	-0.23097	0.24520	-0.12500

$$[\cos n\theta_m][n]=$$

1.00000	3.00000	5.00000	7.00000	9.00000	11.00000	13.00000	15.00000
0.98079	2.40441	2.77785	1.38563	-1.76581	-6.11127	-10.80911	-14.71185
0.92388	1.14804	-1.91340	-6.46716	-8.31492	-4.20948	4.97484	13.88820
0.83147	-0.58527	-4.90395	-3.88899	5.00013	10.78899	2.53177	-12.47205
0.70711	-2.12133	-3.53555	4.94977	6.38399	-7.77821	-9.19443	10.66665
0.55557	-2.94237	0.97645	5.82029	-7.48323	-2.14699	12.75027	-8.33355
0.38268	-2.77164	4.01940	-2.67876	-3.44412	10.16298	-12.01044	5.74020
0.19509	-1.66671	4.16735	-6.86563	8.82711	-9.14617	7.22441	-2.92635

$$[I_1]=$$

0.06250							
	0.12500						
		0.12500					
			0.12500				
				0.12500			
					0.12500		
						0.12500	
							0.12500

$$\left[\frac{\sin n\theta_m}{\sin \theta_m} \right] [n]=$$

1.00000	8.54313	21.30990	35.19159	45.24633	46.88178	37.02023	15.00000
1.00000	7.24272	12.07120	7.00000	-9.00000	-25.55640	-31.38512	-15.00000
1.00000	5.29620	1.75580	-10.47841	-13.46967	3.86276	22.95020	15.00000
1.00000	3.00000	-5.00000	-7.00000	9.00000	11.00000	-13.00000	-15.00000
1.00000	0.70389	-5.89795	4.67719	6.01353	-12.97549	3.05019	15.00000
1.00000	-1.24293	-2.07105	7.00000	-9.06900	4.55631	5.38473	-15.00000
1.00000	-2.54328	2.83220	-1.39237	-1.79019	6.23084	-11.02088	15.00000
1.00000	-3.00000	5.00000	-7.00000	9.00000	-11.00000	13.00000	-15.00000

$$[B_m]=$$

5.1253	-1.8481	0	-0.1514	0	-0.0481	0	-0.0163
-0.9422	2.6131	-1.0193	0	-0.0107	0	-0.0411	0
0	-0.7022	1.7999	-0.7191	0	-0.0815	0	-0.0226
-0.0417	0	-0.5649	1.4142	-0.5739	0	-0.0773	0
0	-0.0468	0	-0.4831	1.2027	-0.4994	0	-0.0506
-0.0102	0	-0.0490	0	-0.4494	1.0824	-0.4814	0
0	-0.0160	0	-0.0567	0	-0.4535	1.0196	-0.4106
-0.0063	0	-0.0251	0	-0.0342	0	-0.8053	1.0000

$$[D]=$$

0.039276	-0.018861	0.011893	-0.007813	0.005220	-0.003236	0.001554
-0.018861	0.050969	-0.026674	0.016913	-0.011048	0.006775	-0.003236
-0.027584	-0.007813	0.044496	-0.022097	0.013246	-0.007813	0.003666
0.011048	-0.034057	-0.003236	0.040330	-0.018861	0.010138	-0.004577
-0.004473	0.015625	-0.037723	0	0.037723	-0.015625	0.006473
0.004577	-0.010138	0.018861	-0.040330	0.003236	0.034056	-0.011048
-0.003666	0.007813	-0.013246	0.022097	-0.044496	0.007813	0.027584
0.003236	-0.006775	0.011048	-0.016913	0.026674	-0.050969	0.018861
-0.001554	0.003236	-0.005220	0.007813	-0.011893	0.018861	-0.039276

(b) Antisymmetrical distributions

$$[\sin n\theta_m]=$$

0.38268	0.70711	0.92388	1.00000	0.92388	0.70711	0.38268
0.70711	1.00000	0.70711	0.00000	-0.70711	-1.00000	-0.70711
0.92388	0.70711	-0.38268	-1.00000	-0.38268	0.70711	0.92388
1.00000	0.00000	-1.00000	0.00000	1.00000	0.00000	-1.00000
0.92388	-0.70711	-0.38268	1.00000	-0.38268	-0.70711	0.92388
0.70711	-1.00000	0.70711	0.00000	-0.70711	1.00000	-0.70711
0.38268	-0.70711	0.92388	-1.00000	0.92388	-0.70711	0.38268

$$[\sin n\theta_m]^{-1}=$$

0.09567	0.17678	0.23097	0.25000	0.23097	0.17678	0.09567
0.17678	0.25000	0.17678	0.00000	-0.17678	-0.25000	-0.17678
0.23097	0.17678	-0.09567	-0.25000	-0.09567	0.17678	0.23097
0.25000	0.00000	-0.25000	0.00000	0.25000	0.00000	-0.25000
0.23097	-0.17678	-0.09567	0.25000	-0.09567	-0.17678	0.23097
0.17678	-0.25000	0.17678	0.00000	-0.17678	0.25000	-0.17678
0.09567	-0.17678	0.23097	-0.25000	0.23097	-0.17678	0.09567

$$[\cos n\theta_m][n]=$$

2.00000	4.00000	6.00000	8.00000	10.00000	12.00000	14.00000
1.84778	2.82844	2.29608	0.00000	-3.82680	-8.48532	-12.93432
1.41422	0.00000	-4.24266	-8.00000	-7.07110	0.00000	9.89954
0.76538	-2.82844	-5.64348	0.00000	9.23880	8.48532	-5.35752
0.00000	-4.00000	0.00000	8.00000	0.00000	-12.00000	0.00000
-0.76538	-2.82844	5.64348	0.00000	-9.23880	8.48532	5.35752
-1.41422	0.00000	4.24266	-8.00000	7.07110	0.00000	-9.89954
-1.84778	2.82844	-2.29608	0.00000	3.82680	-8.48532	12.93432
-2.00000	4.00000	-6.00000	8.00000	-10.00000	12.00000	-14.00000

$$[I_1]=$$

0.06250							
	0.12500						
		0.12500					
			0.12500				
				0.12500			
					0.12500		
						0.12500	
							0.12500

$$\left[\frac{\sin n\theta_m}{\sin \theta_m} \right] [n]=$$

3.92312	14.49812	28.41396	41.00672	47.35660	43.49436	27.46184
3.69556	10.46280	11.08668	0.00000	-18.47780	-31.35780	-25.86892
3.32594	5.09116	-4.13292	-14.39992	-6.88820	15.27348	23.28158
2.82842	-0.00000	-8.48526	0.00000	14.14210	0.00000	-10.78994
2.22228	-3.40172	-2.76150	9.62152	-4.60250	-10.20516	15.55596
1.53074	-4.32956	4.59222	0.00000	-7.65370	12.98868	-10.17618
0.78036	-2.88984	5.65188	-8.15672	9.41980	-8.65152	5.40252

$$[B_m]=$$

5.1259	-1.8448	0.0000	-0.1438	0.0000	-0.0326	0.0000
-0.9405	2.6131	-1.0128	0.0000	-0.0898	0.0000	-0.0166
0.0000	-0.6983	1.7999	-0.7097	0.0000	-0.0619	0.0000
-0.0396	0.0000	-0.5576	1.4142	-0.5576	0.0000	-0.0396
0.0000	-0.0414	0.0000	-0.4742	1.2027	-0.4666	0.0000
-0.0069	0.0000	-0.0372	0.0000	-0.4199	1.0824	-0.3898
0.0000	-0.0065	0.0000	-0.0286	0.0000	-0.3670	1.0196

$$[D]=$$

0.040046	-0.020415	0.014062	-0.011048	0.009396	-0.008456	0.007966	-0.003907
-0.020415	0.064108	-0.031464	0.023459	-0.019505	0.017362	-0.016269	0.007966
-0.025984	-0.011048	0.049442	-0.028872	0.022028	-0.018861	0.017362	-0.003456
0.009396	-0.030649	-0.008456	0.048012	-0.028228	0.022028	-0.019505	0.009396
-0.004666	0.011959	-0.032081	-0.007813	0.048012	-0.028871	0.023459	-0.011048
0.002593	-0.006097	0.012903	-0.032081	-0.008456	0.049442	-0.031464	0.014062
-0.001430	0.003236	-0.006097	0.011959	-0.030649	-0.011048	0.054108	-0.020415
0.000644	-0.001430	0.002593	-0.004666	0.009396	-0.025984	-0.020415	0.040046

TABLE VIII.—COMPUTING PROCEDURE FOR *F* FUNCTIONS

(a) Row 1

⊙ ⊙ ⊙ ⊙ ⊙ ⊙ ⊙ ⊙ ⊙ ⊙	γ^* γ^* γ^* $1/(\gamma^*-\gamma^*)$ $1/(\gamma^*+\gamma^*)$	0.98079 1.00000 -0.01921 -52.05622 0.50485	0.98079 0.98079 0 ∞ 0.50979	0.98079 0.92388 0.05691 17.57160 0.52503	0.98079 0.83147 0.14932 6.69703 0.55180	0.98079 0.70711 0.27368 3.65390 0.59245	0.98079 0.55557 0.42522 2.85172 0.66089	0.98079 0.38268 0.19509 0.69811 1.67193 0.73342	0.98079 0.19509 0 0.78570 1.27276 0.85043	0.98079 0 0.98079 1.01959 1.01959
⊙ ⊙ ⊙ ⊙ ⊙ ⊙ ⊙ ⊙ ⊙ ⊙	$(\gamma^*-\gamma^*)^2$ $(\gamma^*+\gamma^*)^2$ γ^* $c^2/2$ $\tan A$	0.00037 3.92353 0.96195	0 3.84780 0.96195	0.00324 3.62777 0.96195	0.02230 3.28429 0.96195	0.07490 2.84901 0.96195	0.18081 2.36040 0.96195	0.35774 1.85905 0.96195	0.61732 1.38269 0.96195	0.96195 0.96195 0.96195
⊙ ⊙ ⊙ ⊙ ⊙ ⊙ ⊙ ⊙ ⊙ ⊙	$\frac{\odot+\odot}{\odot+\odot}$ $\frac{\odot+\odot}{\sqrt{\odot+\odot}}$ $2 \tan A/\odot$									
⊙ ⊙ ⊙ ⊙ ⊙ ⊙ ⊙ ⊙ ⊙ ⊙	$\odot+\odot \tan A$ $\frac{\odot}{\odot}$ $\frac{\sqrt{\odot+\odot}}{\odot-\odot}$ $\frac{\odot}{\sqrt{\odot+\odot}}$									
⊙ ⊙ ⊙ ⊙ ⊙ ⊙ ⊙ ⊙ ⊙ ⊙	$\frac{\odot}{\odot}-1$ $F_2 = \frac{\odot}{\odot}$ $F_1 = \frac{\odot+\odot}{\odot}$ $2F_2 = \frac{\odot-\odot}{\odot}$ $2F_1 = \frac{\odot+\odot}{\odot}$		(*)							

* For $\gamma^* = \gamma^*$, $\odot = \tan A/\odot$.

(b) Row 2

⊙ ⊙ ⊙ ⊙ ⊙ ⊙ ⊙ ⊙ ⊙ ⊙	0.92388 1.00000 -0.07812 -13.13716 0.51978	0.92388 0.98079 -0.06691 -17.57160 0.52503	0.92388 0.92388 0 ∞ 0.54120	0.92388 0.83147 0.09241 10.82134 0.56969	0.92388 0.70711 0.21677 4.61318 0.61312	0.92388 0.55557 0.36831 2.71510 0.67593	0.92388 0.38268 0.54120 1.84775 0.76537	0.92388 0.19509 0.72879 1.37214 0.82388	0.92388 0 0.92388 1.08239 1.08239
⊙ ⊙ ⊙ ⊙ ⊙ ⊙ ⊙ ⊙ ⊙ ⊙	0.00579 3.70131 0.85355	0.00324 3.62777 0.85355	0 3.41422 0.85355	0.00854 3.08125 0.85355	0.04699 2.66013 0.85355	0.12565 2.18977 0.85355	0.29290 1.70710 0.85355	0.53113 1.25209 0.85355	0.85355 0.85355 0.85355
⊙ ⊙ ⊙ ⊙ ⊙ ⊙ ⊙ ⊙ ⊙ ⊙									
⊙ ⊙ ⊙ ⊙ ⊙ ⊙ ⊙ ⊙ ⊙ ⊙									
⊙ ⊙ ⊙ ⊙ ⊙ ⊙ ⊙ ⊙ ⊙ ⊙			(*)						

* For $\gamma^* = \gamma^*$, $\odot = \tan A/\odot$.

(c) Row 3

⊙ ⊙ ⊙ ⊙ ⊙ ⊙ ⊙ ⊙ ⊙ ⊙	0.83147 1.00000 -0.16853 -5.93268 0.54601	0.83147 0.98079 -0.14932 -6.69703 0.55180	0.83147 0.92388 -0.09241 -10.82134 0.56969	0.83147 0.83147 0 ∞ 0.60134	0.83147 0.70711 0.12436 8.04117 0.64995	0.83147 0.55557 0.27590 3.63450 0.72096	0.83147 0.38268 0.44579 2.22621 0.82362	0.83147 0.19509 0.63638 1.57139 0.97413	0.83147 0 0.83147 1.20269 1.20269
⊙ ⊙ ⊙ ⊙ ⊙ ⊙ ⊙ ⊙ ⊙ ⊙	0.02840 3.35428 0.69134	0.02230 3.28429 0.69134	0.00854 3.08125 0.69134	0 2.76537 0.69134	0.01547 2.36723 0.69134	0.07612 1.92388 0.69134	0.20141 1.47416 0.69134	0.40498 1.05383 0.69134	0.69134 0.69134 0.69134
⊙ ⊙ ⊙ ⊙ ⊙ ⊙ ⊙ ⊙ ⊙ ⊙									
⊙ ⊙ ⊙ ⊙ ⊙ ⊙ ⊙ ⊙ ⊙ ⊙									
⊙ ⊙ ⊙ ⊙ ⊙ ⊙ ⊙ ⊙ ⊙ ⊙				(*)					

* For $\gamma^* = \gamma^*$, $\odot = \tan A/\odot$.

TABLE VIII.—COMPUTING PROCEDURE FOR F FUNCTIONS—Continued

(d) Row 4

⊙	0.70711 1.00000	0.70711 0.98079	0.70711 0.92388	0.70711 0.83147	0.70711 0.70711	0.70711 0.55557	0.70711 0.38268	0.70711 0.19509	0.70711 0
⊙	-0.29289	-0.27368	-0.21677	-0.12436	0	0.15154	0.32443	0.51202	0.70711
⊙	-3.41425	-3.65390	-4.61318	-8.04117	∞	6.59332	3.08233	1.95305	1.41421
⊙	0.53579	0.59245	0.61312	0.64995	0.70710	0.79197	0.91761	1.10840	1.41421
⊙	0.08578	0.07490	0.04899	0.01547	0	0.02296	0.10325	0.26216	0.50000
⊙	2.01422	2.84901	2.66013	2.36723	2.00002	1.59436	1.18764	0.81396	0.50000
⊙	0.50000	0.50000	0.50000	0.50000	0.50000	0.50000	0.50000	0.50000	0.50000
⊙									
⊙									
⊙					(*)				

* For $\eta^* = \gamma^*$, $\ominus = \tan \Delta / \odot$.

(e) Row 5

⊙	0.55557 1.00000	0.55557 0.98079	0.55557 0.92388	0.55557 0.83147	0.55557 0.70711	0.55557 0.55557	0.55557 0.38268	0.55557 0.19509	0.55557 0
⊙	-0.44443	-0.42523	-0.36831	-0.27590	-0.15154	0	0.17289	0.36048	0.55557
⊙	-2.25007	-2.35172	-2.71510	-3.62450	-6.59892	∞	5.78402	2.77408	1.79995
⊙	0.64285	0.65089	0.67593	0.72096	0.79197	0.89998	1.06581	1.33216	1.79995
⊙	0.19752	0.18081	0.13565	0.07812	0.02296	0	0.02989	0.12995	0.30866
⊙	2.41980	2.36040	2.18977	1.92338	1.59436	1.29463	0.89031	0.56349	0.30866
⊙	0.30866	0.30866	0.30866	0.30866	0.30866	0.30866	0.30866	0.30866	0.30866
⊙									
⊙									
⊙						(*)			

* For $\eta^* = \gamma^*$, $\ominus = \tan \Delta / \odot$.

(f) Row 6

⊙	0.38268 1.00000	0.38268 0.98079	0.38268 0.92388	0.38268 0.83147	0.38268 0.70711	0.38268 0.55557	0.38268 0.38268	0.38268 0.19509	0.38268 0
⊙	-0.61732	-0.69811	-0.54120	-0.44879	-0.32443	-0.17289	0	0.18759	0.38268
⊙	-1.61991	-1.67193	-1.84775	-2.22821	-3.08233	-5.78402	∞	5.33077	2.61315
⊙	0.72323	0.73342	0.76537	0.82362	0.91761	1.06581	1.30657	1.73079	2.61315
⊙	0.38108	0.35774	0.29290	0.20141	0.10525	0.02989	0	0.03519	0.14644
⊙	1.91180	1.85905	1.70710	1.47416	1.18764	0.89031	0.58578	0.33382	0.14644
⊙	0.14644	0.14644	0.14644	0.14644	0.14644	0.14644	0.14644	0.14644	0.14644
⊙									
⊙									
⊙							(*)		

* For $\eta^* = \gamma^*$, $\ominus = \tan \Delta / \odot$.

TABLE VIII.—COMPUTING PROCEDURE FOR *F* FUNCTIONS—Concluded

(g) Row 7

⊙ ⊙ ⊙ ⊙ ⊙	0.19509 1.00000 -0.80491 -1.24237 0.83676	0.19509 0.98079 -0.78570 -1.37275 0.85043	0.19509 0.92388 -0.72879 -1.37214 0.89368	0.19509 0.83147 -0.63638 -1.57139 0.97413	0.19509 0.70711 -0.51202 -1.95305 1.10840	0.19509 0.55557 -0.38048 -2.77408 1.33216	0.19509 0.38268 -0.18759 -5.33077 1.73079	0.19509 0.19509 0 ∞ 2.66292	0.19509 0 0.19509 5.12584 5.12584
⊙ ⊙ ⊙ ⊙ ⊙	0.64788 1.42834 0.03806	0.61732 1.38269 0.03806	0.53113 1.25209 0.03806	0.40498 1.05383 0.03806	0.28216 0.81396 0.03806	0.12995 0.56349 0.03806	0.03519 0.33382 0.03806	0 0.15234 0.03806	0.03806 0.03806 0.03806
⊙ ⊙ ⊙ ⊙ ⊙									
⊙ ⊙ ⊙ ⊙ ⊙									
⊙ ⊙ ⊙ ⊙ ⊙								(*)	

* For $\eta^* = \eta^*$, $\ominus = \tan \Delta / \Theta$.

(h) Row 8

⊙ ⊙ ⊙ ⊙ ⊙	0 1.00000 -1.00000 -1.00000 1.00000	0 0.98079 -0.78570 -1.01959 1.01959	0 0.92388 -0.72879 -1.08239 1.08239	0 0.83147 -0.63638 -1.20269 1.20269	0 0.70711 -0.51202 -1.41421 1.41421	0 0.55557 -0.38048 -1.79995 1.79995	0 0.38268 -0.18759 -2.61315 2.61315	0 0.19509 -0.19509 -5.12584 5.12584	0 0 0 ∞ ∞
⊙ ⊙ ⊙ ⊙ ⊙	1.00000 1.00000 0	0.96195 0.96195 0	0.83355 0.86356 0	0.69134 0.69134 0	0.50000 0.50000 0	0.30866 0.30866 0	0.14644 0.14644 0	0.03806 0.03806 0	0 0 0
⊙ ⊙ ⊙ ⊙ ⊙									
⊙ ⊙ ⊙ ⊙ ⊙									
⊙ ⊙ ⊙ ⊙ ⊙									(*)

* For $\eta^* = \eta^*$, $\ominus = \tan \Delta / \Theta$.

TABLE IX.—SYMMETRIC AND ANTISYMMETRIC F MATRICES FOR PLAN FORM 333

$2[F_s] =$

7.5947	8.3357	10.4164	12.6323	14.1611	14.9907	15.4435	15.6705	15.7393
5.4247	5.9650	7.8390	10.0672	12.7094	13.7911	14.3488	14.6188	14.6999
3.3866	3.6601	4.6921	7.1238	10.1734	11.0020	12.7114	13.0781	13.1849
2.0610	2.1859	2.6370	3.7462	6.2896	6.2061	10.6338	11.2167	11.3777
1.2484	1.3057	1.5099	1.9676	3.0125	5.3952	7.9725	9.0854	9.3707
0.7125	0.7409	0.8360	1.0357	1.4434	2.3579	4.4096	6.4724	7.0692
0.3229	0.3345	0.3728	0.4498	0.5975	0.8970	1.5789	3.0437	4.0507

$2[F_a] =$

-8.0860	-8.3357	-8.2265	-3.9097	-2.3552	-1.4171	-0.8120	-0.3720	
-10.2361	-9.7433	-7.5390	-4.9575	-2.8344	-1.6368	-0.9156	-0.4143	
-10.9636	-10.6795	-9.6142	-7.1238	-3.9851	-2.1270	-1.1327	-0.5000	
-10.7385	-10.6013	-10.1123	-8.9332	-6.2896	-3.2216	-1.5732	-0.6636	
-9.9951	-9.9214	-9.6724	-9.1347	-7.9649	-5.3952	-2.5379	-0.9930	
-9.0043	-9.0182	-8.8677	-8.5679	-8.0014	-6.8424	-4.4096	-1.7216	
-8.1161	-8.0817	-7.9720	-7.7636	-7.4021	-6.7815	-5.5163	-3.0437	
-7.2195	-7.1891	-7.0920	-6.9106	-6.6056	-6.0935	-5.1811	-3.3901	

TABLE X.—INTEGRATING MATRICES FOR LOAD AND MOMENT COEFFICIENTS

$[I_{C_L}] =$

[0.01915 0.03757 0.05454 0.06942 0.08163 0.09070 0.09829 0.04909]

$[I_{C_{D_M}}] =$

[0.01878 0.03472 0.04533 0.04913 0.04528 0.03487 0.01833 0.00196]

$[I_{C_{r, \beta}}] =$

[0.01993 0.03596 0.05713 0.06556 0.06736 0.08164 0.11365]

$[I_{C_1}] =$

[0.00939 0.01735 0.02267 0.02454 0.02267 0.01736 0.00939]

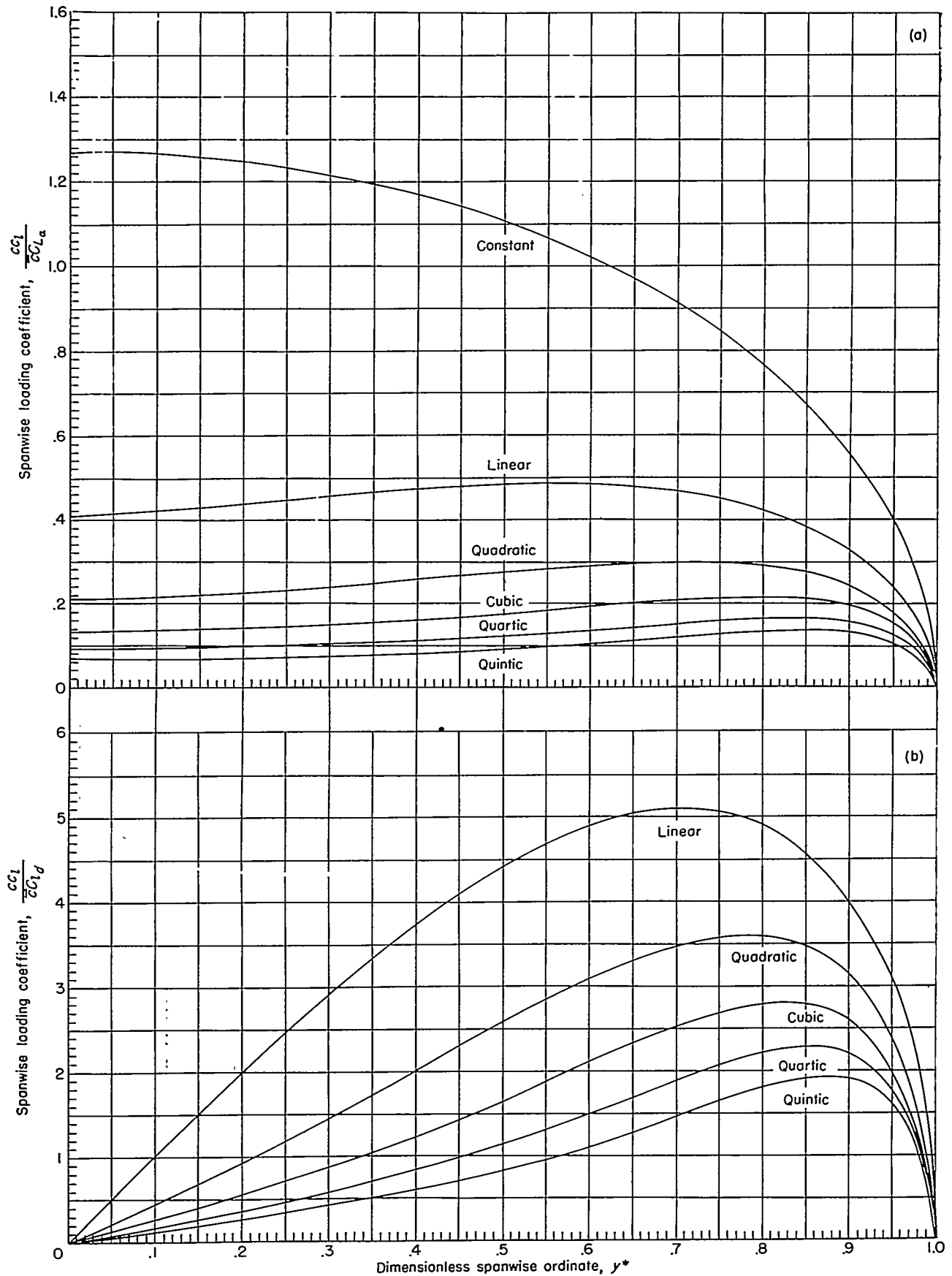
TABLE XI.—VALUES OF $[[\cos n\theta]^{-1} \{H_n(\theta_0)\}]$ FOR FLAP AND AILERON DEFLECTIONS

$[[\cos n\theta]^{-1} \{H_n(\theta_0)\}]$ for—

$\frac{b_{aft}}{b} = 0.1$	$\frac{b_{aft}}{b} = 0.2$	$\frac{b_{aft}}{b} = 0.3$	$\frac{b_{aft}}{b} = 0.4$	$\frac{b_{aft}}{b} = 0.5$	$\frac{b_{aft}}{b} = 0.6$	$\frac{b_{aft}}{b} = 0.7$	$\frac{b_{aft}}{b} = 0.8$	$\frac{b_{aft}}{b} = 0.9$	$\frac{b_{aft}}{b} = 1.0$
-0.04894	-0.07961	-0.08874	-0.09615	-0.11144	-0.11592	-0.11700	-0.12187	-0.12514	-0.12549
-0.09847	-0.12346	-0.16690	-0.19603	-0.19865	-0.21572	-0.23305	-0.23637	-0.23746	-0.23934
0.04411	-0.09144	-0.12048	-0.14009	-0.17888	-0.18994	-0.19251	-0.20405	-0.21175	-0.21257
0.05663	0.09988	-0.03286	-0.09620	-0.10056	-0.12701	-0.15286	-0.15743	-0.15897	-0.16159
0.01030	0.09762	0.17937	0.08128	-0.03033	-0.05553	-0.06038	-0.08125	-0.09471	-0.09611
0.01700	0.02748	0.10254	0.23444	0.22592	0.10376	0.02309	0.01046	0.00692	0.00099
0.00682	0.03686	0.05288	0.08880	0.22801	0.33365	0.28602	0.17519	0.13191	0.11696
0.01140	0.01794	0.05243	0.09196	0.09876	0.18369	0.35407	0.44468	0.39113	0.33720
0.00236	0.01474	0.02078	0.03205	0.06718	0.08312	0.09240	0.17064	0.30809	0.37995

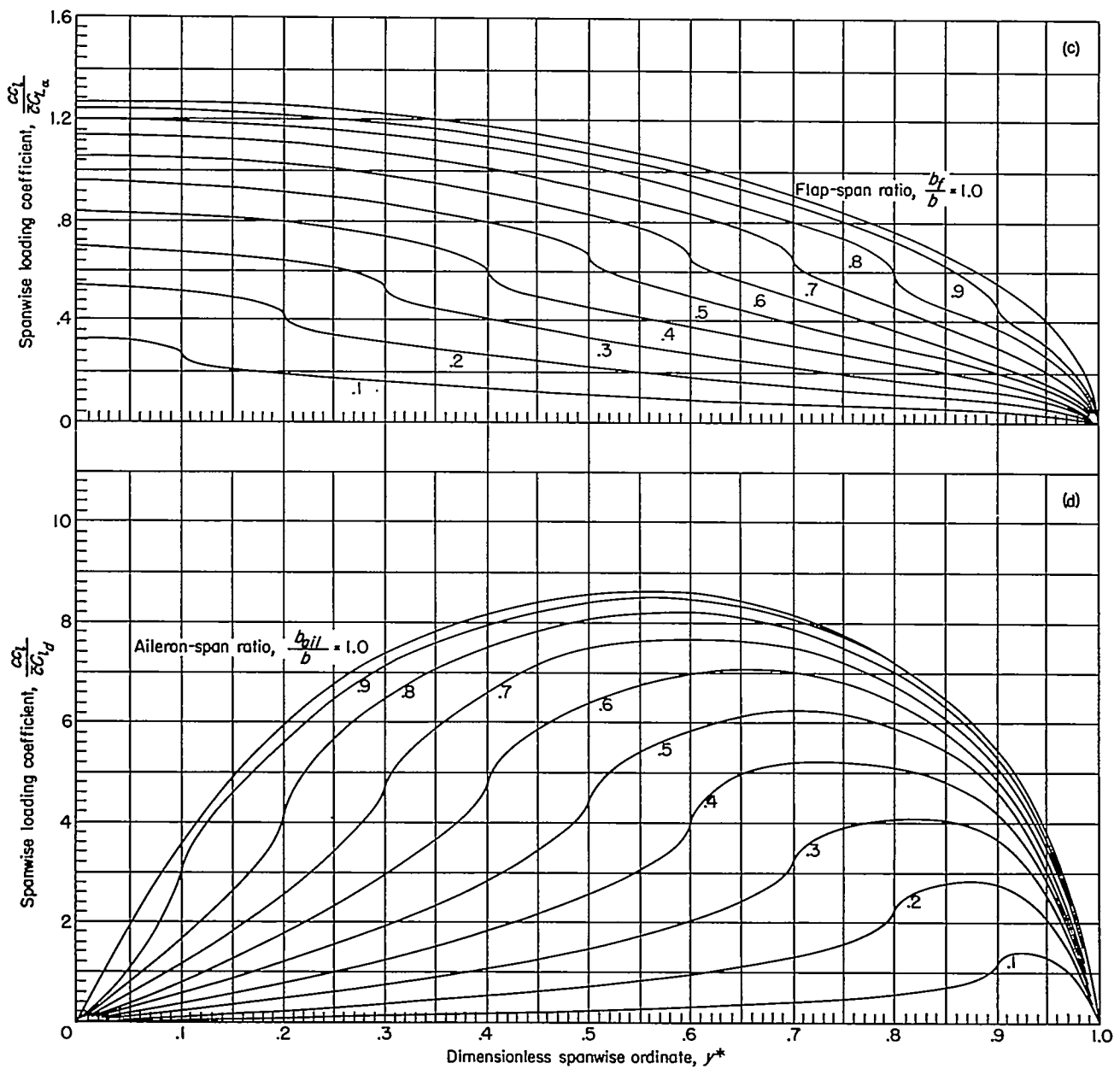
$[[\cos n\theta]^{-1} \{H_n(\theta_0)\}]$ for—

$\frac{b_f}{b} = 0.1$	$\frac{b_f}{b} = 0.2$	$\frac{b_f}{b} = 0.3$	$\frac{b_f}{b} = 0.4$	$\frac{b_f}{b} = 0.5$	$\frac{b_f}{b} = 0.6$	$\frac{b_f}{b} = 0.7$	$\frac{b_f}{b} = 0.8$	$\frac{b_f}{b} = 0.9$
0.00472	0.02580	0.04580	0.04912	0.05868	0.06855	0.06817	0.10994	0.14625
0.04146	0.06006	0.06200	0.10995	0.14795	0.19694	0.19728	0.25848	0.28138
0.01022	0.06006	0.09894	0.10718	0.12894	0.17257	0.22262	0.25718	0.40451
0.04896	0.05117	0.07378	0.13387	0.18370	0.17950	0.26966	0.41746	0.37740
0.01941	0.07451	0.13936	0.14573	0.18360	0.36530	0.43459	0.36916	0.28326
0.07384	0.08839	0.11507	0.24070	0.39275	0.34950	0.29182	0.23504	0.22685
0.02551	0.15548	0.32649	0.38258	0.29445	0.24310	0.17469	0.16677	0.15251
0.22547	0.30508	0.23760	0.14175	0.10390	0.07035	0.08960	0.08047	0.07900



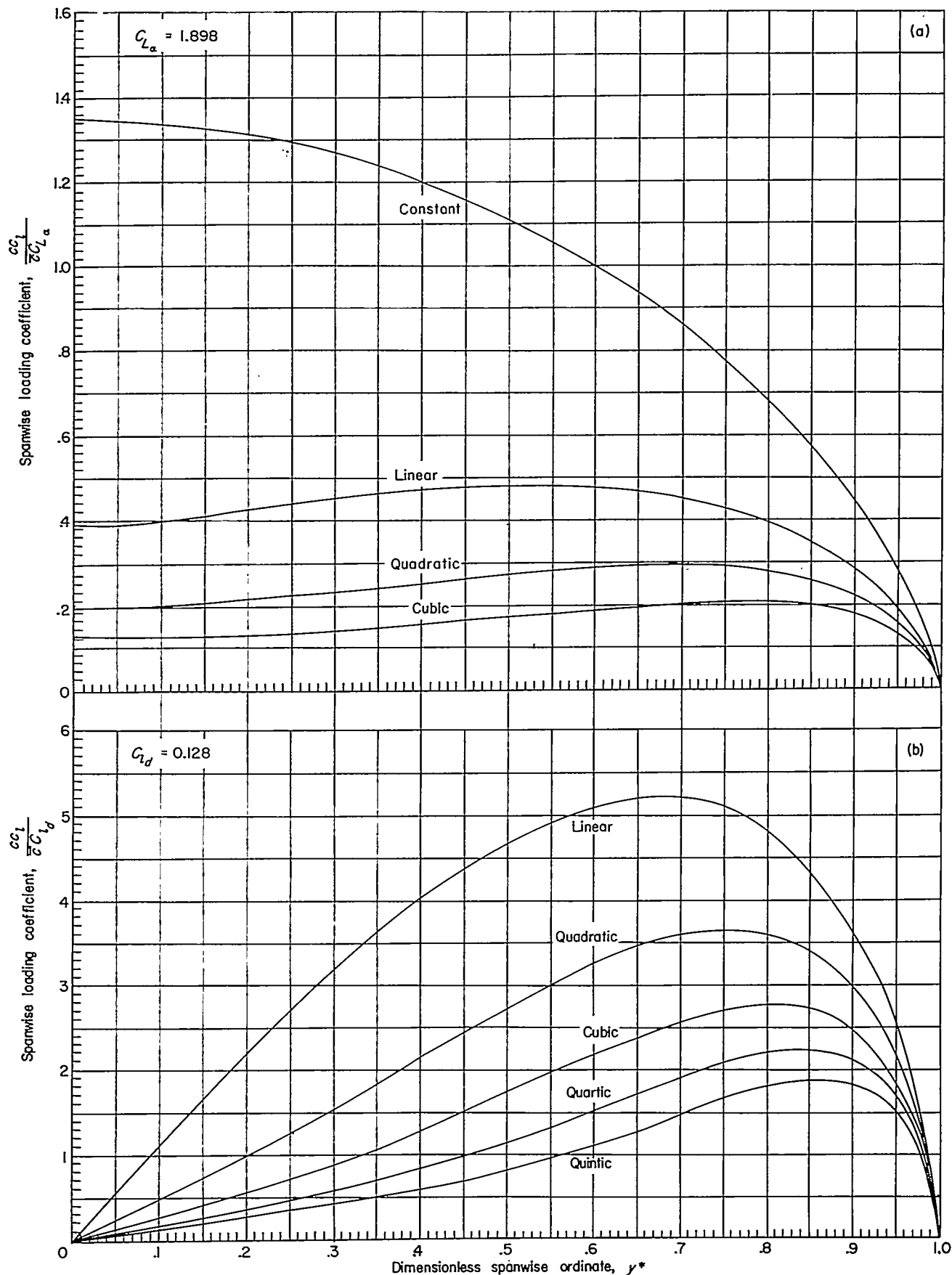
(a) Symmetrical lift distributions.
 (b) Antisymmetrical lift distributions.

FIGURE 1.—Spanwise lift distributions for wings of very low aspect ratio (from ref. 3).



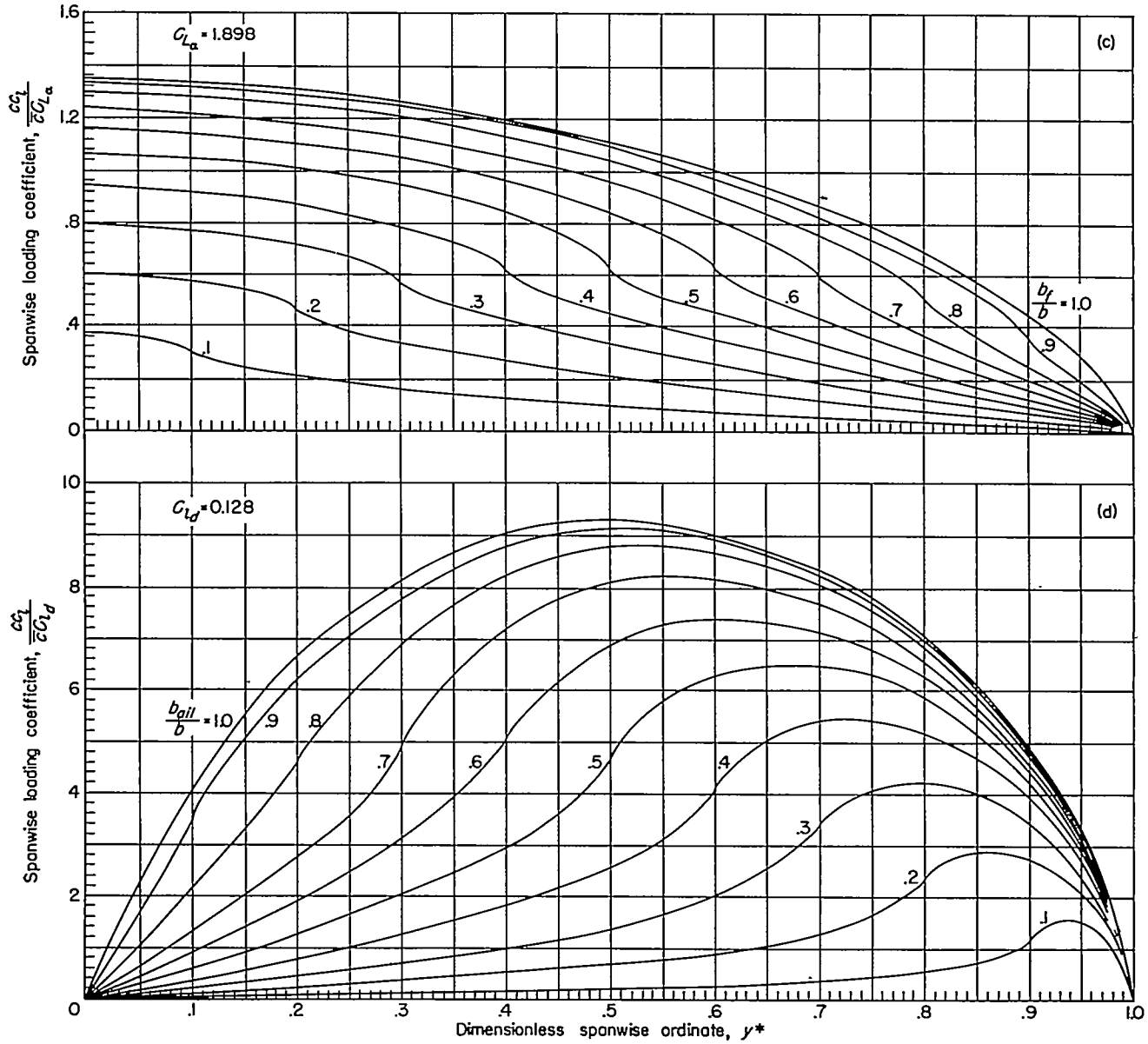
(c) Lift distribution for inboard flap.
(d) Lift distribution for outboard aileron.

FIGURE 1.—Concluded.



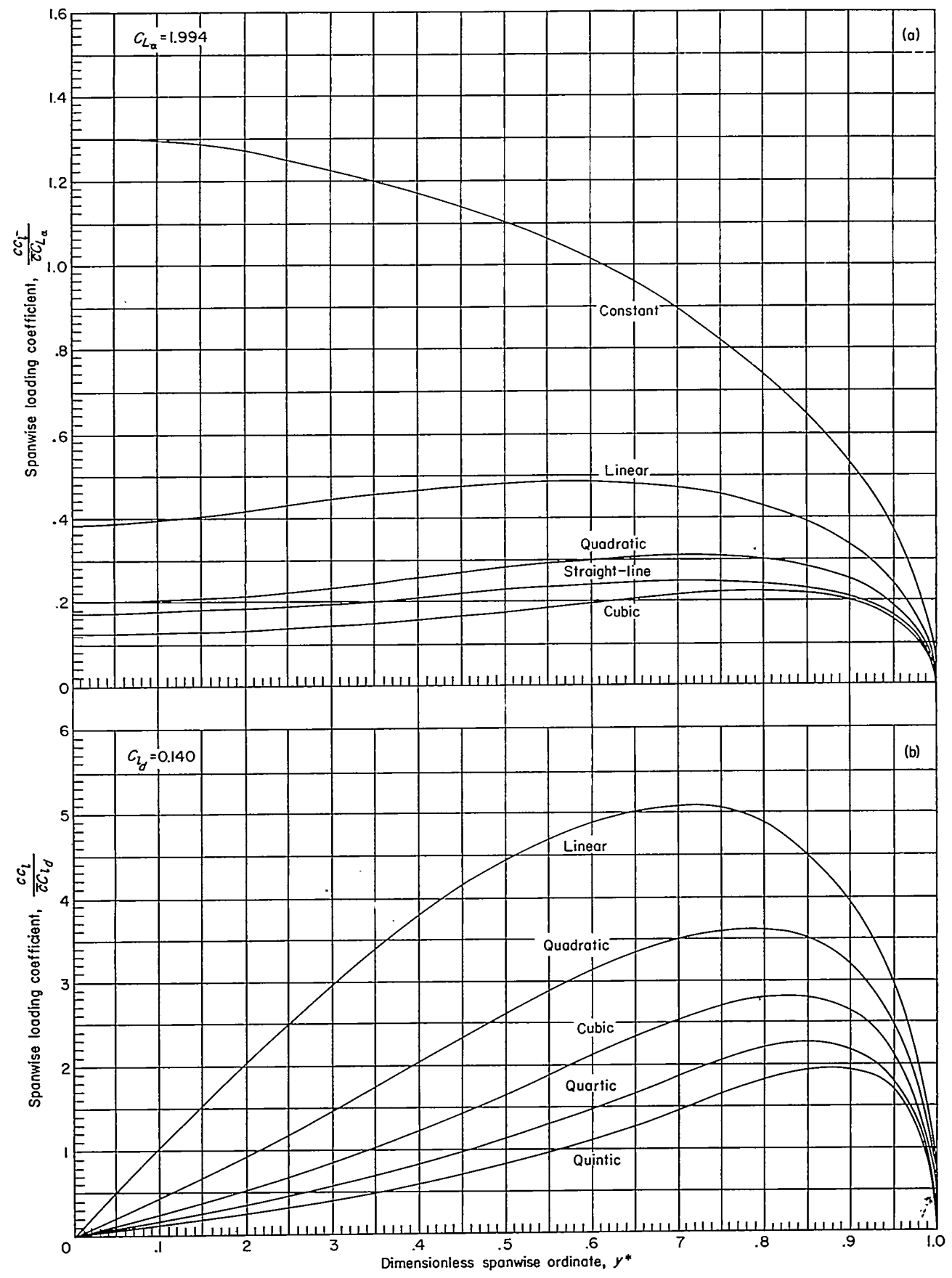
(a) Symmetrical lift distributions.
 (b) Antisymmetrical lift distributions.

FIGURE 2.—Spanwise lift distributions for plan form 311 ($A=1.5$; $\lambda=0$).



(c) Lift distribution for inboard flap.
(d) Lift distribution for outboard aileron.

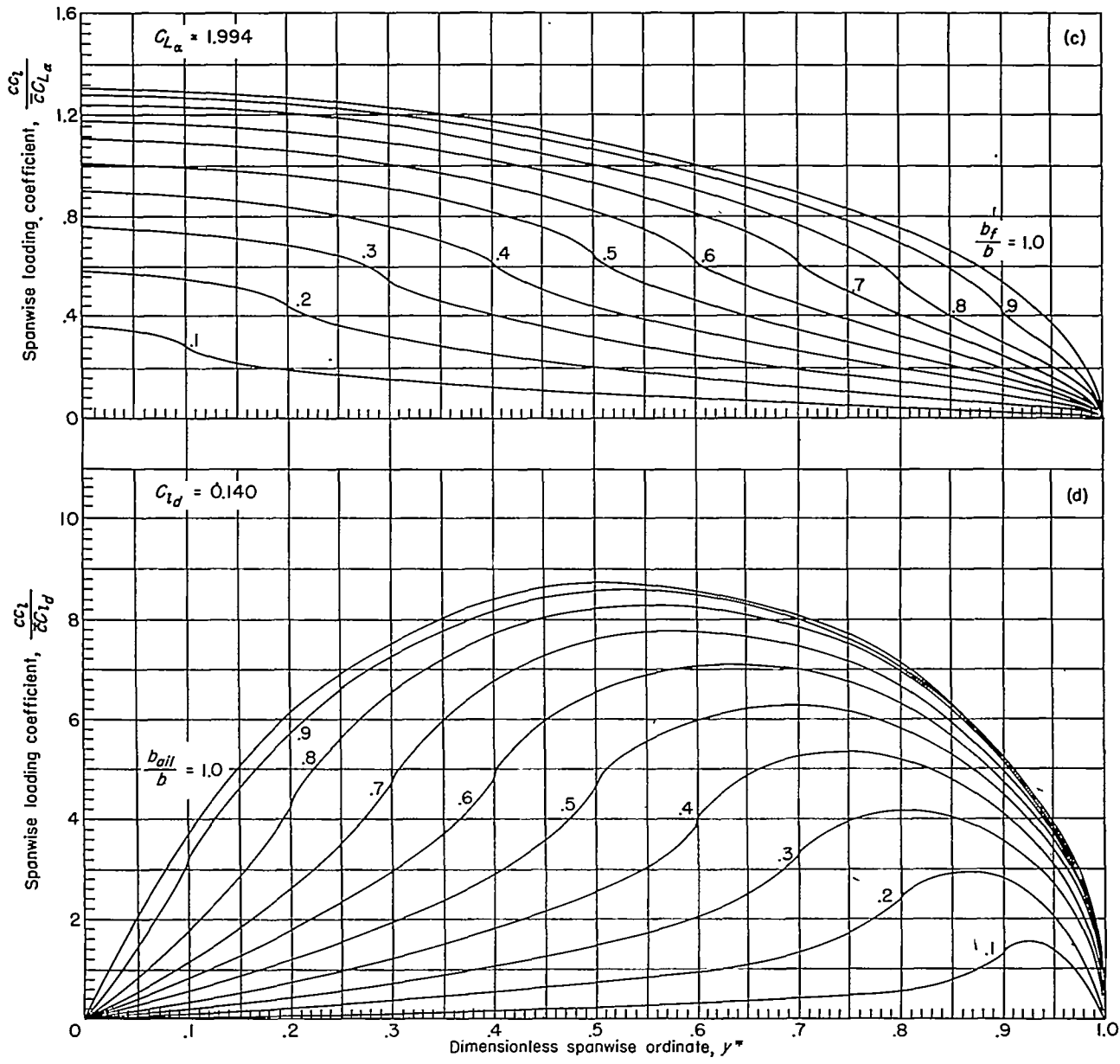
FIGURE 2.—Concluded.



(a) Symmetrical lift distributions.
 (b) Antisymmetrical lift distributions.

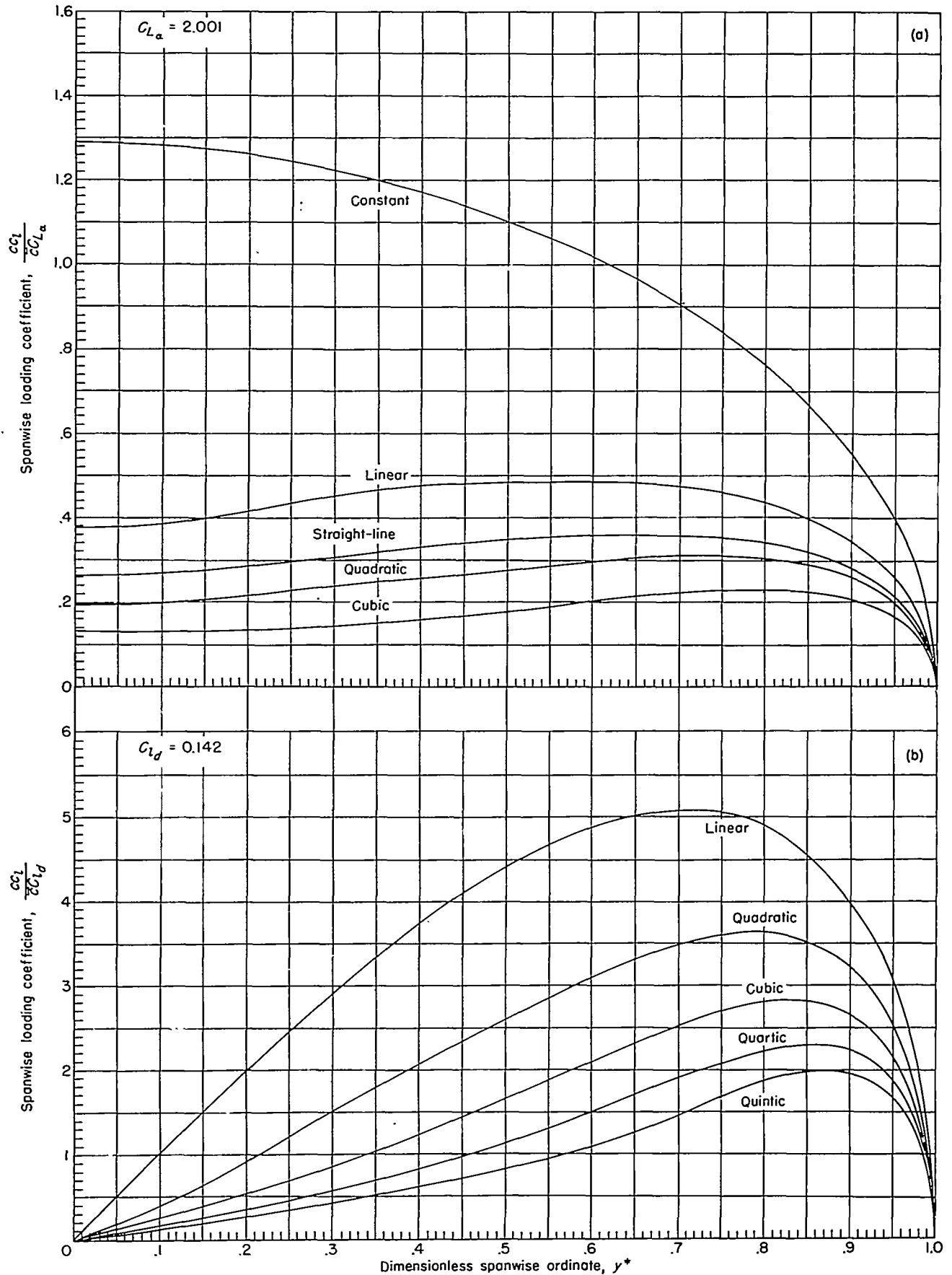
FIGURE 3.—Spanwise lift distributions for plan form 312 ($A=1.5$; $\lambda=0.25$).

SPANWISE LIFT DISTRIBUTIONS AND INFLUENCE FUNCTIONS FOR UNSWEPT WINGS IN SUBSONIC FLOW



(c) Lift distribution for inboard flap.
 (d) Lift distribution for outboard aileron.

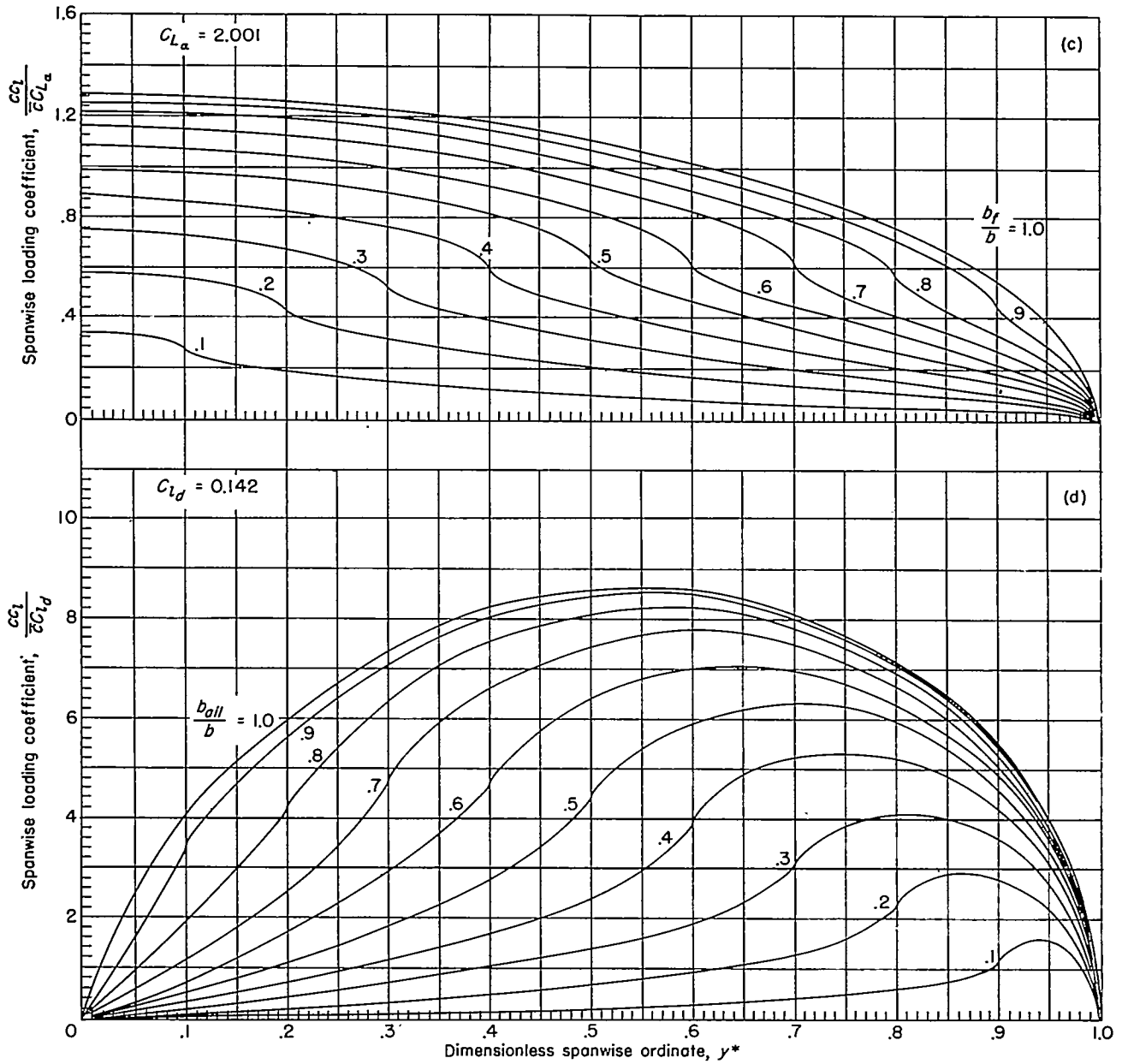
FIGURE 3.—Concluded.



(a) Symmetrical lift distributions.

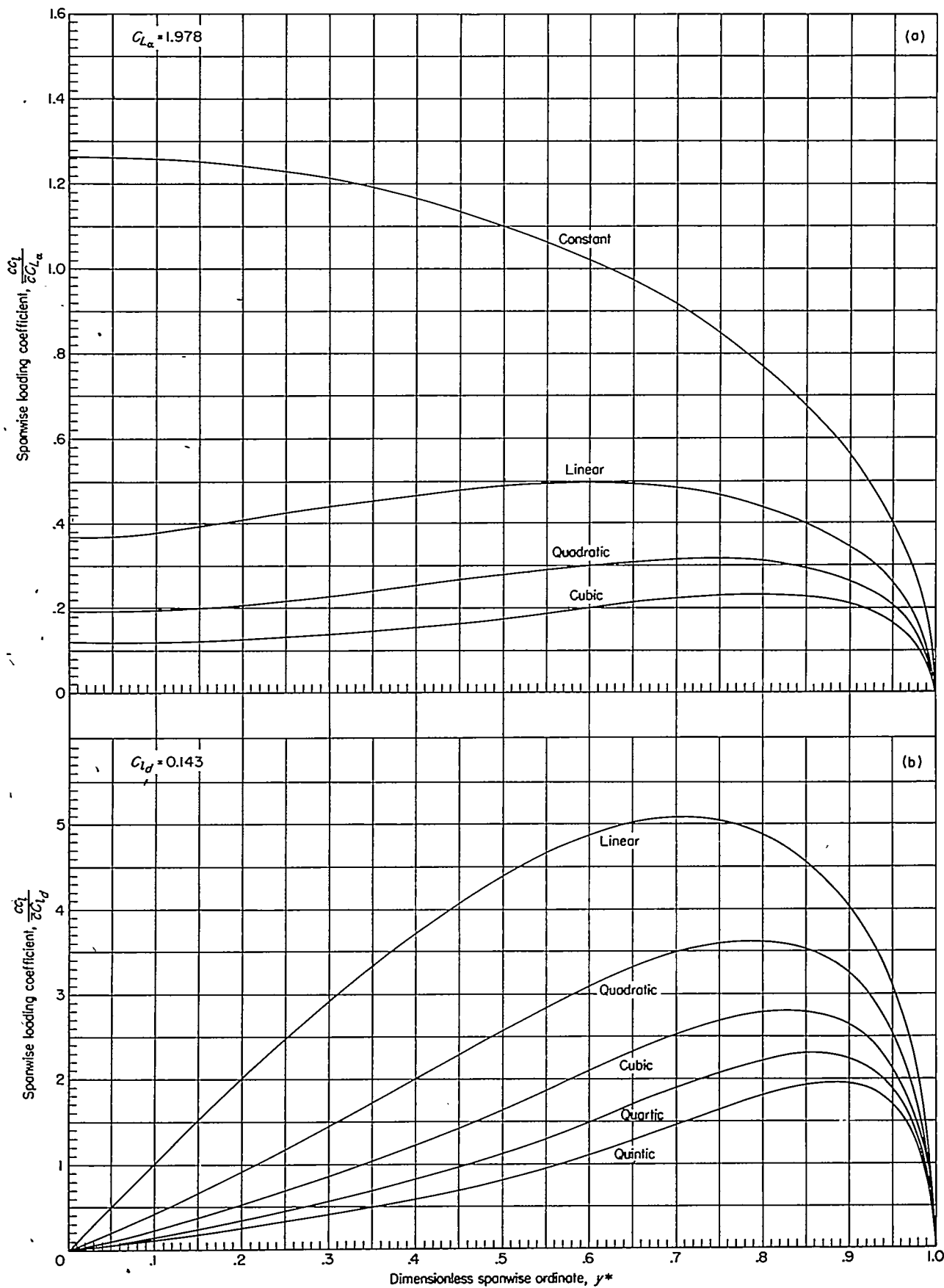
(b) Antisymmetrical lift distributions.

FIGURE 4.—Spanwise lift distributions for plan form 313 ($A=1.5$; $\lambda=0.50$).



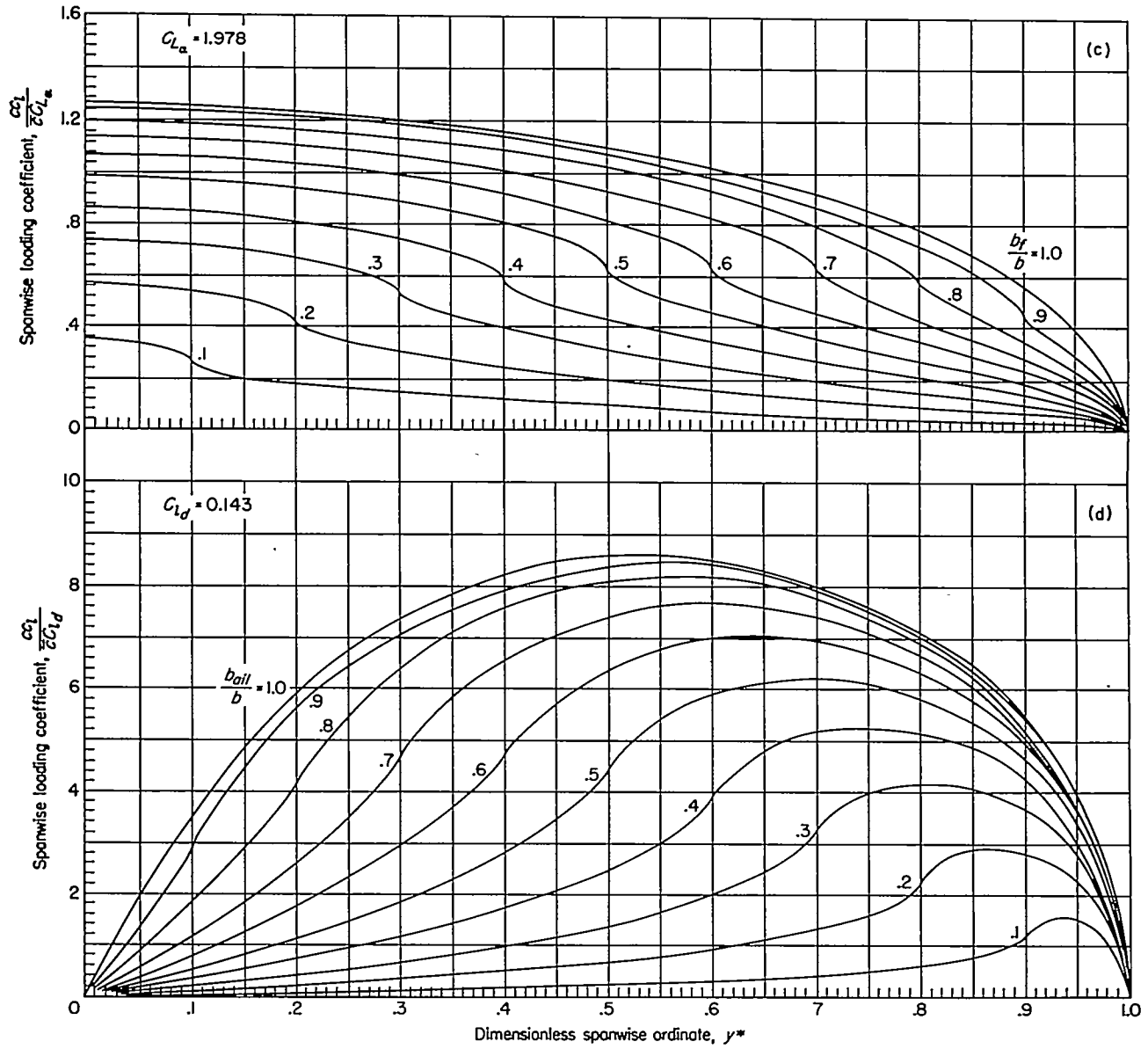
- (c) Lift distribution for inboard flap.
- (d) Lift distribution for outboard aileron.

FIGURE 4.—Concluded.



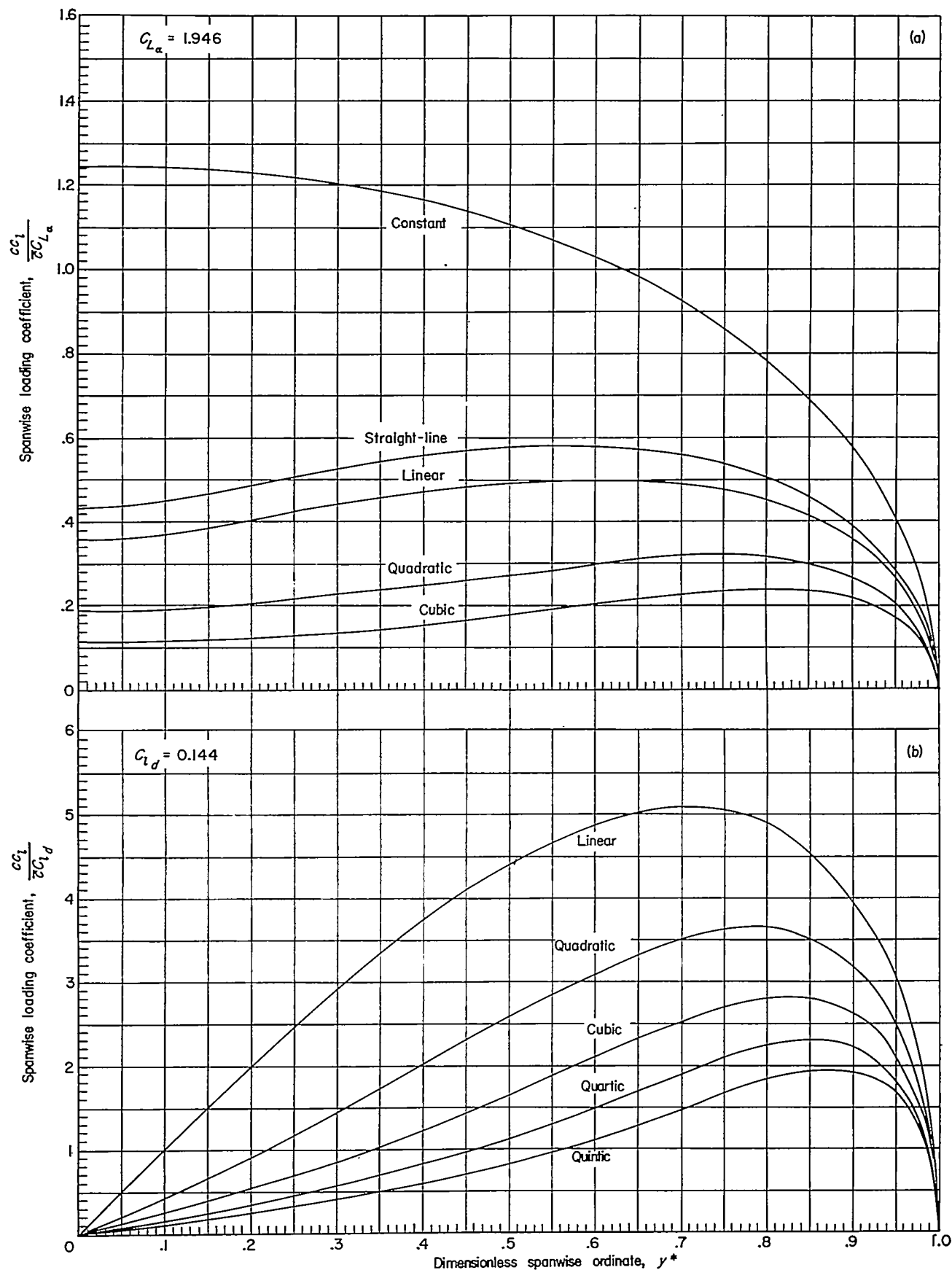
(a) Symmetrical lift distributions.
 (b) Antisymmetrical lift distributions.

FIGURE 5.—Spanwise lift distributions for plan form 314 ($A=1.5$; $\lambda=1.00$).



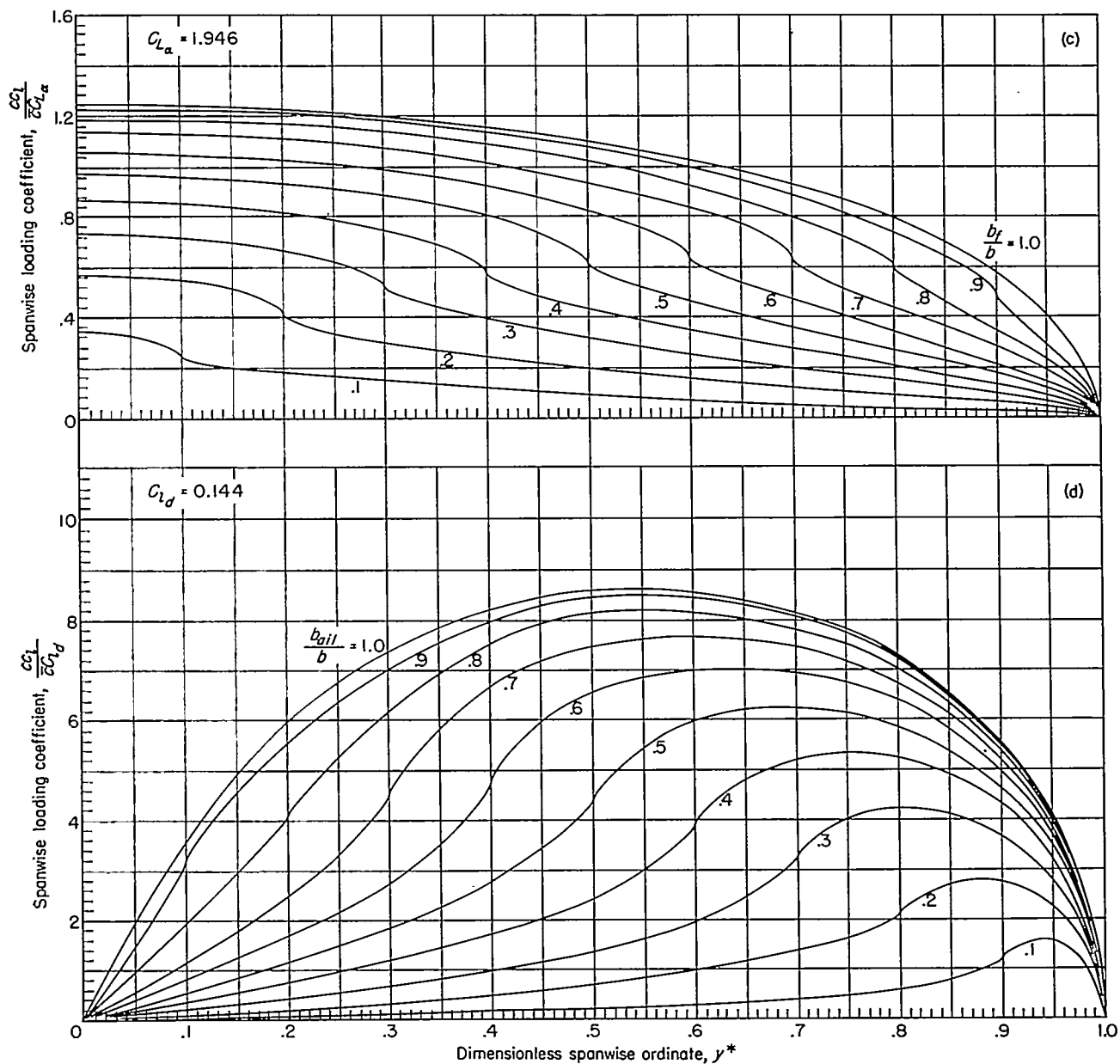
- (c) Lift distribution for inboard flap.
- (d) Lift distribution for outboard aileron.

FIGURE 5.—Concluded.



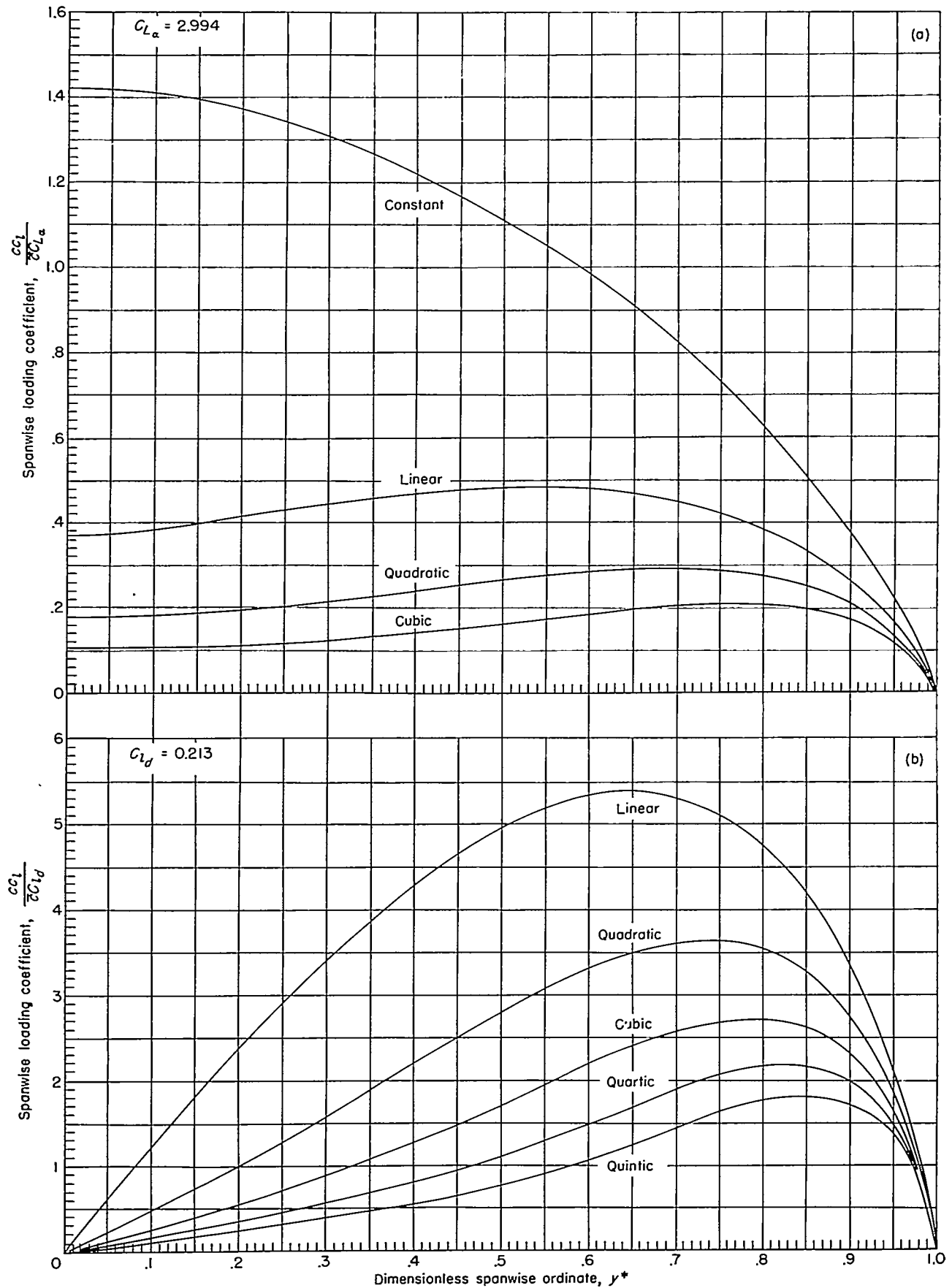
(a) Symmetrical lift distributions.
 (b) Antisymmetrical lift distributions.

FIGURE 6.—Spanwise lift distributions for plan form 315 $\bar{7}$ ($A=1.5$; $\lambda=1.50$).



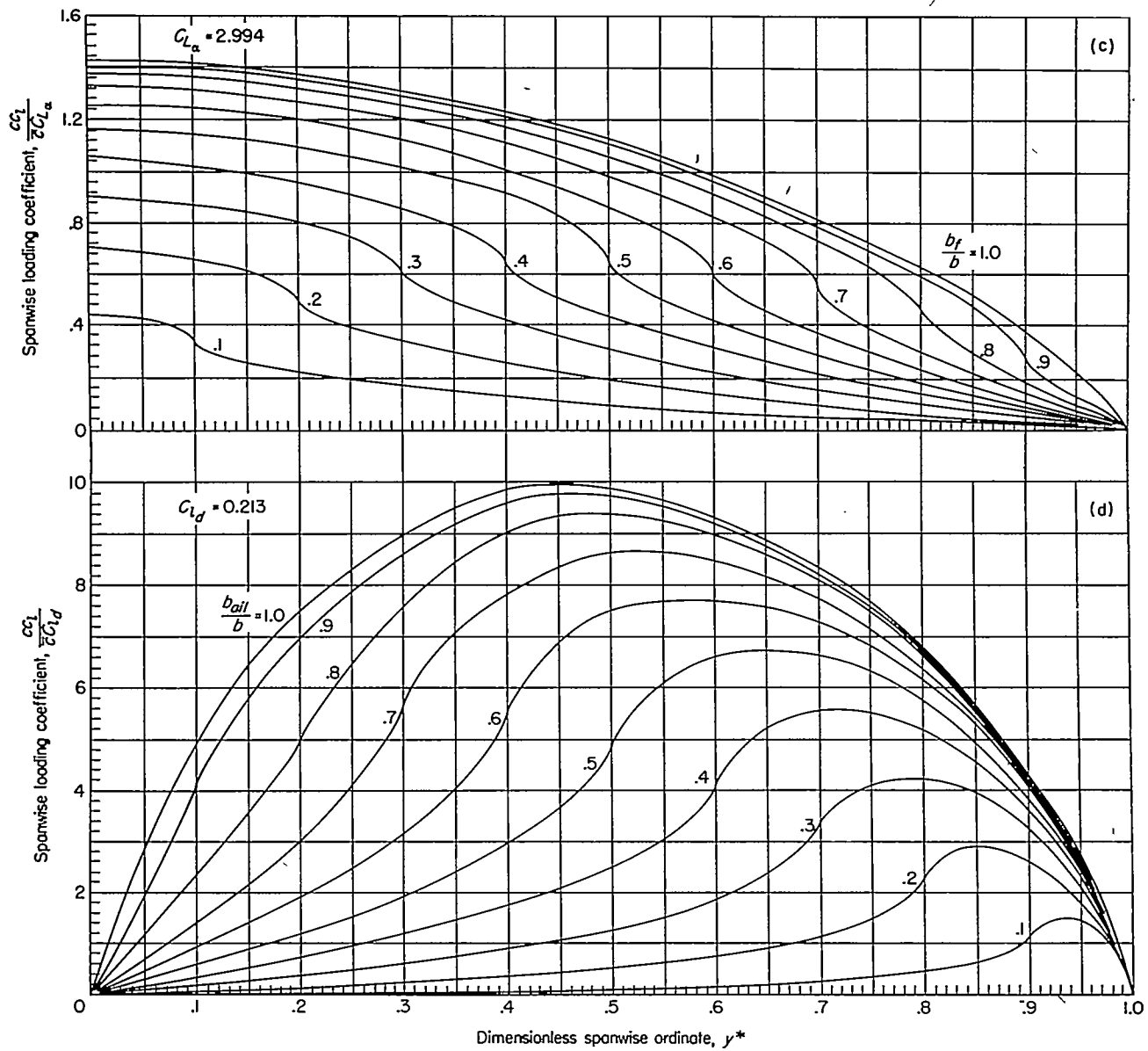
(c) Lift distribution for inboard flap.
 (d) Lift distribution for outboard aileron.

FIGURE 6.—Concluded.



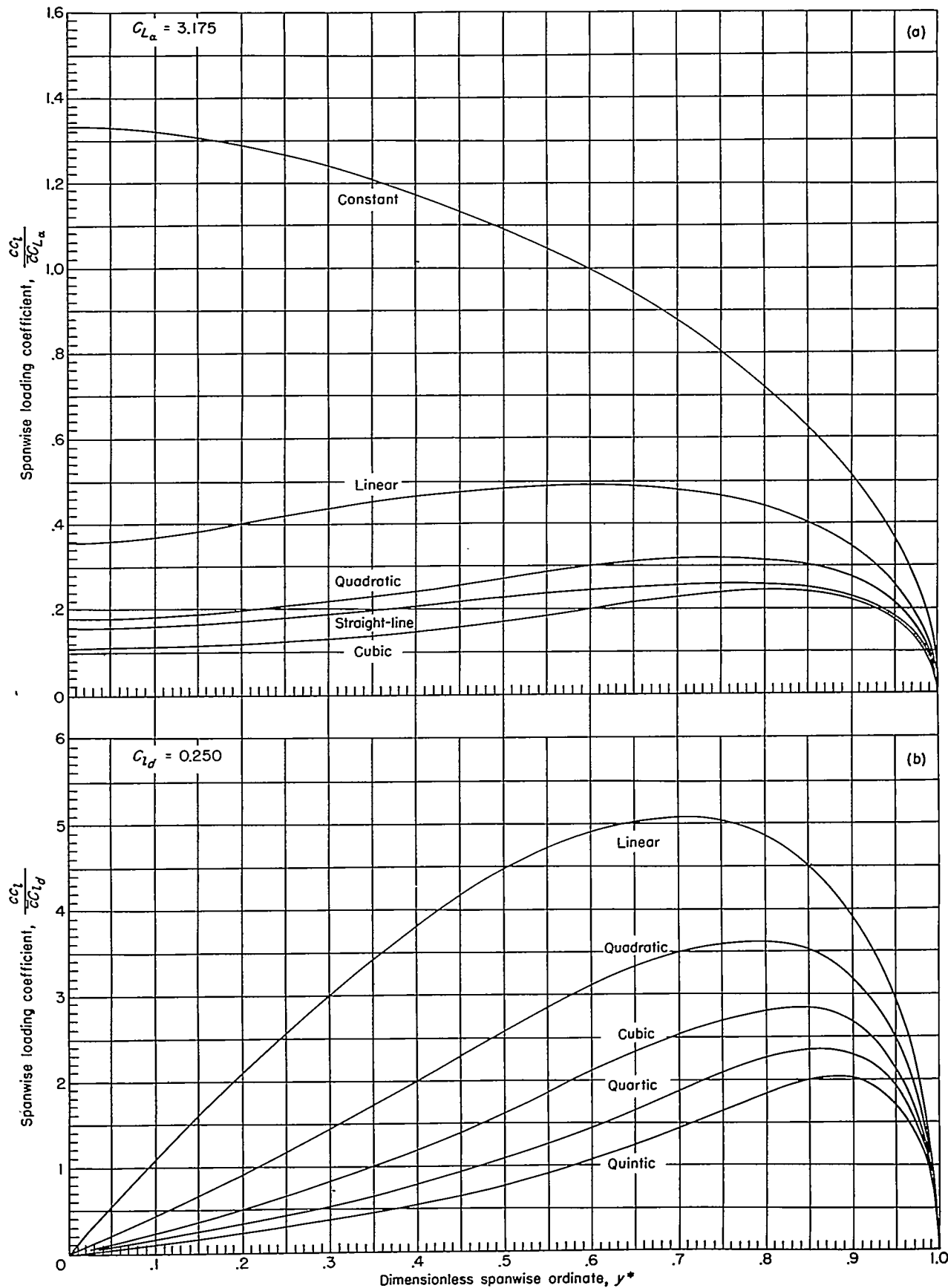
(a) Symmetrical lift distributions.
 (b) Antisymmetrical lift distributions.

FIGURE 7.—Spanwise lift distributions for plan form 321 ($A=3.0$; $\lambda=0$).



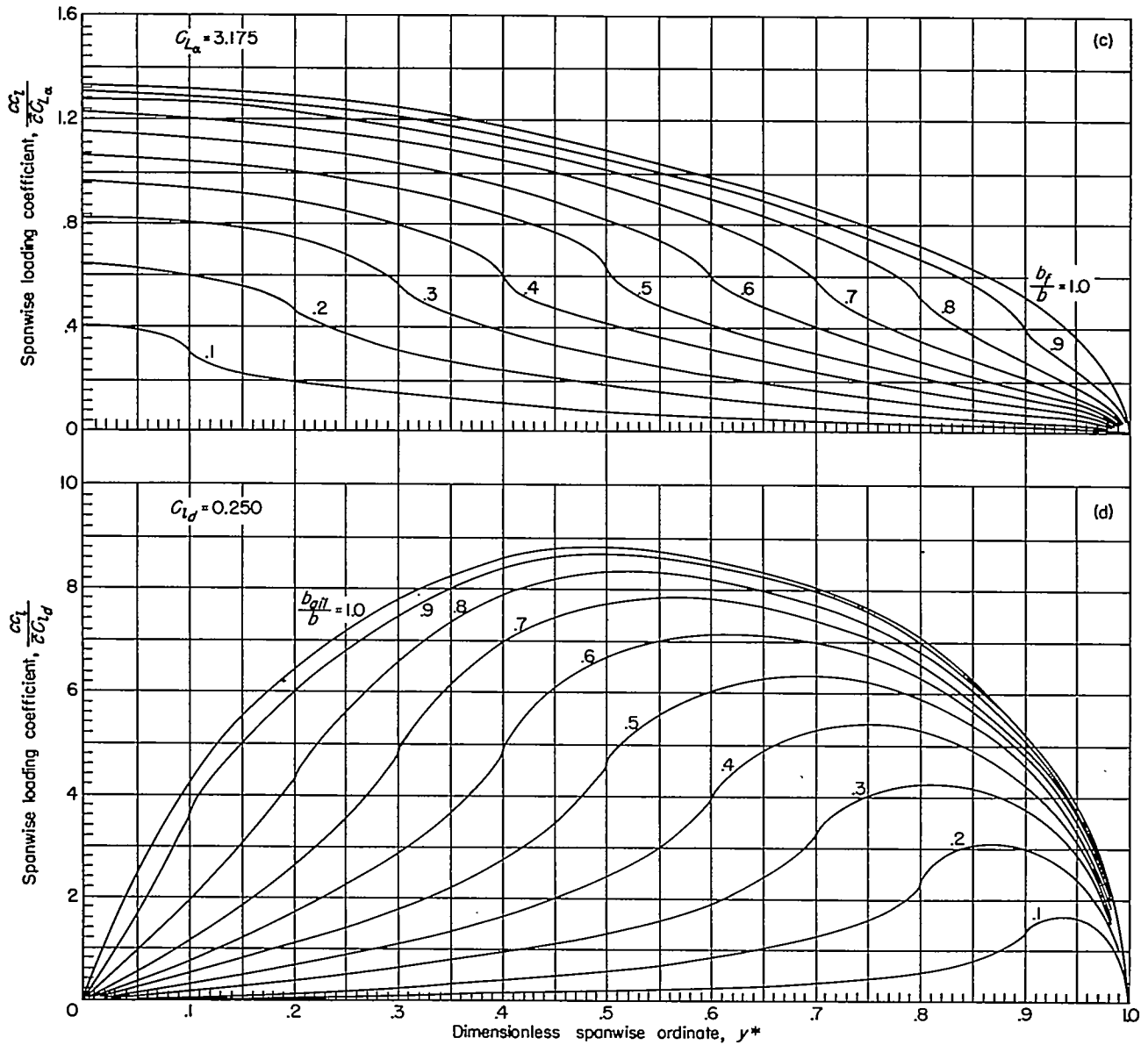
- (c) Lift distribution for inboard flap.
- (d) Lift distribution for outboard aileron.

FIGURE 7.—Concluded.



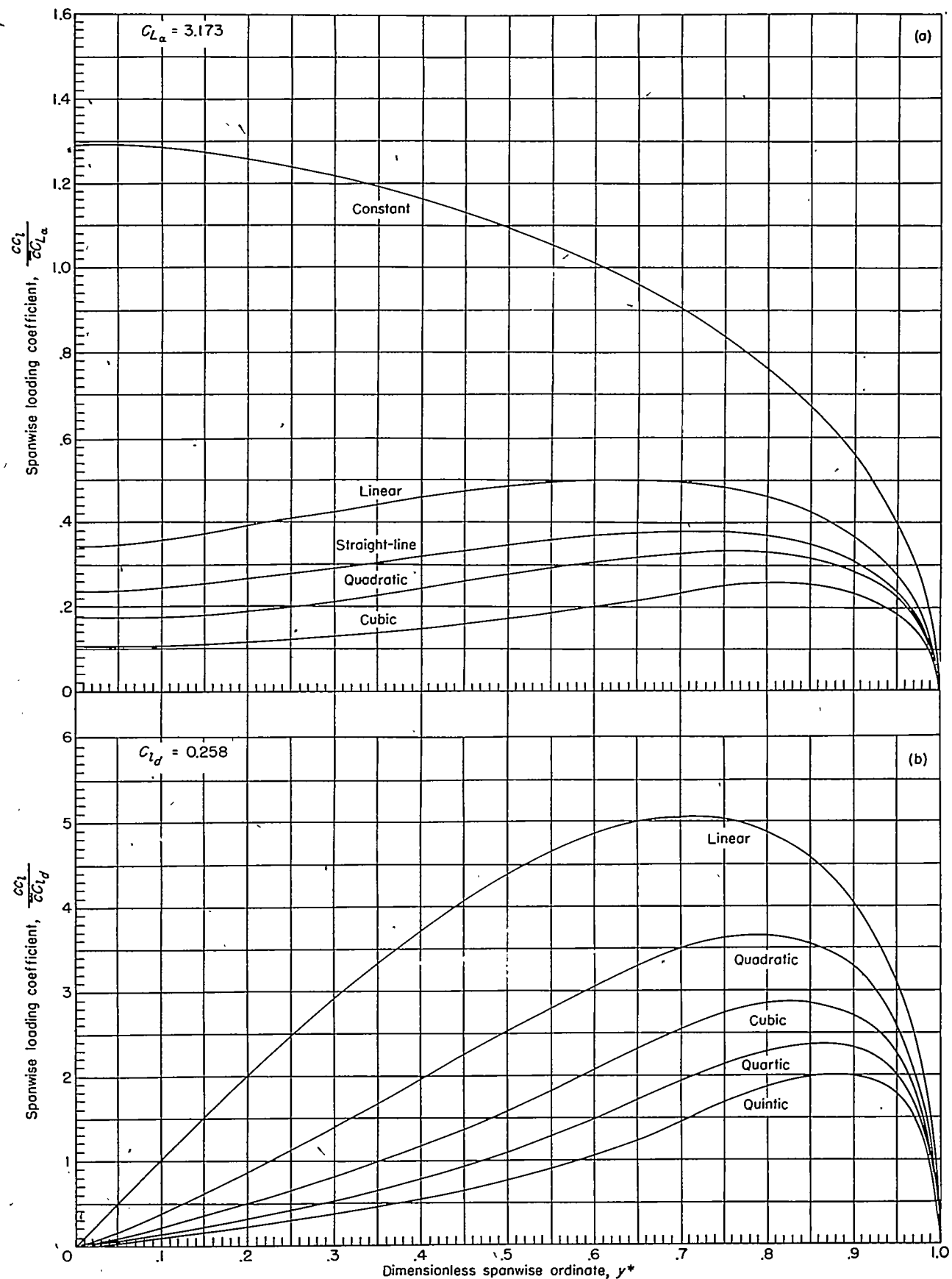
- (a) Symmetrical lift distributions.
- (b) Antisymmetrical lift distributions.

FIGURE 8.—Spanwise lift distributions for plan form 322 ($A=3.0$; $\lambda=0.25$).



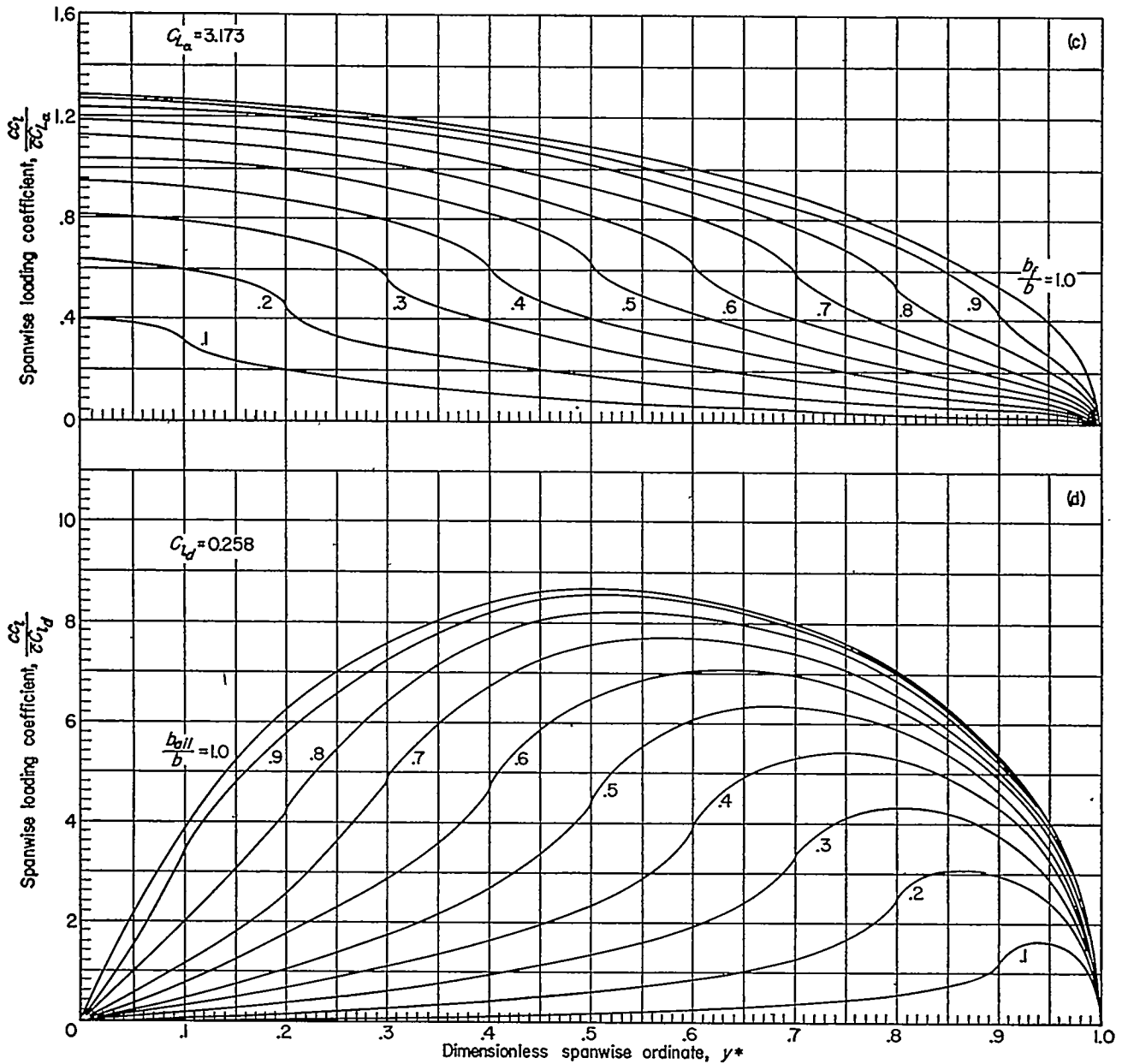
(c) Lift distribution for inboard flap.
 (d) Lift distribution for outboard aileron.

FIGURE 8.—Concluded.



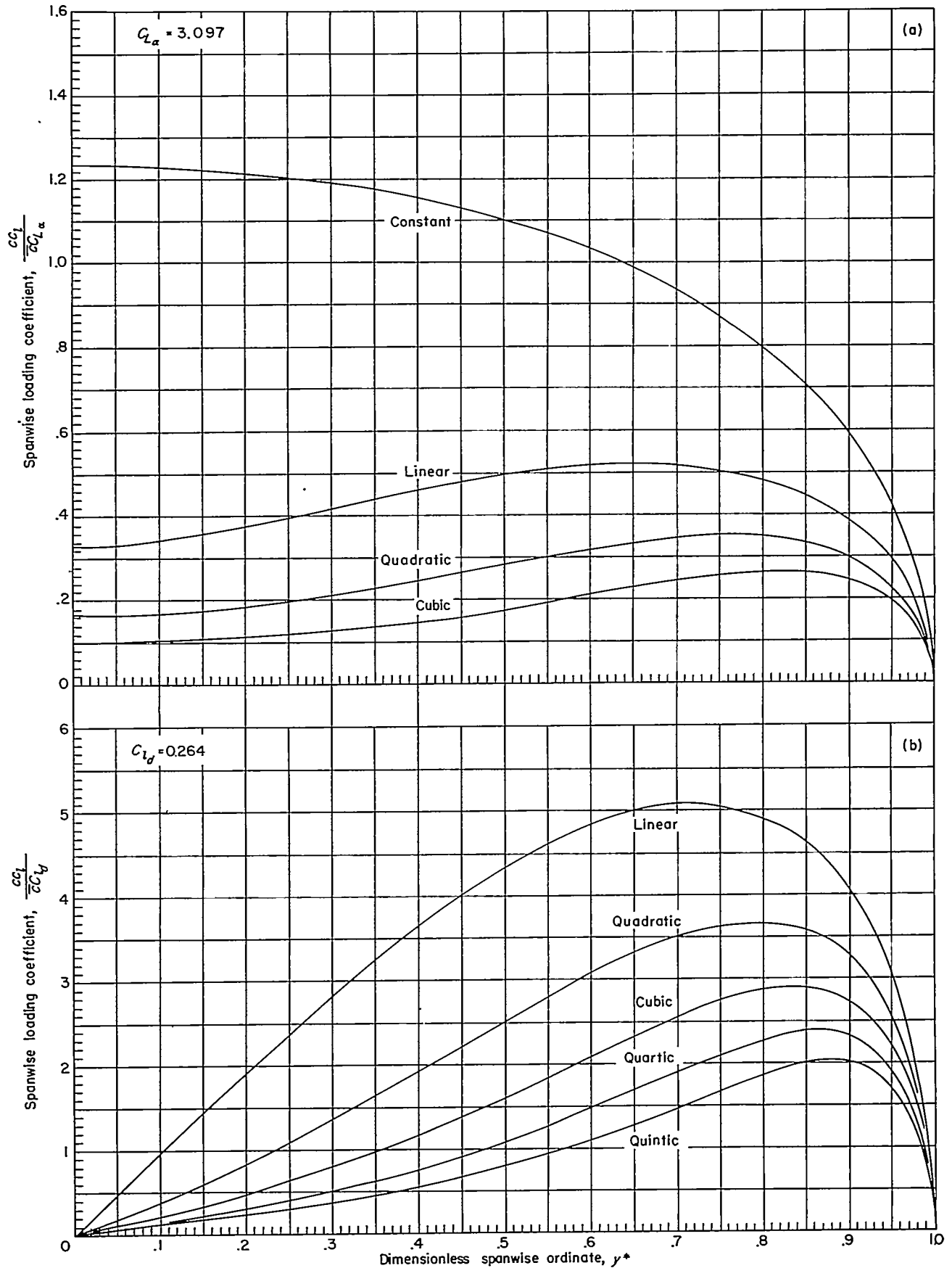
(a) Symmetrical lift distributions.
 (b) Antisymmetrical lift distributions.

FIGURE 9.—Spanwise lift distributions for plan form 323 ($A=3.0$; $\lambda=0.50$).



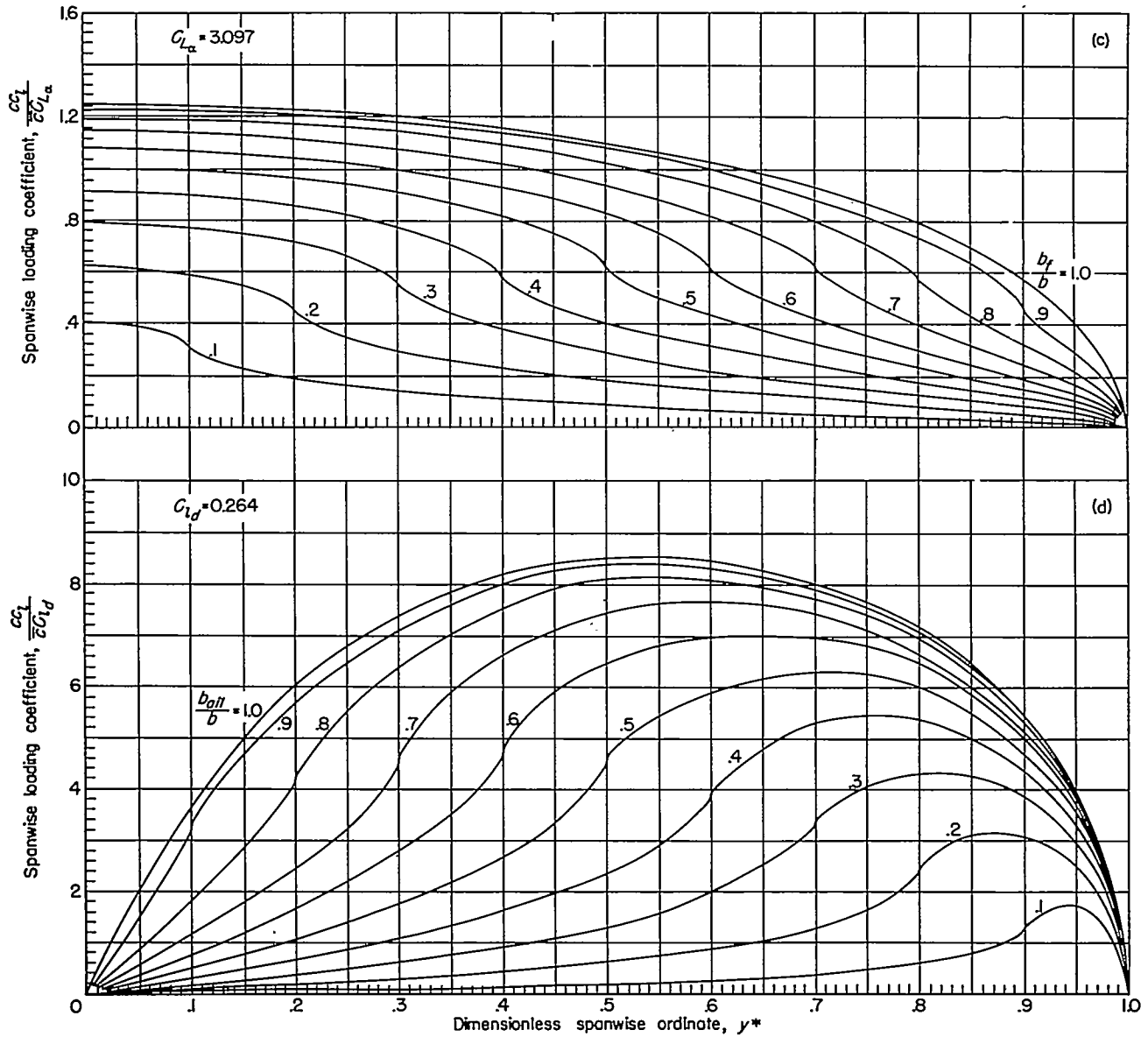
(c) Lift distribution for inboard flap.
 (d) Lift distribution for outboard aileron.

FIGURE 9.—Concluded.



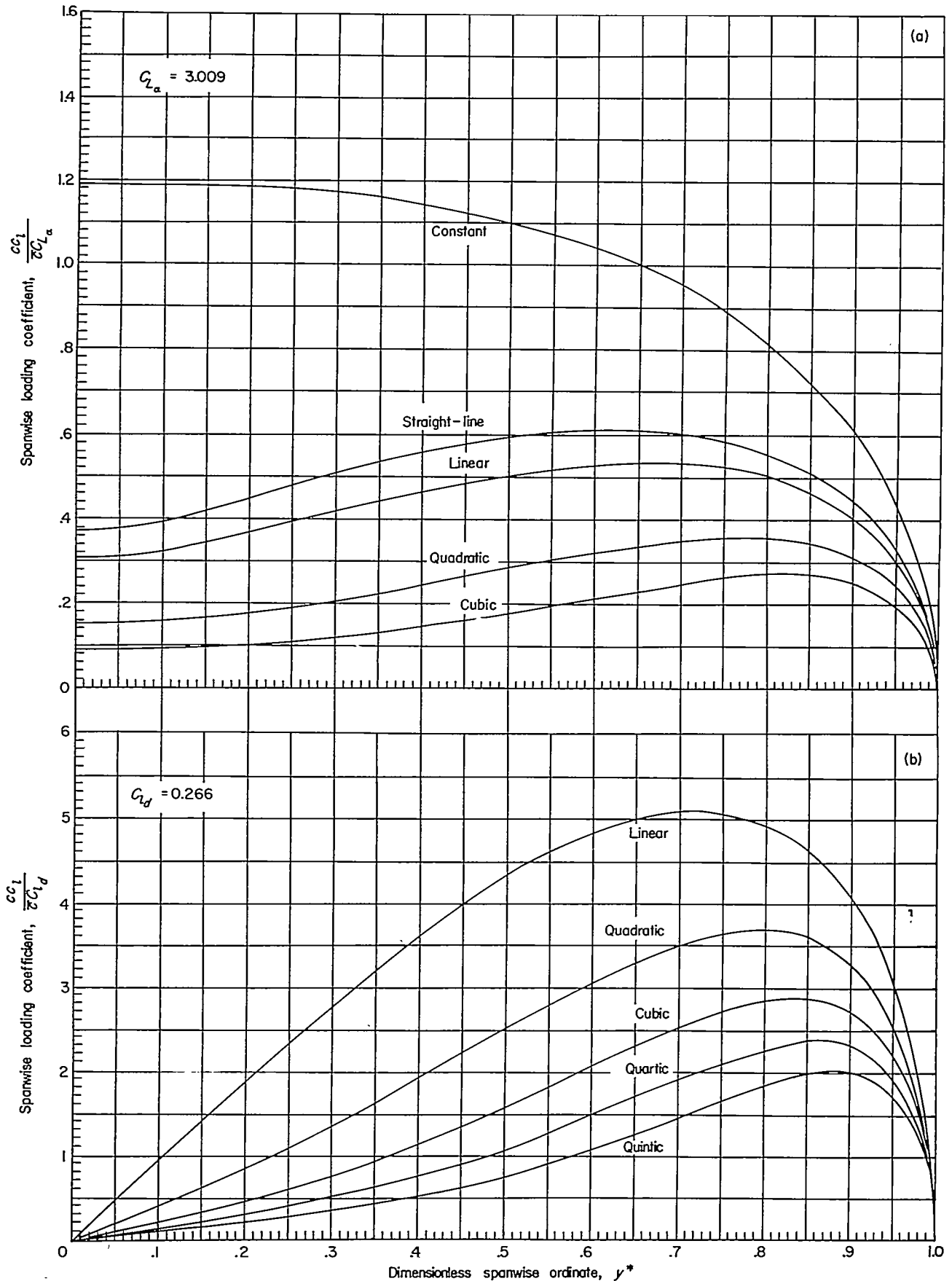
(a) Symmetrical lift distributions.
 (b) Antisymmetrical lift distributions.

FIGURE 10.—Spanwise lift distributions for plan form 324 ($A=3.0$; $\lambda=1.00$).



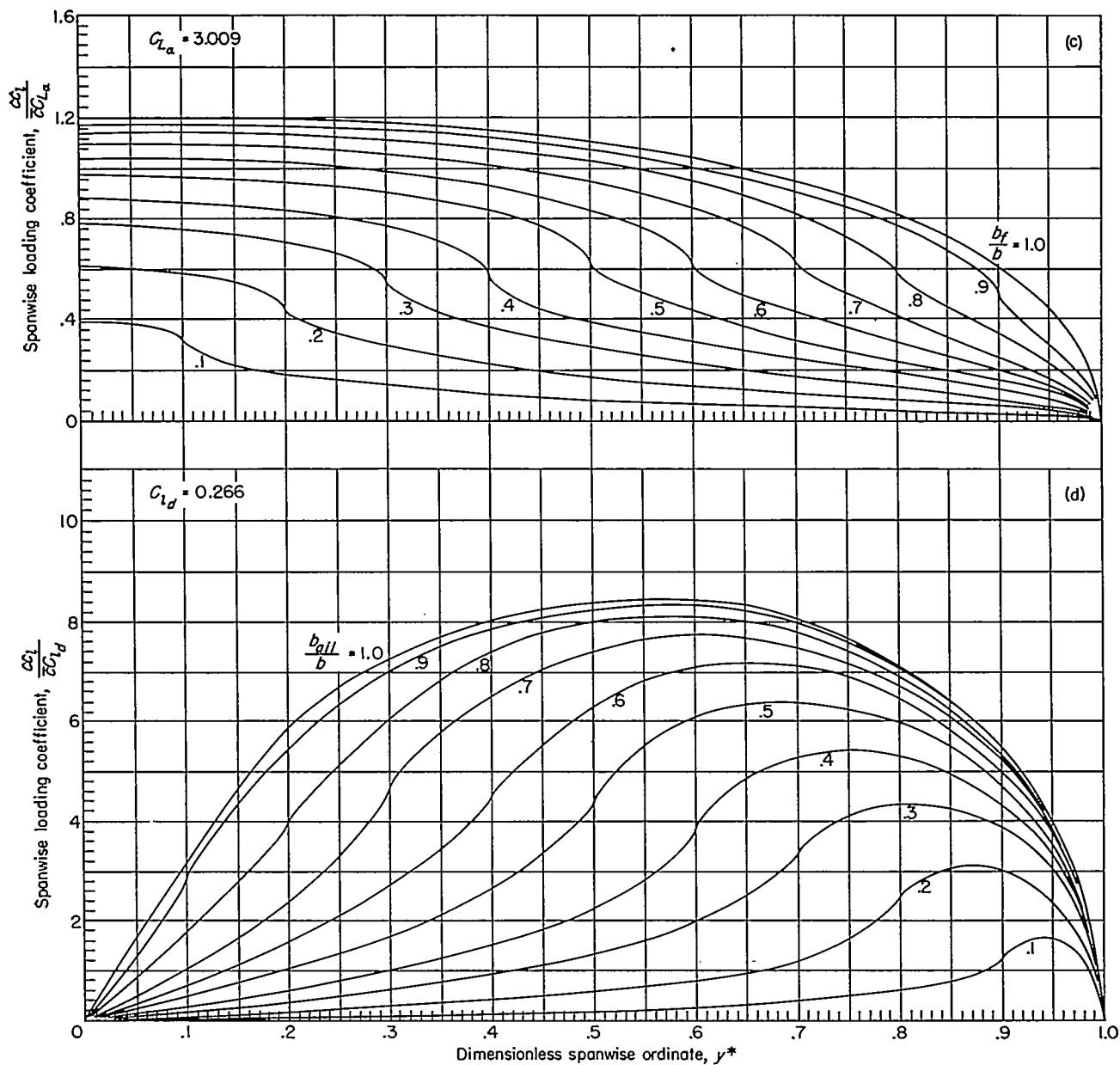
(c) Lift distribution for inboard flap.
(d) Lift distribution for outboard aileron.

Figure 10.—Concluded.



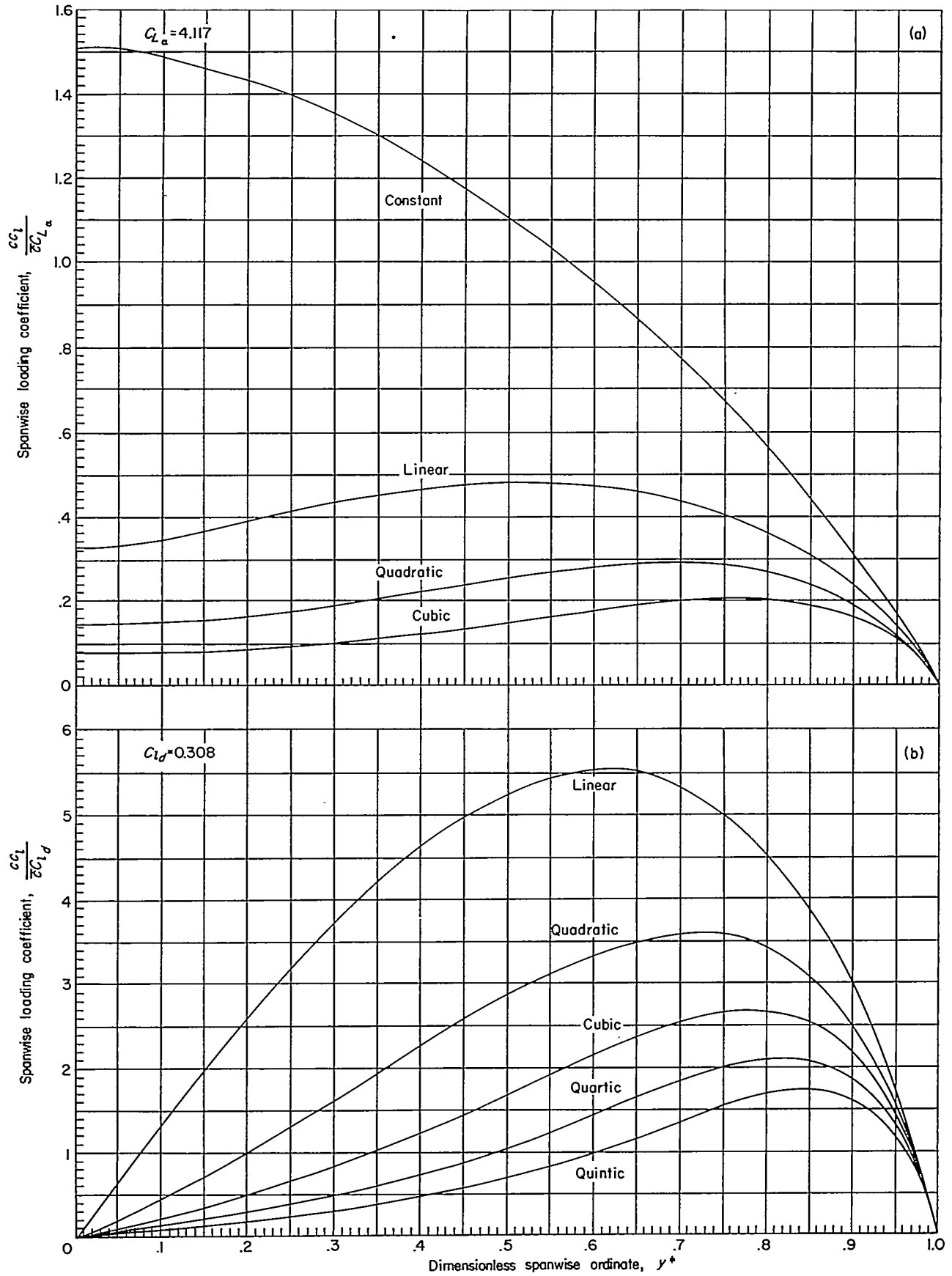
(a) Symmetrical lift distributions.
 (b) Antisymmetrical lift distributions.

FIGURE 11.—Spanwise lift distributions for plan form 325 ($A=3.0$; $\lambda=1.50$).



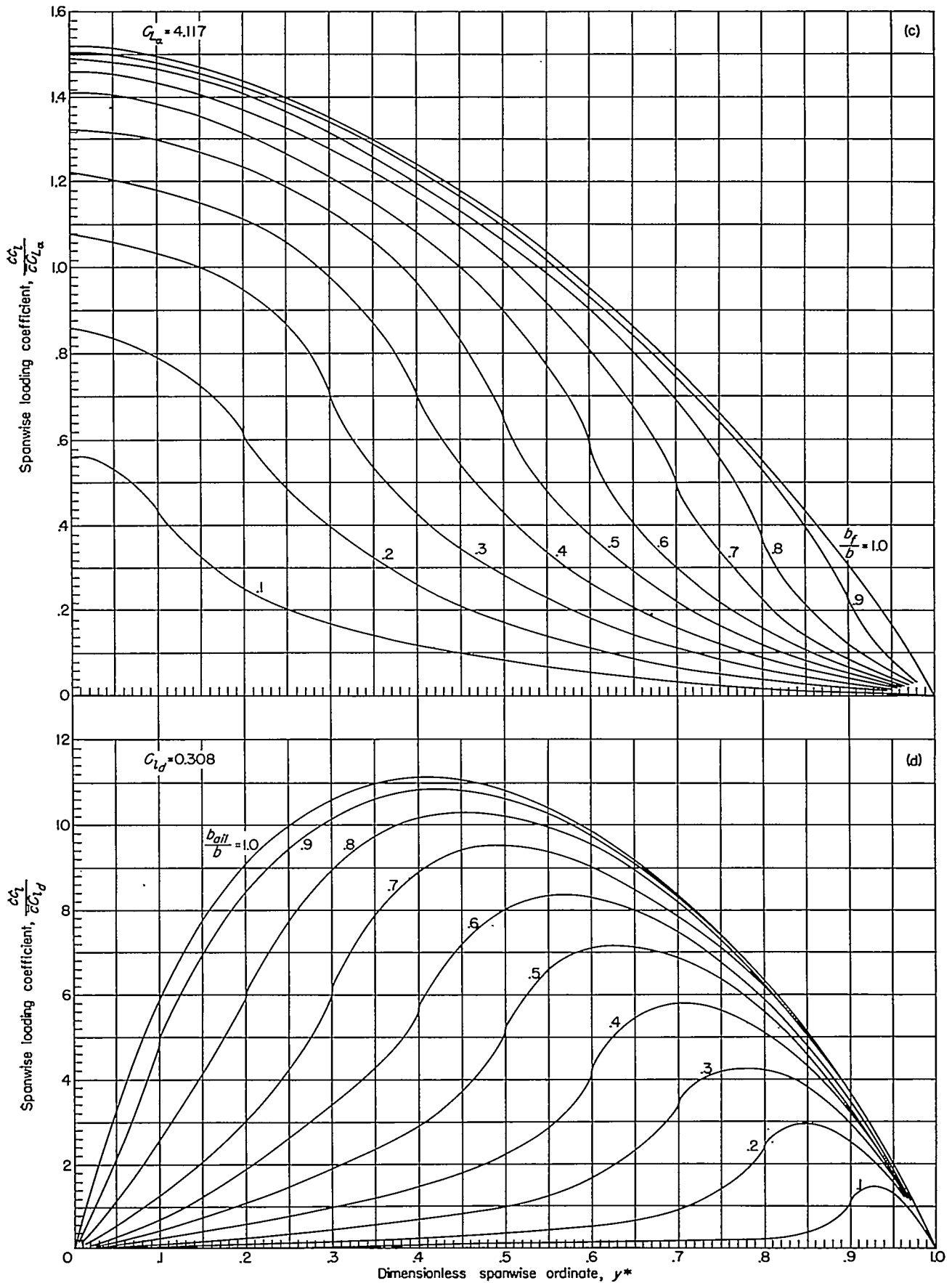
(c) Lift distribution for inboard flap.
 (d) Lift distribution for outboard aileron.

FIGURE 11.—Concluded.



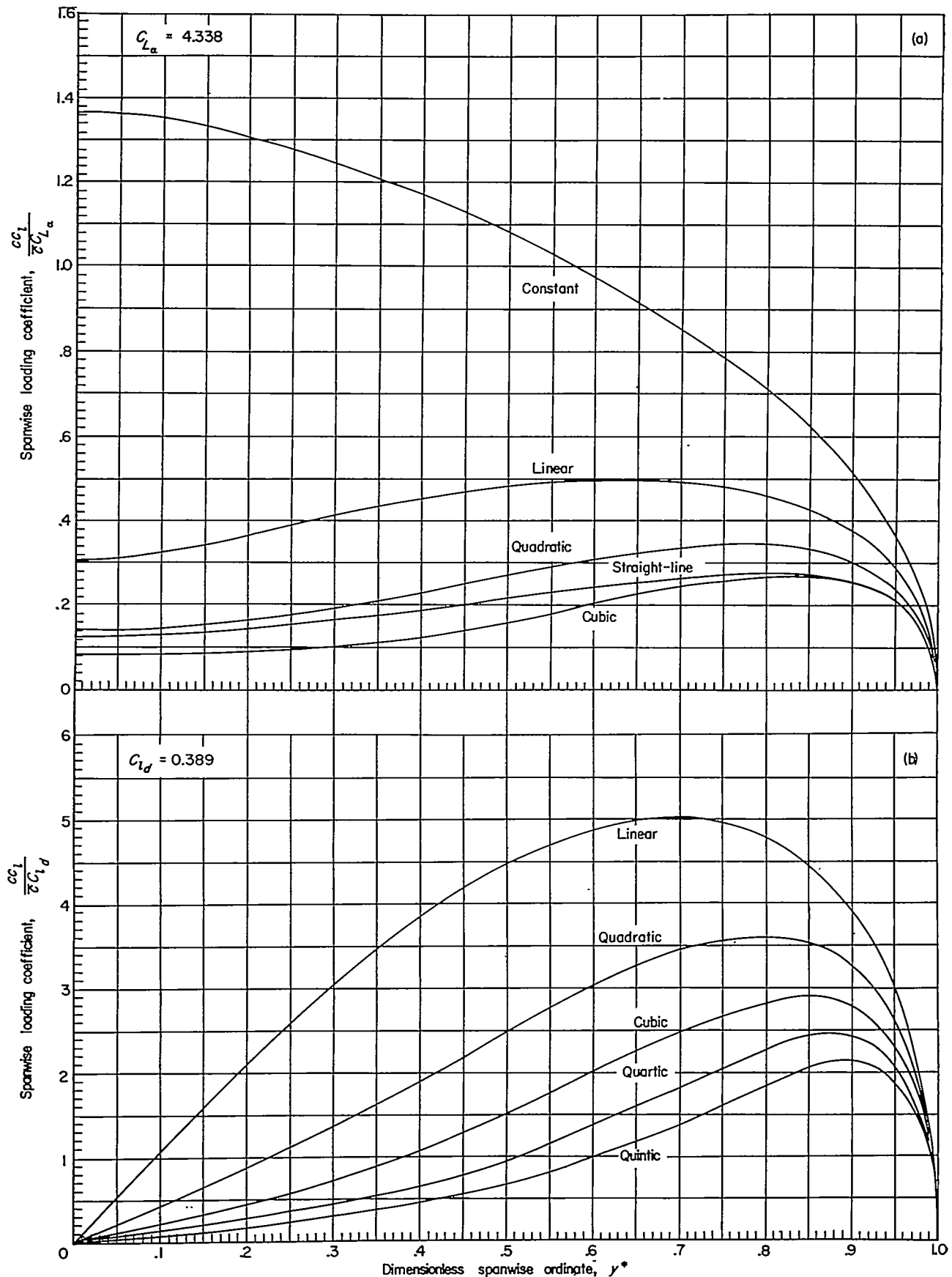
(a) Symmetrical lift distributions.
 (b) Antisymmetrical lift distributions.

FIGURE 12.—Spanwise lift distributions for plan form 331 ($\dot{A}=6.0$; $\lambda=0$).



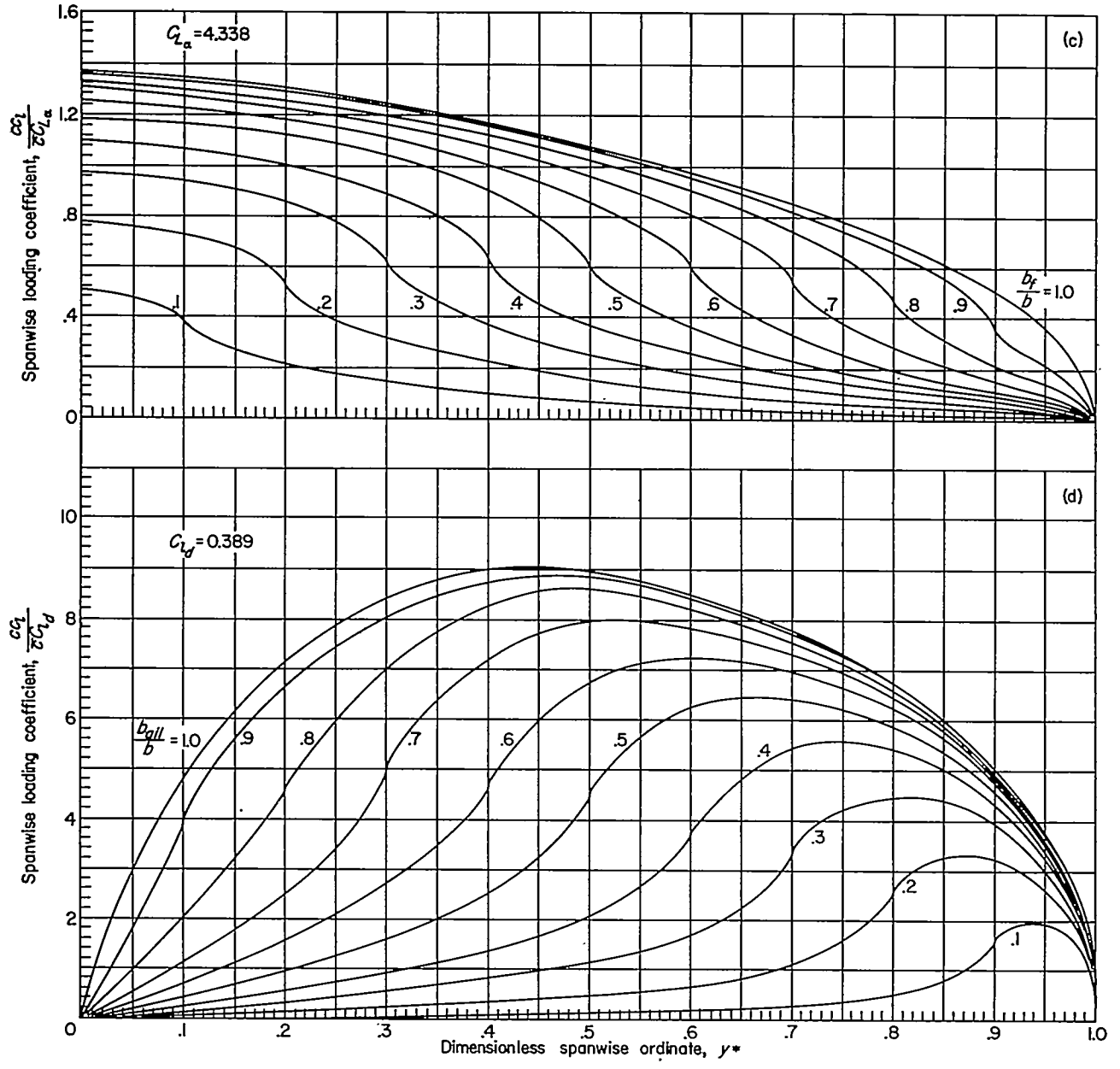
(c) Lift distribution for inboard flap.
 (d) Lift distribution for outboard alleron.

FIGURE 12.—Concluded.



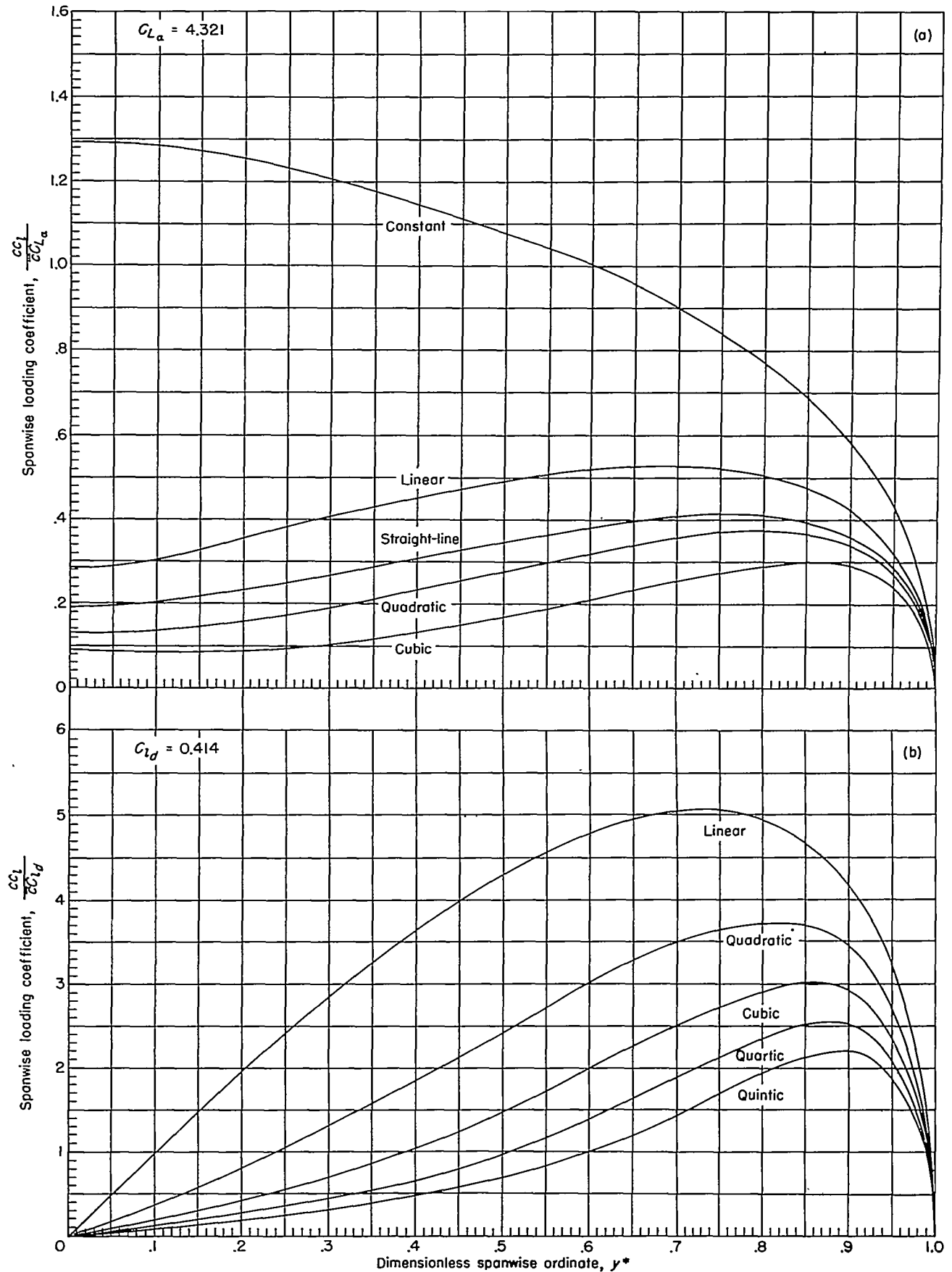
(a) Symmetrical lift distributions.
 (b) Antisymmetrical lift distributions.

FIGURE 13.—Spanwise lift distributions for plan form 332 ($A=6.0$; $\lambda=0.25$).



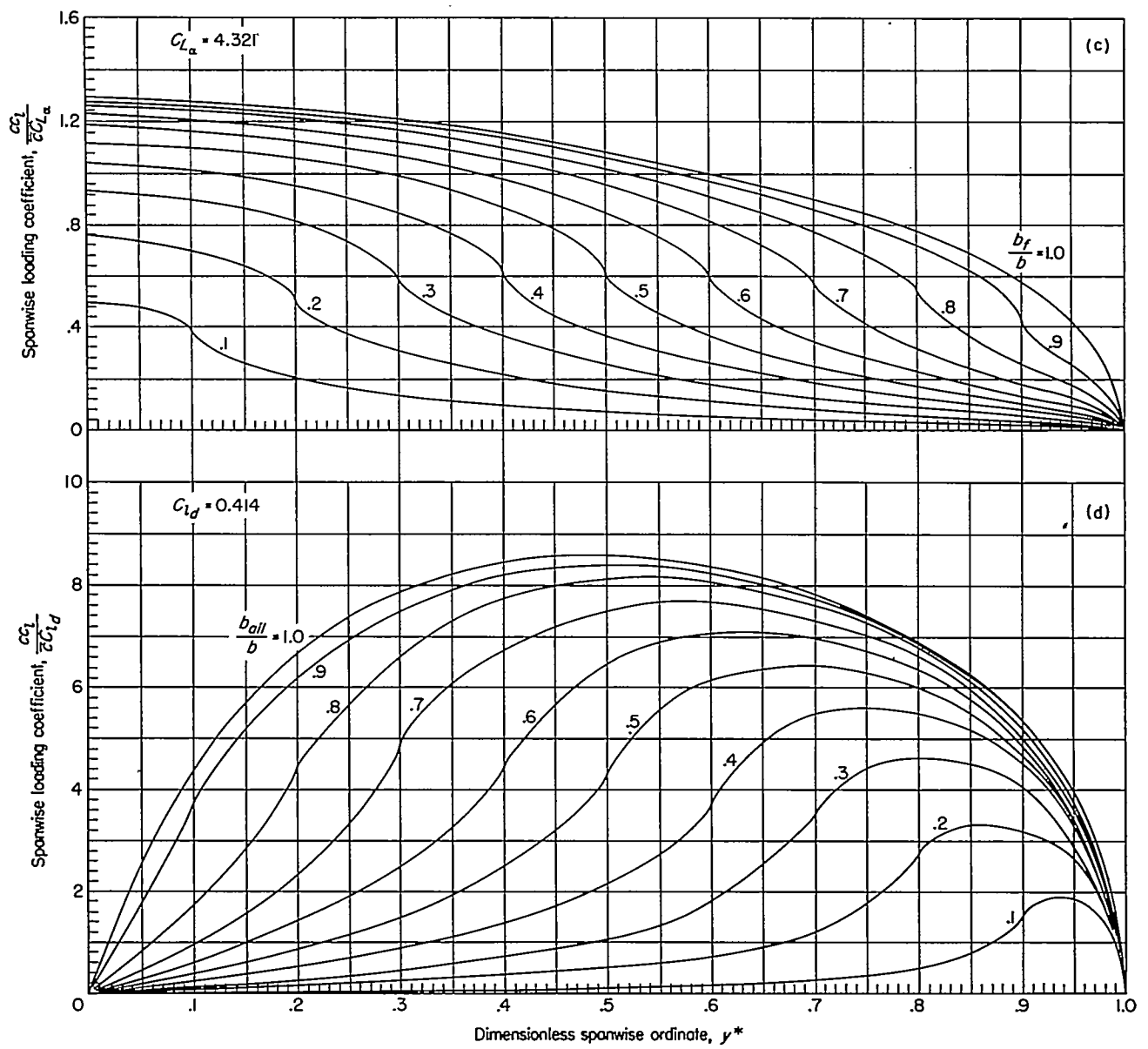
- (c) Lift distribution for inboard flap.
- (d) Lift distribution for outboard aileron.

FIGURE 13.—Concluded.



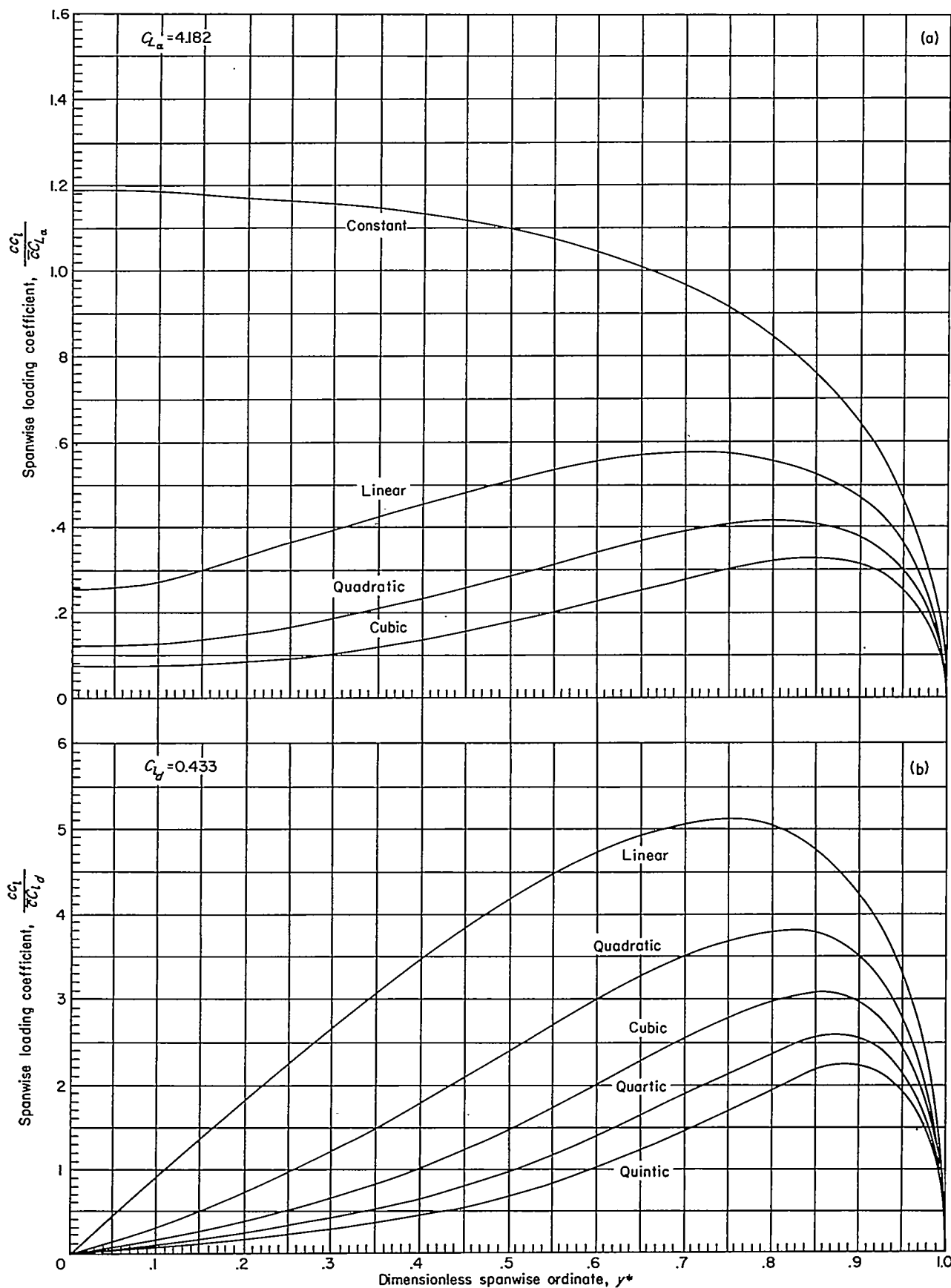
(a) Symmetrical lift distributions.
 (b) Antisymmetrical lift distributions.

FIGURE 14.—Spanwise lift distributions for plan form 333 ($A=6.0$; $\lambda=0.50$).



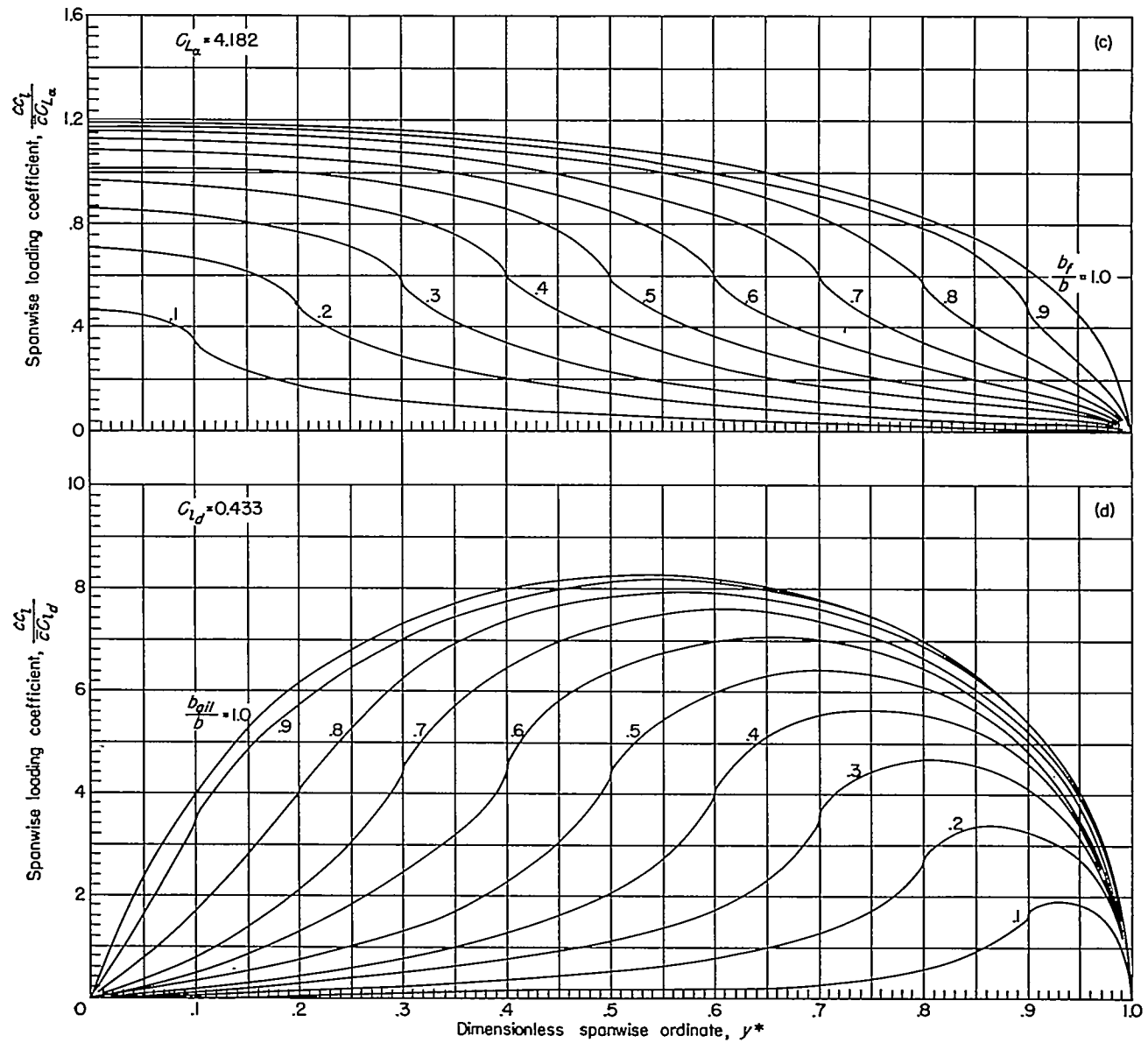
(c) Lift distribution for inboard flap.
 (d) Lift distribution for outboard aileron.

FIGURE 14.—Concluded.



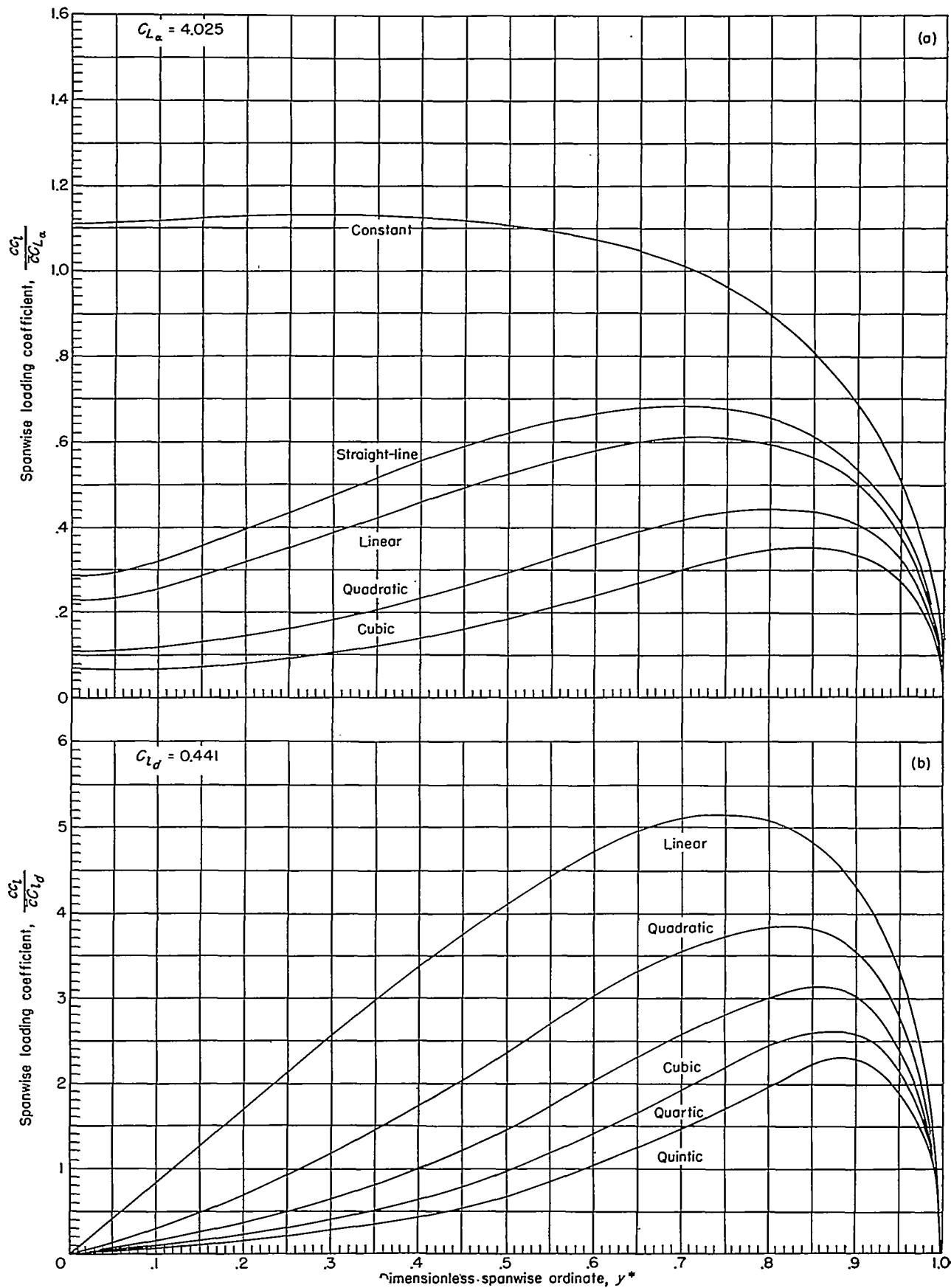
(a) Symmetrical lift distributions.
 (b) Antisymmetrical lift distributions.

FIGURE 15.—Spanwise lift distributions for plan form 334 ($A=6.0$; $\lambda=1.00$).



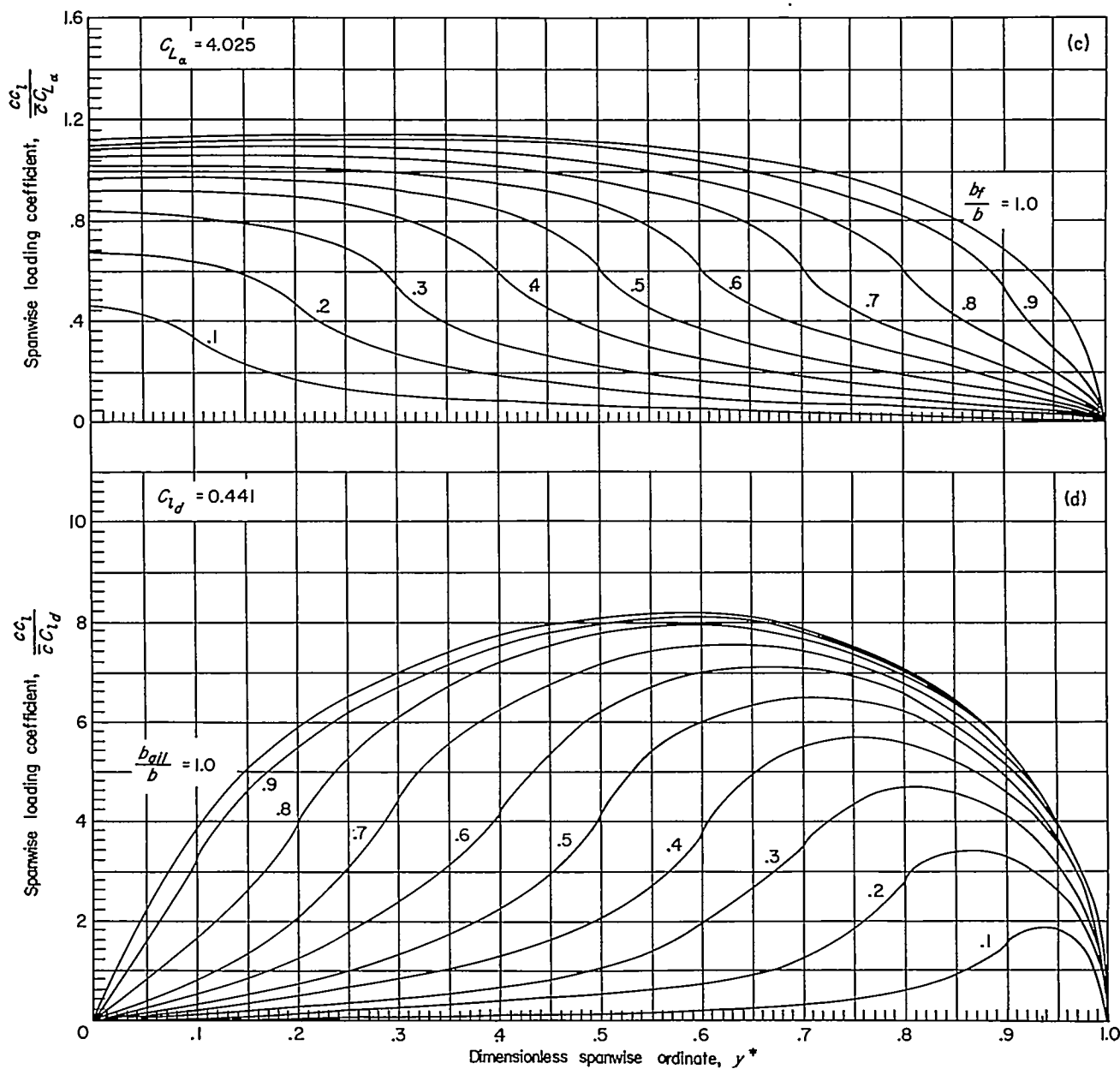
(c) Lift distribution for inboard flap.
(d) Lift distribution for outboard aileron.

FIGURE 15.—Concluded.



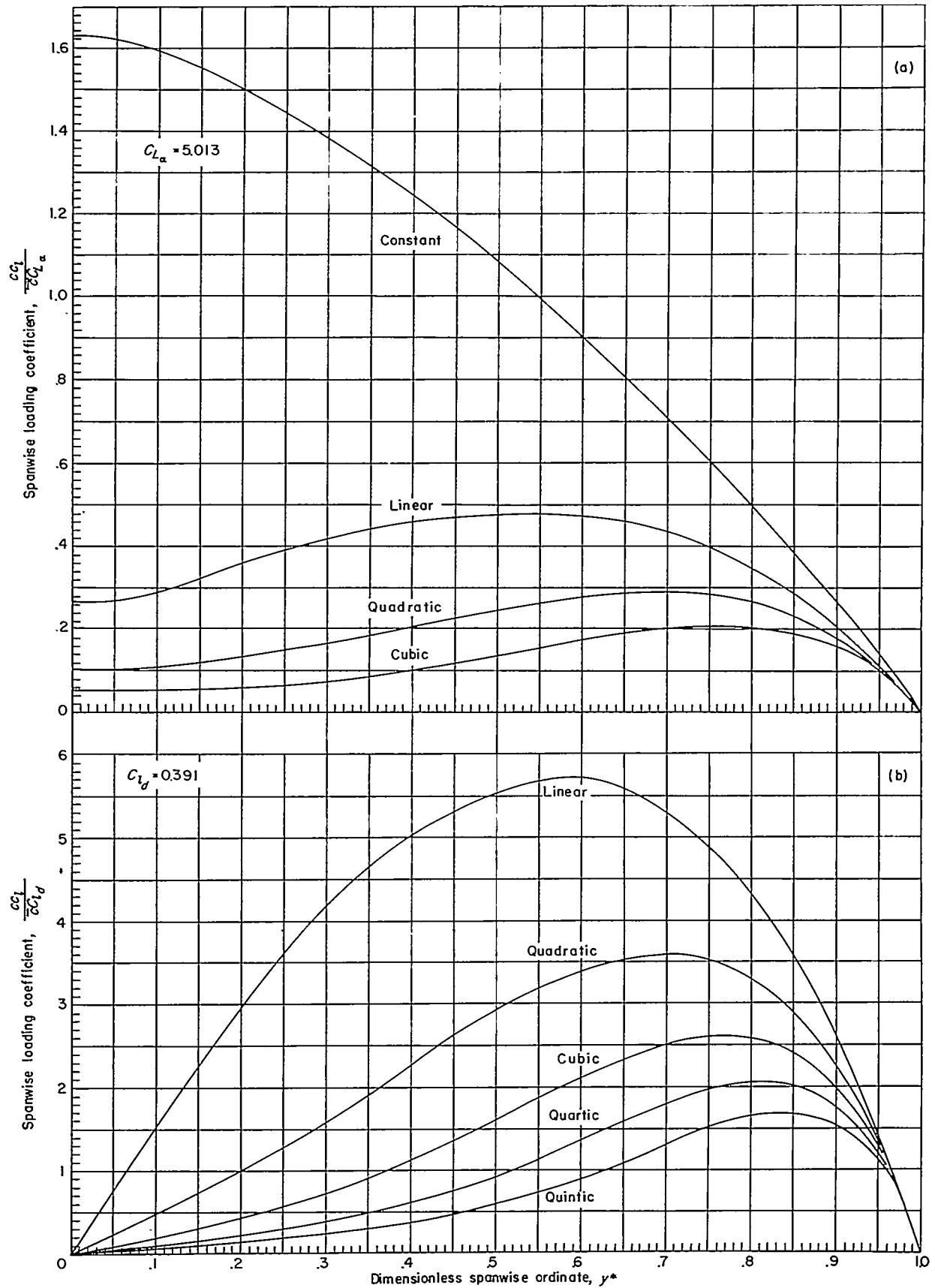
(a) Symmetrical lift distributions.
 (b) Antisymmetrical lift distributions.

FIGURE 16.—Spanwise lift distributions for plan form 335 ($A=6.0$; $\lambda=1.50$).



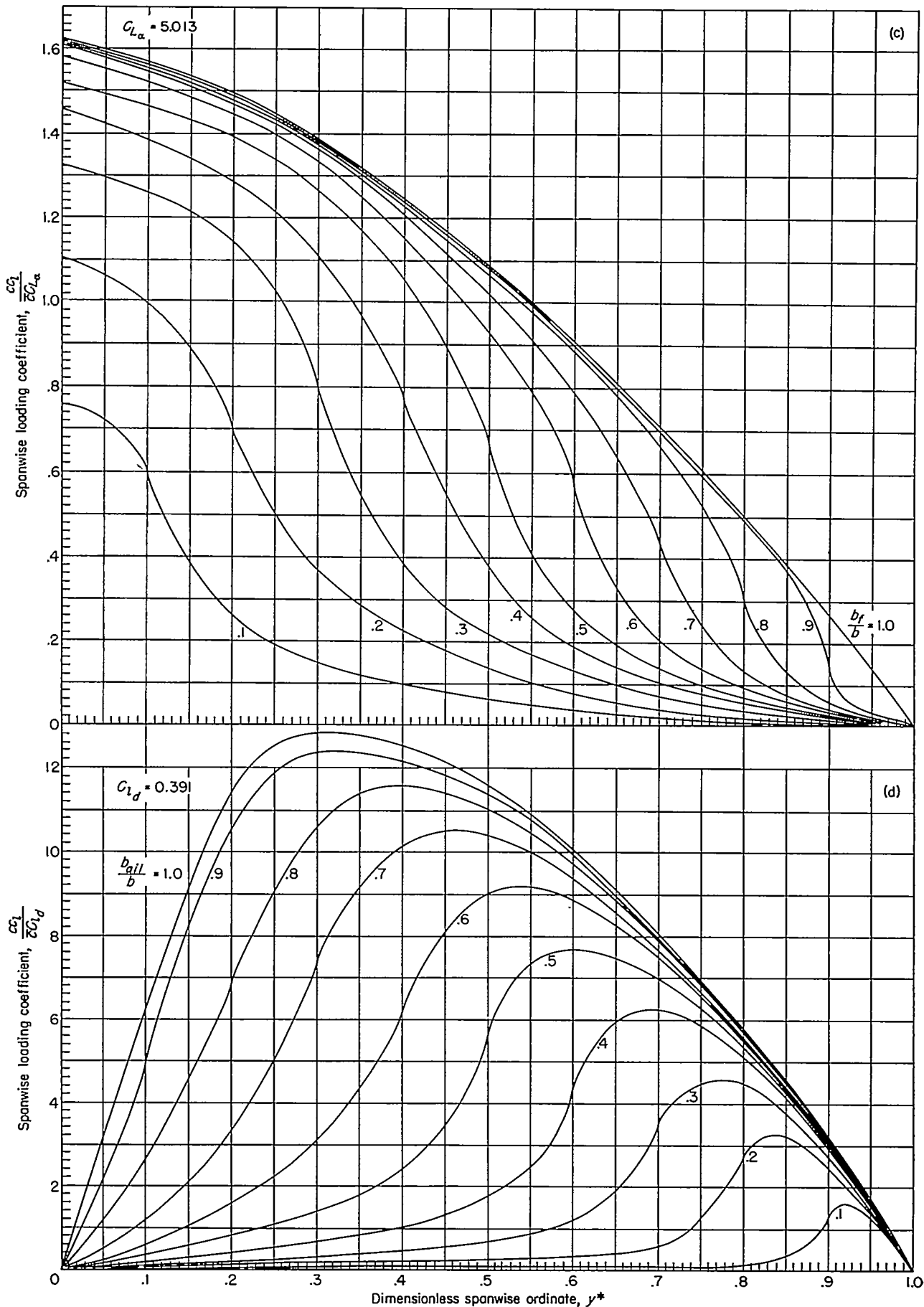
- (c) Lift distribution for inboard flap.
- (d) Lift distribution for outboard aileron.

FIGURE 16.—Concluded.



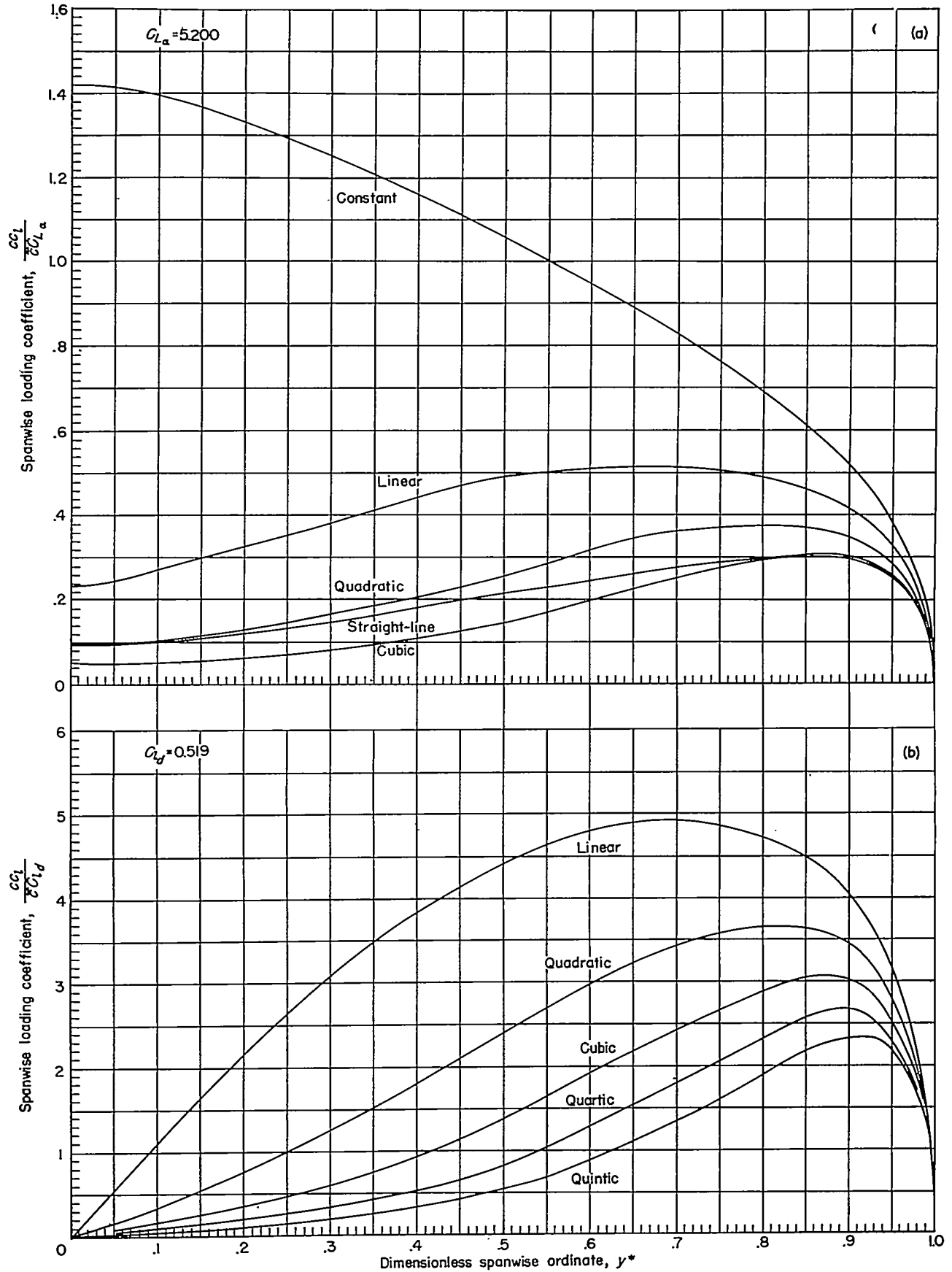
(a) Symmetrical lift distributions.
 (b) Antisymmetrical lift distributions.

FIGURE 17.—Spanwise lift distributions for plan form 341 ($A=12.0$; $\lambda=0$).



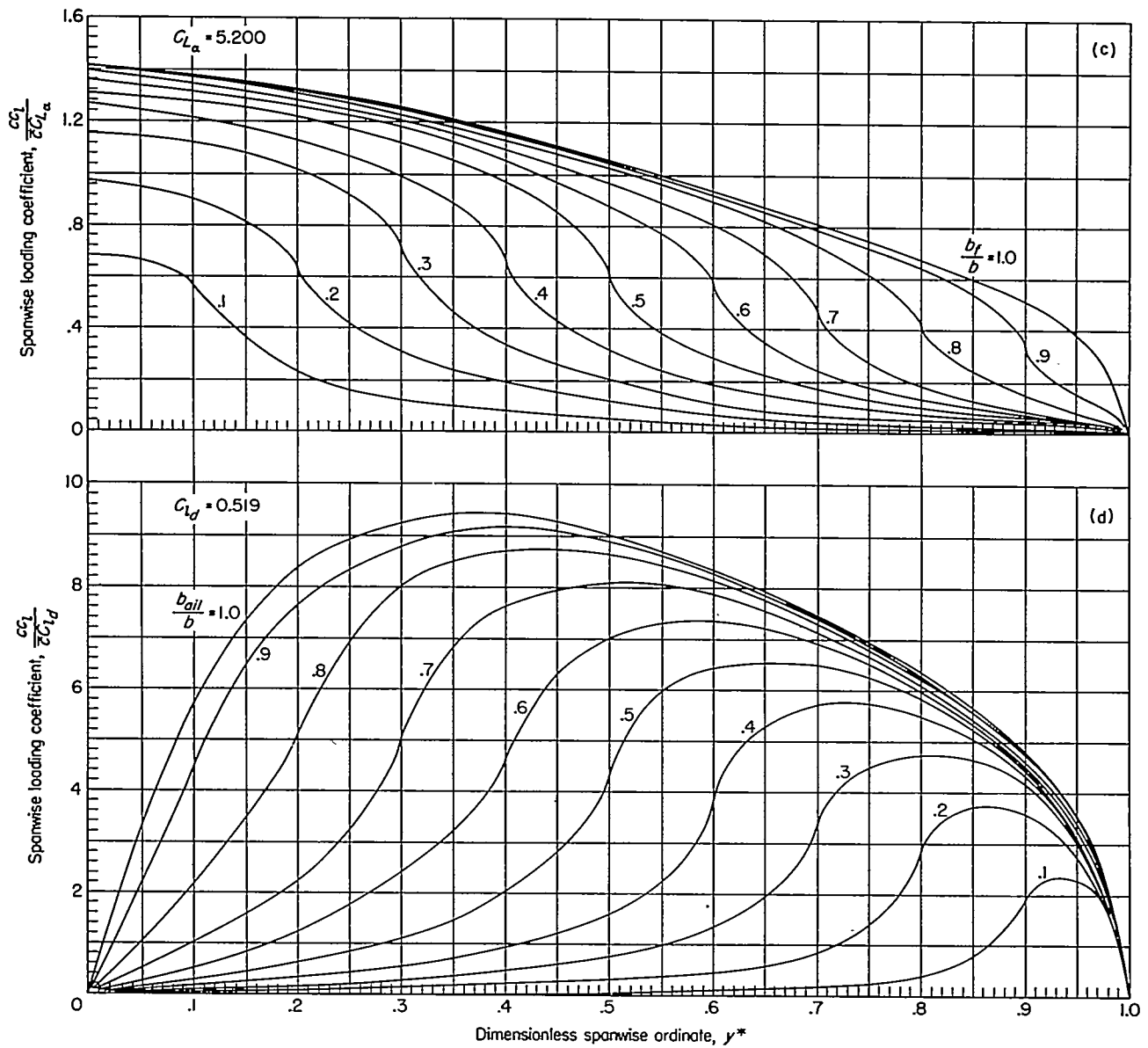
(c) Lift distribution for inboard flap.
 (d) Lift distribution for outboard aileron.

FIGURE 17—Concluded.



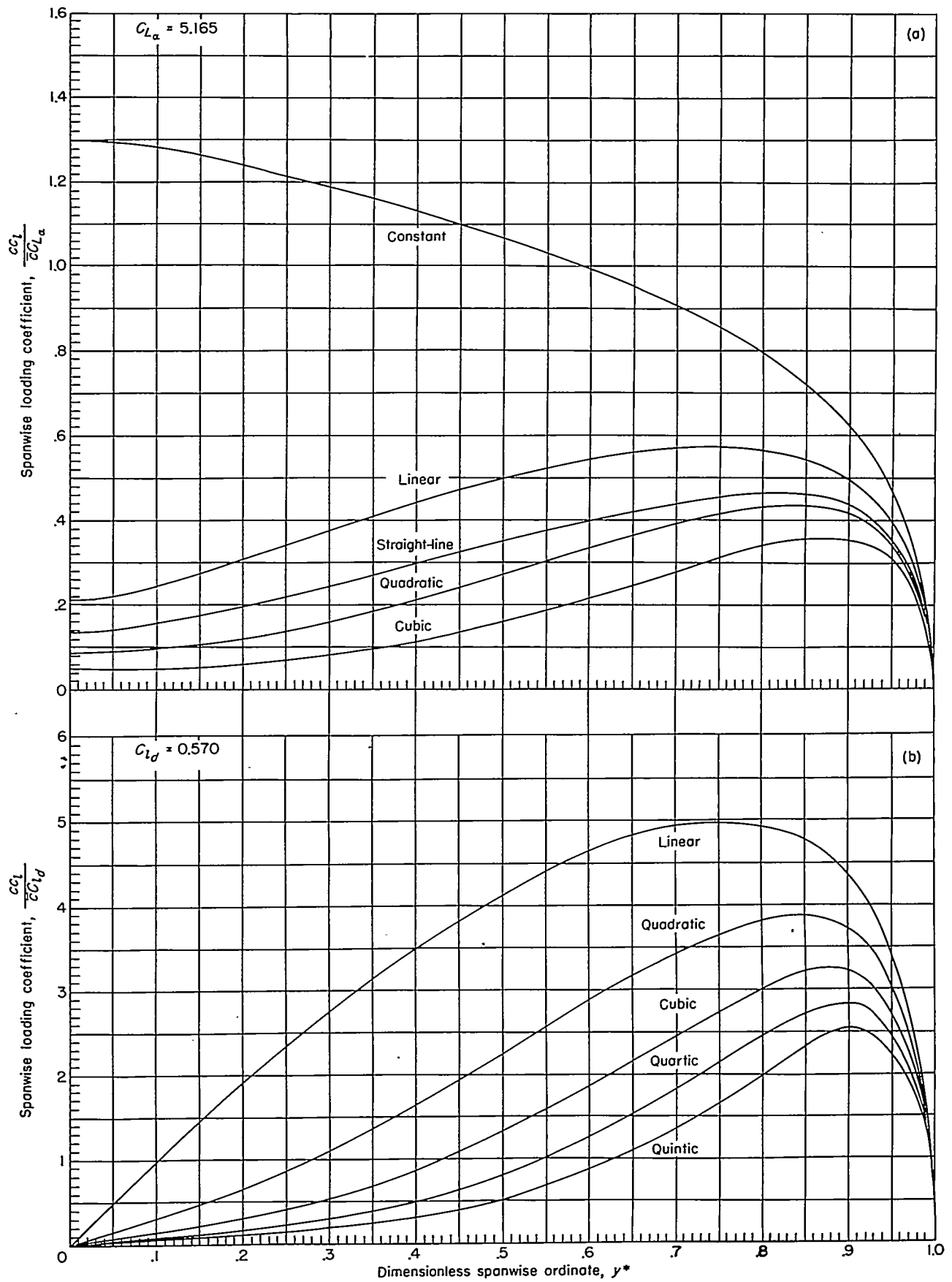
- (a) Symmetrical lift distributions.
- (b) Antisymmetrical lift distributions.

FIGURE 18.—Spanwise lift distributions for plan form 342 ($A=12.0$; $\lambda=0.25$).



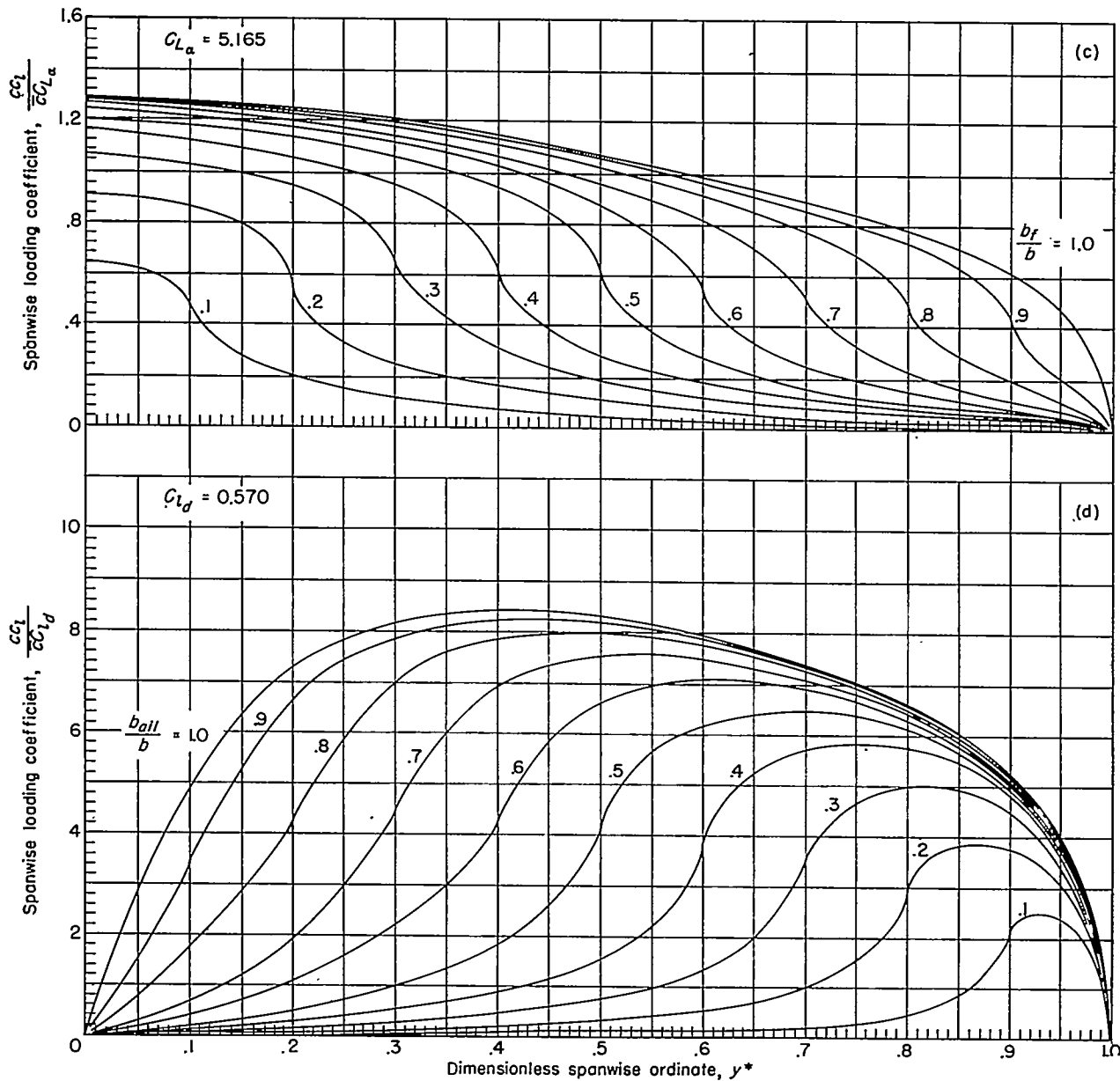
(c) Lift distribution for inboard flap.
 (d) Lift distribution for outboard aileron.

FIGURE 18.—Concluded.



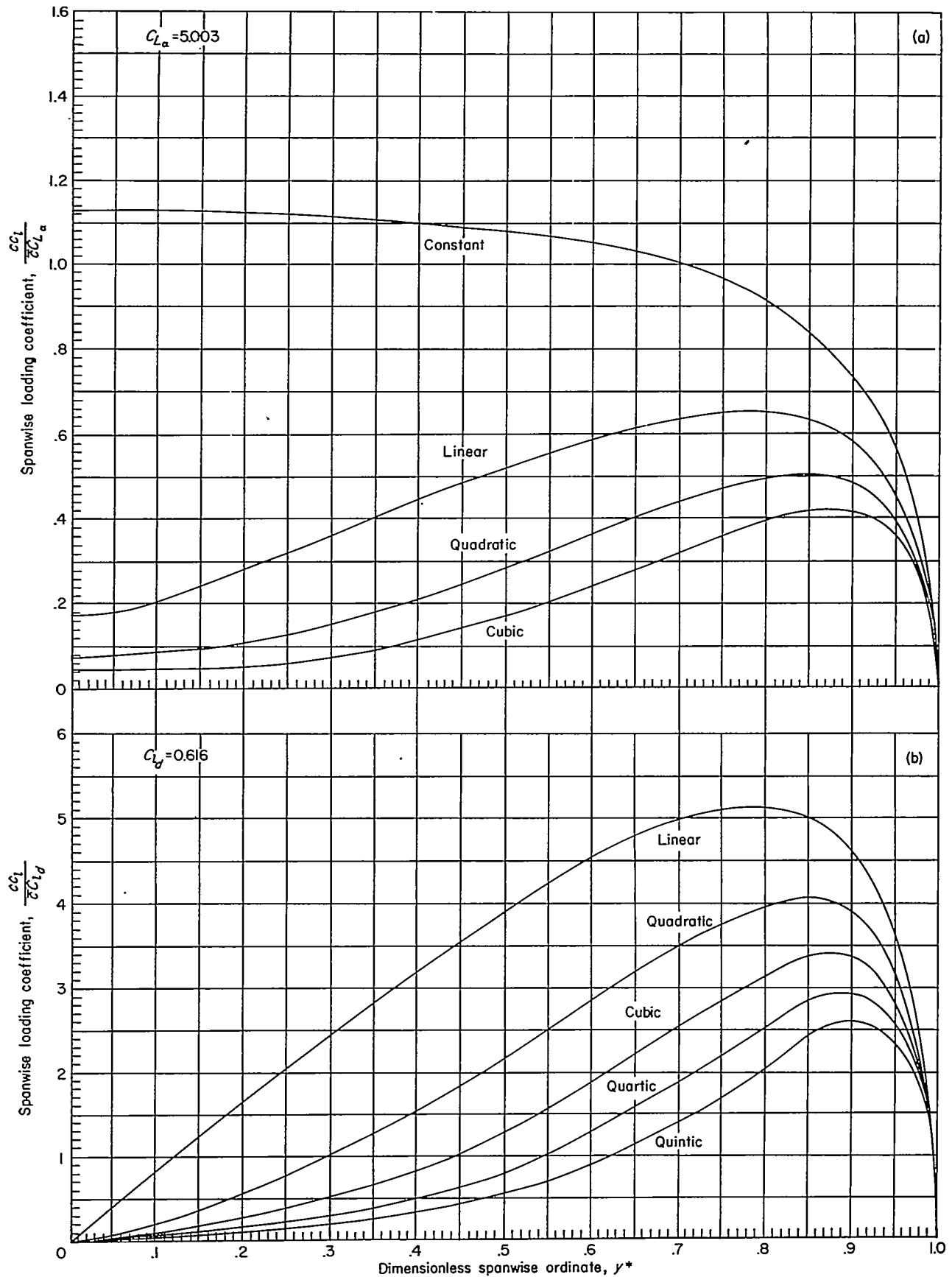
- (a) Symmetrical lift distributions.
- (b) Antisymmetrical lift distributions.

FIGURE 19.—Spanwise lift distributions for plan form 343 ($A=12.0$; $\lambda=0.50$).



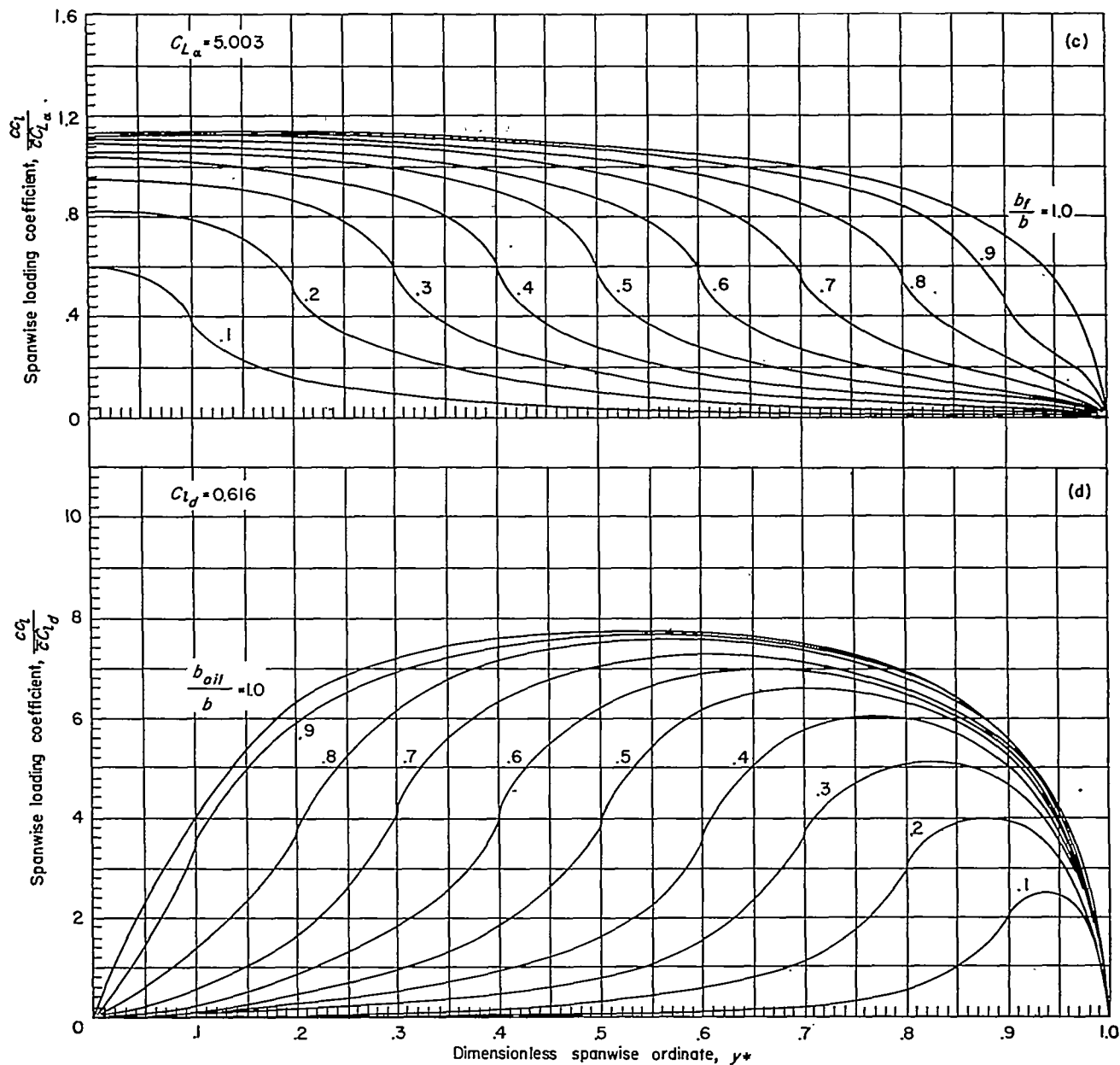
(c) Lift distribution for inboard flap.
 (d) Lift distribution for outboard alleron.

FIGURE 19.—Concluded.



- (a) Symmetrical lift distributions.
- (b) Antisymmetrical lift distributions.

FIGURE 20.—Spanwise lift distributions for plan form 344 ($A=12.0$; $\lambda=1.00$).



(c) Lift distribution for inboard flap.
 (d) Lift distribution for outboard aileron.

FIGURE 20.—Concluded.

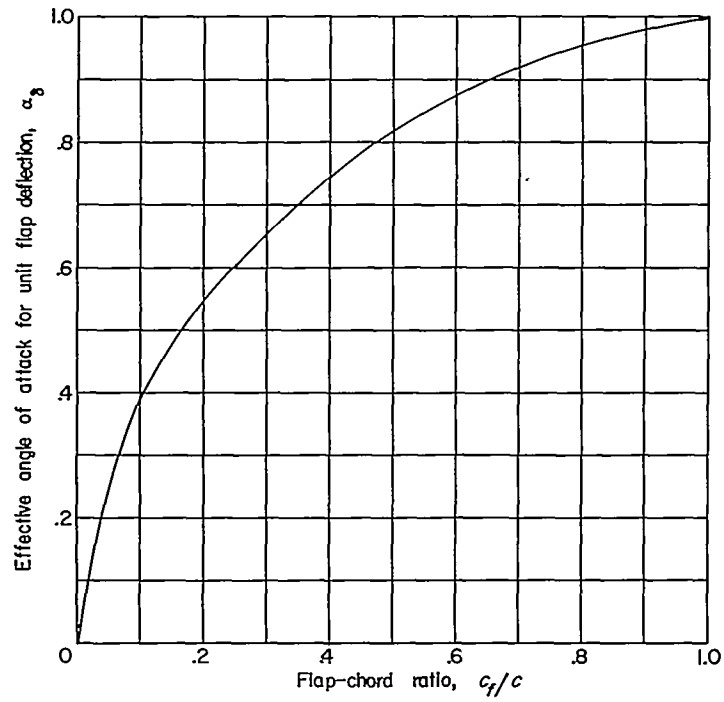


FIGURE 21.—Variation of flap effectiveness with flap-chord ratio.